



HAL
open science

Measurement of exclusive $\gamma\gamma \rightarrow W^+W^-$ production and search for exclusive Higgs boson production in pp collisions at $\sqrt{s} = 8$ TeV using the ATLAS detector

M. Aaboud, S. Albrand, S. Berlendis, A. Bethani, C. Camincher, J. Collot, S. Crépé-Renaudin, P.A. Delsart, C. Gabaldon, M.H. Genest, et al.

► To cite this version:

M. Aaboud, S. Albrand, S. Berlendis, A. Bethani, C. Camincher, et al.. Measurement of exclusive $\gamma\gamma \rightarrow W^+W^-$ production and search for exclusive Higgs boson production in pp collisions at $\sqrt{s} = 8$ TeV using the ATLAS detector. Physical Review D, 2016, 94, pp.032011. 10.1103/PhysRevD.94.032011 . in2p3-01345965

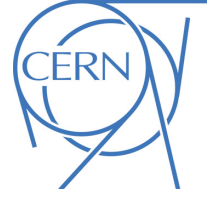
HAL Id: in2p3-01345965

<https://hal.in2p3.fr/in2p3-01345965>

Submitted on 12 Sep 2023

HAL is a multi-disciplinary open access archive for the deposit and dissemination of scientific research documents, whether they are published or not. The documents may come from teaching and research institutions in France or abroad, or from public or private research centers.

L'archive ouverte pluridisciplinaire **HAL**, est destinée au dépôt et à la diffusion de documents scientifiques de niveau recherche, publiés ou non, émanant des établissements d'enseignement et de recherche français ou étrangers, des laboratoires publics ou privés.



Measurement of exclusive $\gamma\gamma \rightarrow W^+W^-$ production and search for exclusive Higgs boson production in pp collisions at $\sqrt{s} = 8$ TeV using the ATLAS detector

The ATLAS Collaboration

Abstract

Searches for exclusively produced W boson pairs in the process $pp(\gamma\gamma) \rightarrow pW^+W^-p$ and exclusively produced Higgs boson in the process $pp(gg) \rightarrow pHp$ have been performed using $e^\pm\mu^\mp$ final states. These measurements use 20.2 fb^{-1} of pp collisions collected by the ATLAS experiment at a center-of-mass energy $\sqrt{s} = 8$ TeV at the LHC. Exclusive production of W^+W^- consistent with the Standard Model prediction is found with 3.0σ significance. The exclusive W^+W^- production cross-section is determined to be $\sigma(\gamma\gamma \rightarrow W^+W^- \rightarrow e^\pm\mu^\mp X) = 6.9 \pm 2.2(\text{stat.}) \pm 1.4(\text{sys.}) \text{ fb}$, in agreement with the Standard Model prediction. Limits on anomalous quartic gauge couplings are set at 95% confidence-level as $-1.7 \times 10^{-6} < a_0^W/\Lambda^2 < 1.7 \times 10^{-6} \text{ GeV}^{-2}$ and $-6.4 \times 10^{-6} < a_C^W/\Lambda^2 < 6.3 \times 10^{-6} \text{ GeV}^{-2}$. A 95% confidence-level upper limit on the total production cross-section for exclusive Higgs boson is set to 1.2 pb.

Contents

| | | |
|-----------|---------------------------------------------------------------------------------------------------------|-----------|
| 1 | Introduction | 2 |
| 2 | The ATLAS detector | 5 |
| 3 | Data and simulated event samples | 6 |
| 4 | Selection of leptons, jets, and charged particles | 7 |
| 5 | Exclusivity selection | 8 |
| 6 | Event selection | 9 |
| 6.1 | Exclusive W^+W^- candidate selection | 10 |
| 6.2 | Exclusive Higgs Boson candidate selection | 10 |
| 7 | Pileup and exclusivity validation with $\gamma\gamma \rightarrow \ell^+\ell^-$ events | 10 |
| 8 | Signal and background control regions | 13 |
| 8.1 | Single-dissociative and double-dissociative contributions | 13 |
| 8.2 | Track multiplicity modeling | 15 |
| 8.3 | Inclusive W^+W^- normalization | 16 |
| 8.4 | Sum of inclusive W^+W^- and other background | 17 |
| 9 | Systematic uncertainties | 20 |
| 10 | Results | 20 |
| 10.1 | Standard Model exclusive W^+W^- production | 20 |
| 10.1.1 | $\gamma\gamma \rightarrow W^+W^-$ cross-section | 22 |
| 10.1.2 | Limits on anomalous Quartic Gauge Couplings | 23 |
| 10.2 | Limits on exclusive Higgs Boson production | 25 |
| 11 | Conclusion | 25 |

1 Introduction

In the Standard Model (SM) of particle physics, the interactions between electroweak gauge bosons are described by the non-Abelian $SU(2) \times U(1)$ structure of the electroweak sector. Measurement of the strengths of the trilinear (VVV , where $V = \gamma, W$, or Z) and quartic ($VVVV$) gauge couplings represent an important test of the SM, as deviations from SM predictions would indicate new physics. The discovery of a Higgs boson [1, 2] at the Large Hadron Collider (LHC) has taken a major step toward confirming the mechanism of electroweak symmetry breaking. Anomalous quartic gauge couplings (aQGCs) provide a window to further probe possible new physics extensions of electroweak theory. Exclusive production of W boson pairs, $pp(\gamma\gamma) \rightarrow pW^+W^-p$, provides an opportunity to study $\gamma\gamma \rightarrow W^+W^-$ aQGC couplings [3, 4].

In pp collisions, exclusive W^+W^- events are produced when each proton emits a photon and the two photons annihilate, either via t - and u -channel W -exchange diagrams involving trilinear gauge couplings

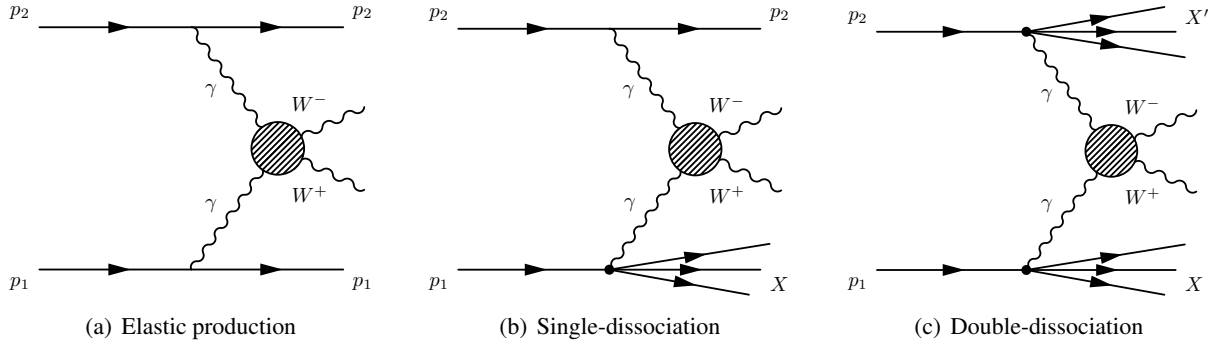


Figure 1: Diagrams for the exclusive $\gamma\gamma \rightarrow W^+W^-$ production representing the (a) elastic process, (b) single-dissociation where one initial proton dissociates (SD) and (c) double-dissociation where both protons fragment (DD). The symbols X and X' denote any additional final state created.

or via quartic gauge coupling diagram, to create a W^+W^- pair. Figure 1 shows the exclusive production of a W^+W^- pair, where the blobs represent the t -channel, u -channel, and quartic diagrams. After the collisions, either both protons remain intact as shown in Fig. 1(a) (referred to as *elastic* hereafter), only one proton remains intact as in Fig. 1(b) (*single-dissociation*, SD), or both protons dissociate as in Fig. 1(c) (*double-dissociation*, DD). In all three cases the trajectories of the protons or their remnants deviate only slightly from their initial directions so that they never enter the acceptance of the ATLAS detector. On the other hand, inclusive processes are produced with accompanying activity such as initial- and final-state radiation and additional scattering in the same pp collision. The accompanying activity is collectively called the underlying event and emits particles into the acceptance of the ATLAS detector.

Photon scattering in hadron colliders can be described in quantum electrodynamics (QED) by the equivalent-photon approximation (EPA) [5, 6]. In this framework the exclusive W^+W^- cross-section can be written as

$$\sigma_{pp(\gamma\gamma) \rightarrow ppW^+W^-}^{\text{EPA}} = \iint f(x_1)f(x_2)\sigma_{\gamma\gamma \rightarrow W^+W^-}(m_{\gamma\gamma}^2)dx_1dx_2, \quad (1)$$

where $f(x_i)$, for $i \in \{1, 2\}$, is the number of equivalent photons carrying a fraction of the proton's energy, x_i , that are emitted, while $m_{\gamma\gamma}$ is the two-photon center-of-mass energy. This approach has been used to describe similar exclusive processes in the CDF [7], STAR [8], and CMS [9, 10] experiments.

Exclusive W^+W^- pair production is particularly sensitive to new physics that may be described by anomalous quartic gauge coupling (aQGC) of the form $WW\gamma\gamma$ [4, 11]. The dimension-6 operators in Ref. [3] are the lowest-dimension operators that give rise to anomalous $WW\gamma\gamma$ couplings, a_0^W/Λ^2 and a_C^W/Λ^2 where Λ is the scale of new physics. A procedure adopted by previous measurements [12–14] uses a dipole form factor to preserve unitarity at high $m_{\gamma\gamma}$. The couplings a_0^W/Λ^2 and a_C^W/Λ^2 then become:

$$a_{0,C}^W/\Lambda^2 \rightarrow \frac{a_{0,C}^W}{\Lambda^2} \frac{1}{\left(1 + \frac{m_{\gamma\gamma}^2}{\Lambda_{\text{cutoff}}^2}\right)^2} \quad (2)$$

where Λ_{cutoff} defines the scale of possible new physics, and the term containing it ensures that unitarity is preserved.

Anomalous triple gauge couplings (aTGCs) could also produce similar effects but the sensitivity of this study to aTGCs is not competitive compared with other processes [4], so these are taken to be zero.

More recent parameterizations of aQGCs are of dimension 8. The parameterization of the dimension-8 couplings, $f_{M,0,1,2,3}/\Lambda^4$, in Ref. [15] are linearly related to the $a_{0,C}^W/\Lambda^2$ as follows:

$$\frac{f_{M,0}}{\Lambda^4} = \frac{a_0^W}{\Lambda^2} \frac{1}{g^2 v^2}, \quad \frac{f_{M,1}}{\Lambda^4} = -\frac{a_C^W}{\Lambda^2} \frac{1}{g^2 v^2}, \quad (3)$$

where $g = e/\sin(\theta_W)$ and v is the Higgs boson vacuum expectation value. Also, with this parameterization, $f_{M,2} = 2 \times f_{M,0}$ and $f_{M,3} = 2 \times f_{M,1}$.

In addition to the discovery of the Higgs boson, several of its properties – such as mass, coupling strengths to various final-state particles, and branching ratios of its decay – have been determined [1, 16] using Higgs boson candidates from inclusive production. Higgs boson candidates from the exclusive production ($pp \rightarrow pggp \rightarrow pHp$) would have lower systematic uncertainties due to their cleaner production environment [17–20]. Since measurements using these Higgs boson candidates would have better precision, they could be used to improve knowledge of the Higgs boson sector. It is therefore interesting to determine the cross-section for exclusive Higgs boson production and examine the feasibility of using exclusive Higgs boson candidates for Higgs boson property measurements. This interest is reflected in the inclusion of the exclusive Higgs boson process studies as part of the physics program of forward proton-tagging detectors [21–23] that extend the ATLAS and CMS coverage for LHC runs at 13 TeV.

Unlike exclusive W^+W^- production, exclusive Higgs boson production proceeds through a quantum chromodynamics (QCD) process involving at least three gluons as shown in Fig. 2. Two gluons from the colliding protons interact through a top-quark loop to produce a Higgs boson while additional gluon exchange between the colliding protons keeps the protons color-neutral and allows the protons to remain intact after the collision. The proton trajectories deviate slightly after the collision. One W boson from Higgs boson decays must be off shell so the event selection for that study needs to be different than the exclusive W^+W^- event selection, and the samples are largely orthogonal.

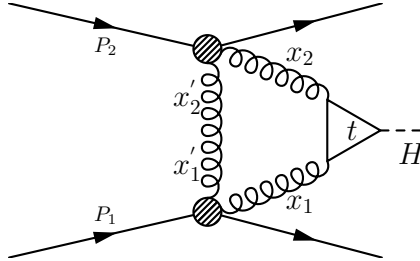


Figure 2: The lowest-order Feynman diagram for the exclusive Higgs boson production. The variables x_1 and x_2 are the fractions of the momenta carried by the gluons that contribute to the production of the Higgs boson, with respect to the momenta of the protons P_1 and P_2 . The variables x'_1 , and x'_2 , on the other hand, are the fractions of the momentum carried by the exchanged third gluon with respect to the momenta of the protons P_1 and P_2 .

The exclusive Higgs boson production cross-section can be written as [24]

$$\sigma_{pp(gg) \rightarrow ppH} \propto \hat{\sigma}(gg \rightarrow H) \left(\int \frac{dQ_t^2}{Q_t^4} f_g(x_1, x'_1, Q_t^2) f_g(x_2, x'_2, Q_t^2) \right)^2 \quad (4)$$

where $\hat{\sigma}(gg \rightarrow H)$ is the cross-section for the gluon fusion process that produces the Higgs boson. The functions f_g [25] are the generalized gluon densities for the finite proton size, that take into account the impact parameter. The variables x_1 and x_2 are the fractions of the momenta carried by the gluons that

contribute to the production of the Higgs boson, with respect to the momenta of the protons P_1 and P_2 . The variables x'_1 and x'_2 are the fractions of the momentum carried by the exchanged third gluon with respect to the momenta of the protons P_1 and P_2 as shown in Fig. 2. These gluon densities are integrated over the exchanged (third) gluon transverse momentum Q_T . This formalism, used in several theoretical calculations, predicts cross-sections that vary by over an order of magnitude [24, 26]. This wide disparity in predictions is an additional motivation for this measurement. While either proton could dissociate, the predictions presented here are for elastic production only and could underestimate the cross-section by an order of magnitude [24].

This paper describes searches for exclusive W^+W^- and $H \rightarrow W^+W^-$ production using $e^\pm\mu^\mp$ final states. Events where a W boson decays to a τ lepton that subsequently decays to an electron or muon are also included. This final state is denoted $e\mu X$, where X represents the neutrinos. Section 2 describes the experimental setup. Section 3 describes the dataset and simulation tools used to model signal and background processes. Initial selection of electron, muon, jet and track candidates is discussed in Section 4. Section 5 introduces a new approach to separate exclusive from inclusive production processes. Section 6 describes the event selections including signal regions for both the exclusive W^+W^- and Higgs boson processes. Section 7 outlines studies of the exclusive event selection and underlying-event models using samples of same-flavor opposite-sign lepton pairs in $p\gamma\gamma p \rightarrow p\ell^+\ell^-p$ candidates ($\ell = \mu$ or e) to validate modeling and selection criteria. In Section 8, data control regions designed to test and correct physics and detector modeling are described. Systematic uncertainties are summarized in Section 9 and the results of the study are described in detail in Section 10. Section 11 summarizes the findings.

2 The ATLAS detector

ATLAS [27] is a multipurpose cylindrical detector¹ that consists of an inner detector surrounded by a superconducting solenoid, a calorimeter system, and a muon spectrometer that includes superconducting toroidal magnets. The inner detector system consists of three subsystems: a pixel detector, a silicon microstrip detector, and a transition radiation tracker. Immersed in a 2 T magnetic field provided by the superconducting solenoid, these three subsystems enable the inner detector to accurately reconstruct the trajectories of charged particles in a pseudorapidity range $|\eta| < 2.5$ and measure their momenta and charges. The inner detector is surrounded by high-granularity lead/liquid-argon (LAr) sampling electromagnetic calorimeters covering the pseudorapidity range $|\eta| < 3.2$. A steel/scintillator tile calorimeter provides hadronic energy measurements in the pseudorapidity region $|\eta| < 1.7$. In the regions $1.5 < |\eta| < 4.9$ the hadronic energy measurements are provided by two endcap LAr calorimeters using copper or tungsten as absorbers. The calorimeters are surrounded by a muon spectrometer that provides muon tracking beyond the calorimeters in the range $|\eta| < 2.7$, and improves muon momentum resolution, charge measurements, and identification including triggering.

Events are selected using a three-level trigger system [28]. A hardware-based Level-1 trigger uses a subset of detector information to reduce the event rate to 75 kHz or less. The rate of accepted events is then reduced to about 400 Hz by two software-based trigger levels, Level-2 and the Event Filter. These events are then stored for later offline reconstruction and analysis.

¹ The ATLAS experiment uses a right-handed coordinate system with its origin at the nominal interaction point (IP) in the center of the detector and the z -axis along the beam direction. The x -axis points from the IP to the center of the LHC ring and the y -axis points upward. Cylindrical coordinates (r, ϕ) are used in the transverse (x, y) plane, ϕ being the azimuthal angle around the z -axis. The pseudorapidity is defined in terms of the polar angle θ as $\eta = -\ln \tan(\theta/2)$. The angular distance ΔR in the η - ϕ space is defined as $\Delta R = \sqrt{(\Delta\eta)^2 + (\Delta\phi)^2}$.

3 Data and simulated event samples

This analysis uses a data set of pp collisions collected at a center-of-mass energy $\sqrt{s} = 8$ TeV during 2012 under stable beam conditions. After applying data quality requirements, the data set has a total integrated luminosity of $20.2 \pm 0.4 \text{ fb}^{-1}$ [29].

The exclusive SM $\gamma\gamma \rightarrow W^+W^-$ signal sample is generated using the HERWIG++ [30] Monte Carlo (MC) generator, while $\gamma\gamma \rightarrow W^+W^-$ signal samples with both the SM and non-SM aQGC predictions are generated by FPMC [31]. These two generators use the EPA formalism with a standard dipole parameterization [32] of the proton electromagnetic form factors to produce an equivalent photon flux in pp collisions. FPMC is used in these studies to generate $pp \rightarrow pggp \rightarrow pHp$ events. None of these exclusive W^+W^- and Higgs boson generators support the case where one or both of the initial protons dissociate.

Produced via a mechanism similar to that for the exclusive W^+W^- signal, exclusive $\tau^+\tau^-$ production is an irreducible background when the two τ leptons decay to an $e^+\mu^\mp$ final state. Elastic $\gamma\gamma \rightarrow \tau^+\tau^-$, $\gamma\gamma \rightarrow \mu^+\mu^-$ and $\gamma\gamma \rightarrow e^+e^-$ backgrounds are generated using HERWIG++. Single- and double-dissociative $\gamma\gamma \rightarrow \mu^+\mu^-$ and $\gamma\gamma \rightarrow e^+e^-$ backgrounds are produced using LPAIR 4.0 [33], while PYTHIA 8 [34] is used to produce single-dissociative $\gamma\gamma \rightarrow \tau^+\tau^-$ candidates. Double-dissociative $\gamma\gamma \rightarrow \tau^+\tau^-$ samples are not available but their contribution is small. This paper refers to the τ processes described in this paragraph as the exclusive background. In the exclusive Higgs boson search, exclusive W^+W^- production is an additional background.

Inclusive W^+W^- production is a dominant background and has similar final states to the signal process, except that it is usually accompanied by additional charged particles from the underlying event. The inclusive W^+W^- background is the sum of nonresonant $q\bar{q} \rightarrow W^+W^-$ events, $gg \rightarrow W^+W^-$ events from nonresonant direct production, and resonant production and decay of the 125 GeV Higgs boson. The $q\bar{q} \rightarrow W^+W^-$ and $H \rightarrow W^+W^-$ samples are generated using the POWHEG-Box [35–39] generator (hereafter referred to as POWHEG) interfaced to PYTHIA8 (POWHEG+PYTHIA8) for parton showering, hadronization, and underlying-event simulation. The AU2 [40] parameter set (“tune”) is used for the underlying event. For the nonresonant $gg \rightarrow W^+W^-$ sample, the GG2WW [41] program is used and the showering, hadronization, and underlying event are simulated using HERWIG [42] and JIMMY [43], with the AUET2 [44] tune. The CT10 PDF set [45] is employed for all of these samples. The contribution from vector-boson fusion production of W^+W^- events, generated with SHERPA [46] with CT10 PDFs, is also included. In all regions of phase space, a normalization factor of 1.2 is applied to inclusive W^+W^- background as a correction to the cross-section as described in Section 8.3.

Other backgrounds such as W/Z +jets are easier to reject than inclusive W^+W^- production, because, in addition to being produced with extra charged particles, their final state topologies are also different. However, their contribution is non-negligible due to their several orders of magnitude higher cross-section. Both W/Z +jets processes are modeled with ALPGEN [47] interfaced to PYTHIA6 [48] (ALPGEN+PYTHIA6) using the CTEQ6L1 PDF set [49] and Perugia 2011C [50] tune. Diboson processes such as WZ and ZZ ² are also sources of background if exactly two charged lepton candidates are reconstructed and identified. The WZ and ZZ samples are generated using POWHEG+PYTHIA8 [51] with the AU2 tune and the CT10 PDF set. Other diboson processes ($W\gamma$ and $Z\gamma$) are also considered, but their contributions are found to be negligible. The POWHEG generator interfaced to PYTHIA6 with the CT10 PDF set is used to simulate $t\bar{t}$ background. Single-top-quark production through the t -channel is modeled with ACERMC [52] interfaced

² The symbol Z in WZ and ZZ is used here for both Z and γ^* production decaying to a lepton pair.

to PYTHIA6 with the CTEQ6L1 PDF set, while s -channel and Wt single-top-quark backgrounds are simulated using MC@NLO [53] interfaced to HERWIG and JIMMY with the CT10 PDF set and AUET2 tune. The underlying event AUET2B [44] tune is employed for the $t\bar{t}$ and t -channel single-top-quark backgrounds. A summary of the processes and simulation tools used in this paper are given in Table 1.

The same background samples are used for the exclusive Higgs boson search, except for Z +jets, which is modeled with ALPGEN interfaced to HERWIG and JIMMY (ALPGEN+HERWIG) and top-quark background whose contribution to the exclusive Higgs boson signal region is negligible. The CTEQ6L1 PDF set is employed for the ALPGEN+HERWIG Z +jets samples. Two more sets of Z +jets samples, generated using POWHEG+PYTHIA8 and SHERPA with CT10 PDF set, are used for additional background studies.

All the background samples mentioned above are processed through a simulation of the ATLAS detector [54] based on GEANT4 [55]. The signal samples are processed through the fast detector simulation program ATLFAS2 [56]. The effect of the multiple pp collisions, which is referred to as pileup throughout this paper, is also simulated by overlaying minimum-bias events generated using PYTHIA 8 and corrected to agree with data.

| Process | MC Generator |
|-----------------------------------------------------------------------------------------------------------|-----------------------------------------------|
| Exclusive W^+W^- signal | |
| $\gamma\gamma \rightarrow W^+W^- \rightarrow \ell^+\nu\ell'^-\bar{\nu}$ ($\ell, \ell' = e, \mu, \tau$) | HERWIG++ |
| aQGC signal | |
| $\gamma\gamma \rightarrow W^+W^- \rightarrow \ell^+\nu\ell'^-\bar{\nu}$ with $a_{0,C}^W/\Lambda^2 \neq 0$ | FPMC |
| Exclusive Higgs boson signal | |
| Exclusive $gg \rightarrow H \rightarrow W^+W^- \rightarrow \ell^+\nu\ell'^-\bar{\nu}$ | FPMC |
| Exclusive dilepton | |
| $\gamma\gamma \rightarrow \ell^+\ell^-$ ($\ell = e, \mu, \tau$) | HERWIG++, LPAIR, PYTHIA8 |
| Inclusive W^+W^- | |
| $W^+W^- \rightarrow \ell^+\nu\ell'^-\bar{\nu}$ ($\ell, \ell' = e, \mu, \tau$) | POWHEG+PYTHIA8, GG2WW+HERWIG |
| Inclusive $gg \rightarrow H \rightarrow W^+W^- \rightarrow \ell^+\nu\ell'^-\bar{\nu}$ | POWHEG+PYTHIA8 |
| Vector-boson fusion $W^+W^- \rightarrow \ell^+\nu\ell'^-\bar{\nu}$ | SHERPA |
| Non- W^+W^- diboson (Other- VV diboson) | |
| WZ, ZZ | POWHEG+PYTHIA8 |
| Other background | |
| W + jets | ALPGEN+PYTHIA6 |
| Z + jets | ALPGEN+PYTHIA6, ALPGEN+HERWIG |
| $t\bar{t}$, single top-quark, Wt | POWHEG+PYTHIA6, ACERMC+PYTHIA6, MC@NLO+HERWIG |

Table 1: A list of the simulated samples used for estimating the expected contributions to the exclusive W^+W^- signal region and exclusive Higgs boson signal region. The exclusive W^+W^- production is treated as background in the exclusive Higgs boson channel. Similarly, the exclusive Higgs boson production is a background to exclusive W^+W^- signal.

4 Selection of leptons, jets, and charged particles

Selection criteria are applied to the data and simulated samples to identify events that have good quality electron and muon candidates. Electron candidates are reconstructed from clusters of energy deposited

in the electromagnetic calorimeter that are matched to tracks in the inner detector. They are required to have transverse momentum $p_T > 10$ GeV, and be within a pseudorapidity range $|\eta| < 2.47$, excluding the region $1.37 \leq |\eta| \leq 1.52$. Also, they satisfy shower shape and track selection criteria that make up the “very tight” likelihood criteria [57] defined by a multivariate likelihood algorithm. Electrons are required to be isolated based on tracking and calorimeter information. Efficiencies for very tight electron identification range from 60% to 70%. Muon candidates with $p_T > 10$ GeV are reconstructed from tracks in the inner detector matched to tracks in the muon spectrometer. Muon candidates are required to be within a pseudorapidity range $|\eta| < 2.5$ and must satisfy the criteria outlined in Ref. [58], providing muon identification efficiencies of up to 95%. The tracking and calorimeter isolation criteria for muon and electron candidates are the same as those used in Ref. [59].

Jets with $|\eta| < 4.5$ are reconstructed from energy clusters in the calorimeter using the anti- k_t algorithm [60] with a radius parameter of 0.4. To suppress jets from pileup, only jets with $p_T > 25$ GeV are considered. Missing transverse momentum $\mathbf{p}_T^{\text{miss}}$ with magnitude E_T^{miss} is reconstructed as the magnitude of the negative vector sum of the momentum of reconstructed physics objects – e , μ , photons, and jets – and remaining calorimeter clusters that are not associated with any hard objects are also included with the proper calibration [61].

Charged particle tracks having $p_T > 0.4$ GeV and $|\eta| < 2.5$ reconstructed by the inner detector are used in this paper to reject nonexclusive production. They are required to leave at least one hit in the pixel detector and at least four hits in the silicon microstrip detector.

5 Exclusivity selection

Exclusive candidates are characterized by large rapidity gaps [62, 63] between the protons and the system of interest – a W^+W^- pair or Higgs boson. A signature for this, in the ATLAS detector, is an absence of tracks, other than tracks from the W^+W^- pair or Higgs boson decay products. Inclusive candidates, in contrast, are produced with extra particles that originate from the emission and hadronization of additional gluons, and the underlying event. These extra particles usually produce tracks in the inner detector. This analysis takes advantage of the absence of additional charged particle tracks to separate exclusive from inclusive (color processes) production.

In exclusive Higgs boson and W^+W^- production, no further charged particles are produced apart from the two final-state leptons. So in order to select exclusive events, the distance between the z_0 of the leptons is required to be less than 1 mm, where z_0 is the z -coordinate at the point of closest approach of a lepton (or track) to the beam line in the r - ϕ plane. Then the average z_0 of the two leptons, z_0^{av} , is taken as the event vertex and is referred to as the *lepton vertex*. In this paper, an *exclusivity selection* is applied, which requires zero additional tracks with $p_T > 0.4$ GeV near z_0^{av} with $|z_0^{\text{track}} - z_0^{\text{av}}| < \Delta z_0^{\text{iso}}$. To improve the efficiency for exclusive events whose leptons have more than one associated track (due to bremsstrahlung for example), candidate tracks considered for this selection are required to be unmatched to either of the final-state leptons. Therefore, a candidate track within an angular distance $\Delta R < 0.01$ and within 1 mm in z_0 of either of the final-state leptons is considered matched and is ignored. The value Δz_0^{iso} is optimized using exclusive Higgs boson and exclusive W^+W^- simulated samples. A value of $\Delta z_0^{\text{iso}} = 1$ mm is chosen for all results in this paper. The exclusivity selection efficiency is found to be 58% and is largely process independent as is discussed in Section 8.1. In Fig. 3 the exclusivity efficiency is extracted from exclusive Higgs boson signal simulated by FPMC, plotted against the average number of interactions per beam crossing μ . For the dataset used in this study $\langle \mu \rangle$ is 20.7.

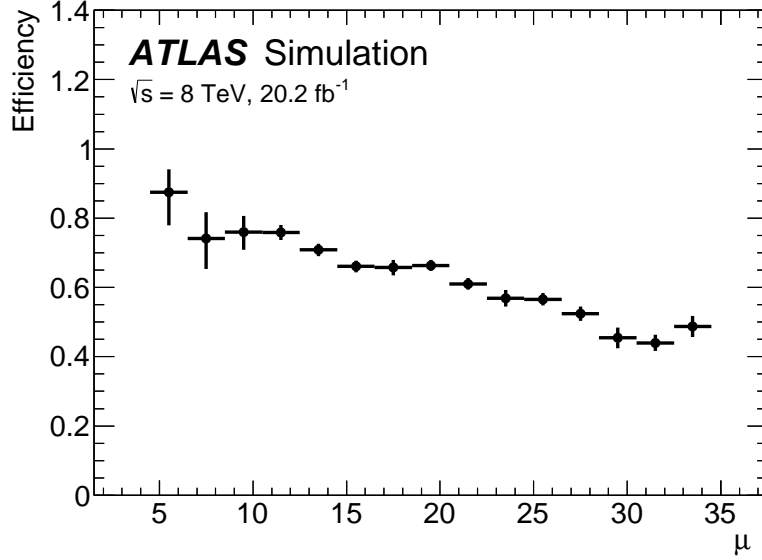


Figure 3: Efficiency of the exclusivity selection, extracted from the exclusive Higgs boson signal simulation, is plotted against the average number of interactions per beam crossing μ . The average is 20.7 for the current dataset.

6 Event selection

Events are required to satisfy at least one of the single- and dilepton triggers in Table 2. They are further categorized into ee , $\mu\mu$, and $e\mu$ final states. A combination of single-lepton and different-flavor dilepton triggers is used to select the signal events, while the same-flavor dilepton triggers are used to select ee and $\mu\mu$ events for validation and control regions.

For both the exclusive W^+W^- and Higgs boson channels, this analysis selects candidates consistent with leptonic decays of W -boson pairs into oppositely charged different-flavor leptons. Additional kinematic requirements reject background while retaining as much of the signal as possible. Exclusive W^+W^- production is a large background in the exclusive Higgs boson search, while the exclusive Higgs boson contribution to the exclusive W^+W^- signal is negligible. So the kinematic requirements for the two channels differ slightly. Table 3 summarizes the selection criteria for both channels.

| Trigger | Lepton p_T criteria [GeV] |
|----------------------|-----------------------------------|
| Single electron | $p_T^e > 24$ |
| Single muon | $p_T^\mu > 24$ |
| Symmetric dielectron | $p_T^{e1} > 12, p_T^{e2} > 12$ |
| Asymmetric dimuon | $p_T^{\mu1} > 18, p_T^{\mu2} > 8$ |
| Electron-muon | $p_T^e > 12, p_T^\mu > 8$ |

Table 2: Single-lepton and dilepton triggers are used to select event candidates. Single-lepton triggers require either of the leptons to satisfy the specified p_T criterion, while dilepton triggers have two specific p_T criteria.

6.1 Exclusive W^+W^- candidate selection

For the exclusive W^+W^- channel, requiring oppositely charged $e^\pm\mu^\mp$ leptons rejects same-flavor lepton events from Drell-Yan and exclusive dilepton processes. The invariant mass of the dilepton system is required to be greater than 20 GeV. This rejects a significant fraction of the remaining background in which jets have non-prompt or fake electron and/or muon signatures. The lepton with the higher p_T is referred to as the leading lepton ($\ell 1$) and the other, the subleading lepton ($\ell 2$). The p_T requirement on the leading lepton is chosen to be higher than the single-lepton trigger threshold, resulting in different leading and subleading leptons requirements: $p_T^{\ell 1} > 25$ GeV and $p_T^{\ell 2} > 20$ GeV, respectively. These selection criteria define *preselection*.

To reduce $\gamma\gamma \rightarrow \tau^+\tau^-$ and $Z/\gamma^* \rightarrow \tau^+\tau^-$ contamination, the magnitude of the transverse momentum of the dilepton system ($p_T^{e\mu}$) is required to be greater than 30 GeV. The exclusivity requirement rejects most of the remaining inclusive background. After applying these selection criteria, 70% of the predicted background is due to inclusive W^+W^- production, while $\gamma\gamma \rightarrow \tau^+\tau^-$ contributes 15% and the contributions from other categories are negligible.

The limits on aQGCs are extracted from the region with $p_T^{e\mu} > 120$ GeV. This requirement considerably reduces the SM contribution.

6.2 Exclusive Higgs Boson candidate selection

The Higgs boson decays to W^+W^- give one on-shell and one off-shell W boson. Thus the subleading lepton minimum p_T is lowered to 15 GeV. For the same reason, the $m_{e\mu}$ threshold is lowered to 10 GeV. The other requirements in the preselection are the same as for the exclusive W^+W^- sample. In contrast to the W^+W^- topology, the zero spin of the Higgs boson implies that the final-state leptons have small angular separation. Therefore the angular separation of the leptons in the transverse plane ($\Delta\phi_{e\mu}$) and the dilepton mass ($m_{e\mu}$) are two good discriminating variables against the remaining exclusive W^+W^- background, which has a wider angular separation and relatively higher dilepton mass. Thus, $m_{e\mu}$ and $\Delta\phi_{e\mu}$ selection criteria are further imposed in the Higgs boson search. The transverse mass of the Higgs boson system, m_T , is defined as:

$$m_T = \sqrt{(E_T^{e\mu} + E_T^{\text{miss}})^2 - |\mathbf{p}_T^{e\mu} + \mathbf{p}_T^{\text{miss}}|^2}, \quad (5)$$

where $E_T^{e\mu} = \sqrt{|\mathbf{p}_T^{e\mu}|^2 + m_{e\mu}^2}$ and $|\mathbf{p}_T^{\text{miss}}| = E_T^{\text{miss}}$. Requiring $m_T < 140$ GeV further reduces both the inclusive and exclusive W^+W^- backgrounds and improves the signal significance by 20% (see Fig. 15). The exclusivity selection uses $\Delta z_0^{\text{iso}} = 1$ mm here as well.

7 Pileup and exclusivity validation with $\gamma\gamma \rightarrow \ell^+\ell^-$ events

The selection strategy described in Section 5 represents a new approach to extract exclusive processes without using usual vertex reconstruction [64]. This section describes two studies designed to validate this technique. The first one demonstrates how the Δz_0^{iso} selection gives results comparable to those of previous strategies employed by the ATLAS Collaboration in a related measurement at $\sqrt{s} = 7$ TeV [65], and the second one shows how simulation of pileup and modeling of underlying event activity are verified.

| | W^+W^- selection | Higgs boson selection |
|---------------------|-----------------------------------------------------|-----------------------------------------------------|
| <i>Preselection</i> | Oppositely charged $e\mu$ final states | |
| | $p_T^{\ell^1} > 25$ GeV and $p_T^{\ell^2} > 20$ GeV | $p_T^{\ell^1} > 25$ GeV and $p_T^{\ell^2} > 15$ GeV |
| | $m_{e\mu} > 20$ GeV | $m_{e\mu} > 10$ GeV |
| | $p_T^{e\mu} > 30$ GeV | |
| | Exclusivity selection, Δz_0^{iso} | |
| aQGC signal | $p_T^{e\mu} > 120$ GeV | – |
| Spin-0 Higgs boson | – | $m_{e\mu} < 55$ GeV |
| | – | $\Delta\phi_{e\mu} < 1.8$ |
| | – | $m_T < 140$ GeV |

Table 3: Selection criteria for the two analysis channels.

Except for possible non-standard couplings, the exclusive production of W^+W^- and $\ell^+\ell^-$ are similar. Exclusive dilepton candidates are therefore used in both studies because elastic $\gamma\gamma \rightarrow \ell^+\ell^-$ production can be separated from SD and DD production using dilepton transverse momentum, $p_T^{\ell\ell}$, and acoplanarity ($1 - |\Delta\phi_{\ell\ell}|/\pi$) of the dilepton system, where $\Delta\phi_{\ell\ell}$ is the dilepton azimuthal separation. The $\gamma\gamma \rightarrow \mu^+\mu^-$ candidates are used for these studies while $\gamma\gamma \rightarrow e^+e^-$ candidates are used for cross-checks.

First, a measurement is made of the correction factor, f_{EL} , defined as the ratio of observed elastic $\gamma\gamma \rightarrow \mu^+\mu^-$ candidates to the HERWIG++ prediction based on the EPA formalism. This factor is expected to be lower than 1.0 due to the finite size effects of the proton [66]. Alternative formulations give similar results [67]. Candidates are required to have two muons with $p_T^\mu > 20$ GeV, invariant mass $45 < m_{\mu\mu} < 75$ GeV or $m_{\mu\mu} > 105$ GeV and pass the exclusivity selection ($\Delta z_0^{\text{iso}} = 1$ mm). The Drell-Yan $Z/\gamma^* \rightarrow \mu^+\mu^-$ process is the dominant background while contributions from other backgrounds are negligible. The elastic $\gamma\gamma \rightarrow \mu^+\mu^-$ signal is enhanced by selecting the low- $p_T^{\ell\ell}$ region with an upper limit on $p_T^{\ell\ell}$ varied between 3 GeV to 5 GeV to study systematic uncertainties.

The value of f_{EL} is extracted from template fits in acoplanarity. Some of the contributing processes have similar acoplanarity shapes; in particular the Drell-Yan and DD backgrounds are not distinguishable. Two fitting strategies are pursued. The first template strategy attempts to distinguish three shapes: elastic, SD, and combined DD plus background. The relative weighting of DD and background is varied to estimate the associated systematic uncertainty. The second template strategy uses the elastic and combined SD and DD shapes, with the background yield constrained to the simulation's prediction. These two fitting strategies give consistent results and are stable at the level of 10% under the variation of $p_T^{\mu\mu}$ and Δz_0^{iso} selections, the four different Drell-Yan generators, bin width, and fit range. These variations reflect mis-modeling of $p_T^{\mu\mu}$ and systematic uncertainties related to shape correlations and signal strength. The effect of these variations is much larger than the 3% combined effect of the systematic uncertainties discussed in Ref. [65], which can then be ignored. The best-fit value is $f_{\text{EL}} = 0.76 \pm 0.04(\text{stat.}) \pm 0.07(\text{sys.})$, where the systematic uncertainty covers the spread of fit values, and Fig. 4 shows the acoplanarity distribution compared to SM expectation normalized by the factors determined in this fit. An additional uncertainty of 10% related to pileup is discussed in the following paragraph. A similar study using $\gamma\gamma \rightarrow e^+e^-$ candidates yields a consistent correction factor but with lower precision; thus the final value for f_{EL} is

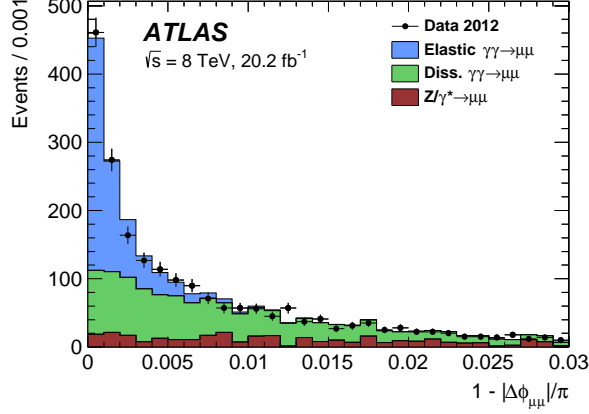


Figure 4: Dimuon acoplanarity distributions after applying the exclusivity selection and requiring $p_T^{\mu\mu} < 3$ GeV. The expected Drell-Yan shape and the elastic and combined SD and DD (Dissociative) shapes normalized from the fit are stacked. This fit determines the factor f_{EL} .

taken from the $\gamma\gamma \rightarrow \mu^+\mu^-$ sample. This correction factor is used to correct the number of $\gamma\gamma \rightarrow \tau^+\tau^-$ candidates predicted by simulation in both the exclusive W^+W^- and the exclusive Higgs boson signal regions. Similar suppression is expected [66] and observed [65] in dissociative events, so the f_{EL} factor is applied to dissociative events as well.

In the second study, the impact of pileup on the signal efficiency and accuracy of the modeling in the simulation is evaluated. A kinematic selection is defined to enhance the fraction of elastic events. Events with $p_T^{\mu\mu} < 3$ GeV and acoplanarity < 0.0015 are studied with both the nominal exclusivity selection criteria and by demanding exactly one extra track within $\Delta z_0^{\text{iso}} = 3$ mm. In the case of exclusive signal, when there is one extra track, the extra track is from pileup and its $\Delta z_0 = |z_0^{\text{track}} - z_0^{\text{av}}|$ has a locally constant distribution while for any inclusive background the track originates from the same vertex and the Δz_0 distribution peaks at zero as can be seen in Fig. 5. A normalization factor, the background-subtracted ratio of observed exclusive events to the predicted sum of elastic, SD, and DD is determined for both selections. For nominal (zero track) exclusivity this normalization factor is $0.73 \pm 0.03(\text{stat.}) \pm 0.01(\text{sys.})$. The one-track selection, illustrated in Fig. 5, gives a factor of $0.70 \pm 0.06(\text{stat.}) \pm 0.03(\text{sys.})$ where the systematic uncertainties result from the uncertainty in the background normalization factor. The zero-track and one-track normalization factors are consistent at the level of 10%, which is taken to be a measure of the accuracy of the pileup simulation in predicting signal efficiency.

The value of f_{EL} with the additional $\pm 10\%$ relative systematic uncertainty for signal efficiency added in quadrature with the previous systematic uncertainty

$$f_{\text{EL}} = 0.76 \pm 0.04(\text{stat.}) \pm 0.10(\text{sys.}) \quad (6)$$

is consistent with the value of $0.791 \pm 0.041(\text{stat.}) \pm 0.026(\text{sys.}) \pm 0.013(\text{theory})$ obtained in an earlier analysis using data from pp collisions at $\sqrt{s} = 7$ TeV [65]. This value is also consistent with the theoretical estimate of $f_{\text{EL}} \sim 0.73\text{--}0.75$, related to the proton size effects in the probed region of dimuon mass [66].

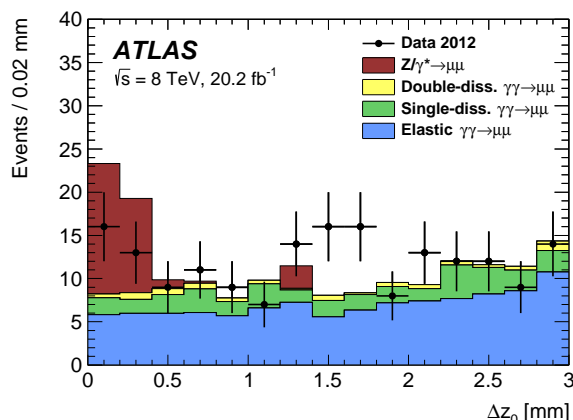


Figure 5: Absolute Δz_0 of the extra track to the lepton vertex in the region defined by acoplanarity < 0.0015 . The exclusivity requirement was changed to select exactly one extra track within 3 mm. The exclusive predictions are scaled by a factor of 0.70.

8 Signal and background control regions

Several control regions are established to use data events to cross-check simulations in areas where they are known to be less reliable. The ratio of elastic to dissociative contributions is extracted from one control region, since a simulation for $\gamma\gamma \rightarrow W^+W^-$ dissociative events is not available. Another set of control regions is used to study the proximity of small numbers of extra tracks to the lepton vertex. This is another regime where the underlying-event models have not been thoroughly tested, so relying on the data is preferred. Finally a control region is established for inclusive W^+W^- production, a predominant background. This control region has a different exclusivity requirement, one to four extra tracks, in order to increase the fraction of inclusive W^+W^- events. The inclusive W^+W^- contribution to the exclusive W^+W^- signal region is estimated using a data-driven method. Based on the number of events observed in this control region, this method makes some assumptions about the rejection of background when going from the control (one to four tracks) to the nominal (zero tracks) exclusivity requirement, and derives an estimate for the background from inclusive W^+W^- , Drell-Yan, W +jets, and top-quark production. The latter three processes have collectively a smaller contribution and are referred to as *other background*. Other contributions to the background are derived from Monte Carlo simulation and are found to be negligible.

8.1 Single-dissociative and double-dissociative contributions

Without detecting the outgoing protons, the elastic $\gamma\gamma \rightarrow W^+W^-$ events are indistinguishable from SD and DD candidates. However, simulations are only available for the elastic $\gamma\gamma \rightarrow W^+W^-$ process; predictions for dissociative production of W^+W^- are not available. Following the strategy in Ref. [68] a normalization factor, f_γ , is determined. This factor is used to correct the prediction for elastic $\gamma\gamma \rightarrow W^+W^-$ to account for dissociative events. It is computed from data using $\gamma\gamma \rightarrow \mu^+\mu^-$ candidates that satisfy the exclusivity selection with $\Delta z_0^{\text{iso}} = 1$ mm, $p_T^\mu > 20$ GeV and $m_{\mu\mu} > 160$ GeV ($\sim 2m_W$). The factor f_γ is defined as the

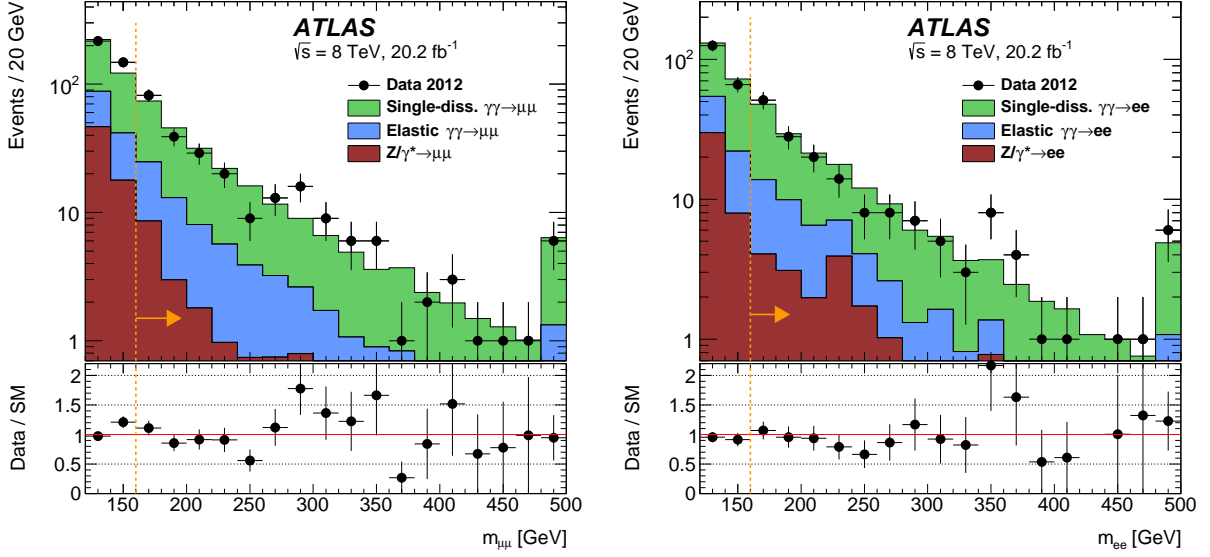


Figure 6: The dilepton invariant mass distribution for muon candidates (left) and electron candidates (right). The elastic yield is scaled by $f_{\text{EL}} = 0.76$ and the SD distribution is scaled to bring the sum of the elastic and SD contributions to the HERWIG++ prediction for the elastic process multiplied by the f_γ factor in the mass region above 160 GeV. The last bin includes overflow.

ratio of observed dimuons in data to the HERWIG++ prediction for elastic dimuon production:

$$f_\gamma = \frac{N_{\text{Data}} - N_{\text{Background}}^{\text{POWHEG}}}{N_{\text{Elastic}}^{\text{HERWIG++}}} \Big|_{m_{\mu\mu} > 160 \text{ GeV}} = 3.30 \pm 0.22(\text{stat.}) \pm 0.06(\text{sys.}), \quad (7)$$

where N_{Data} is the number of candidates in the data, $N_{\text{Background}}^{\text{POWHEG}}$ is the expected number of background events, and $N_{\text{Elastic}}^{\text{HERWIG++}}$ is the expected number of elastic $\gamma\gamma \rightarrow \mu^+\mu^-$ candidates directly from HERWIG++, i.e., the unscaled EPA prediction. Drell-Yan processes are the main sources of background, whereas inclusive and exclusive W^+W^- processes contribute less than 10%. The uncertainty is predominantly statistical, but also contains a systematic component estimated by varying the POWHEG+PYTHIA8 Drell-Yan correction factor by $\pm 20\%$, as is discussed in Section 8.2. Predictions for this ratio are becoming available [69].

The dilepton invariant mass distributions for the $\mu^+\mu^-$ and e^+e^- final states are shown in Fig. 6. The elastic contribution is scaled by $f_{\text{EL}} = 0.76$ and the SD contribution is normalized so that the sum of the elastic and SD contributions corresponds to $f_\gamma \times N_{\text{Elastic}}^{\text{HERWIG++}}$. The shapes of the SD and DD samples are quite similar, so the SD shape is used to describe both the SD and DD processes. The data are well described by the simulation over the full mass range. While the range of $m_{\ell\ell} > 160$ GeV was chosen to correspond to the threshold $m_{WW} > 2m_W$, the value of f_γ is in fact rather insensitive to the choice of this threshold. The W^+W^- sample tends to have higher m_{WW} than these dilepton control samples $m_{\ell\ell}$. The m_{ee} distribution in Fig. 6 shows that f_γ is also valid for the electron channel. Therefore, the total expected $\gamma\gamma \rightarrow W^+W^-$ event yield in both the exclusive W^+W^- and the exclusive Higgs boson channels is taken to be the product of f_γ times the HERWIG++ prediction for elastic $\gamma\gamma \rightarrow W^+W^-$ production.

The dimuon signal sample with mass above 160 GeV is also used to determine the signal efficiency for

exclusivity, which is 0.58 ± 0.06 where the 10% uncertainty arises from pileup modeling as described in Section 7. Other signal samples give compatible results.

8.2 Track multiplicity modeling

In pp collisions, inclusive Drell-Yan, W^+W^- , $t\bar{t}$, and many other events are initiated by quarks or gluons. Through hard radiation and the accompanying underlying event, such events are produced with several additional charged particles. The exclusivity selection is designed to reject such inclusive candidates that have additional tracks near the dilepton vertex. To estimate inclusive backgrounds from Drell-Yan production of $\tau^+\tau^-$ and inclusive W^+W^- production, the track multiplicity modeling of low-multiplicity candidates is studied with a high-purity Z boson sample and scaled with appropriate correction factors.

Drell-Yan candidates are selected by requiring exactly two muons with $p_T^\mu > 20$ GeV and $|\eta| < 2.4$, and satisfying $m_{\mu\mu} > 45$ GeV. The Z -resonance region, $80 < m_{\mu\mu} < 100$ GeV, is used to measure the efficiency of the exclusivity selection in both the data and simulation. The contributions from non- Z processes are subtracted before and after the exclusivity selection for both the data and simulated samples. This non- Z contribution is estimated from the sideband regions $70 < m_{\mu\mu} < 80$ GeV and $100 < m_{\mu\mu} < 110$ GeV. The efficiency of the exclusivity selection for inclusive Z events in data is found to be 0.004. This was compared to efficiencies for simulated Drell-Yan samples from four generators: ALPGEN+PYTHIA6, ALPGEN+HERWIG, POWHEG+PYTHIA8, and SHERPA. In general, the exclusivity criterion rejects more $Z/\gamma \rightarrow \mu^+\mu^-$ candidates in the data than in the simulation. The study was repeated for events with one to four additional tracks.

Correction factors are defined as the ratio of the exclusivity selection efficiency in data to the one in the simulation. They are reported in Table 4 and denoted by $f_{n\text{Tracks}}^{\text{sim}}$, where sim is P for POWHEG+PYTHIA8, AH for ALPGEN+HERWIG, and AP for ALPGEN+PYTHIA6, and $n\text{Tracks}$ is the number of additional tracks. These correction factors are used to scale the Monte Carlo prediction for the inclusive processes considered in the paper. The background event tuning for simulation of low multiplicity in 8 TeV data is seen to vary widely.

The uncertainties in these correction factors are estimated from the variation of the exclusive efficiency as a function of $m_{\mu\mu}$ of the various generators. To check the consistency of the predictions of evolution of underlying event multiplicity as a function of mass, ratios of the predictions of the three generators to the one by SHERPA are listed in Table 5. These are normalized such that the average over the full mass range is 1. The variations are typically within 20%, which is taken as the systematic uncertainty in extrapolating the $f_{n\text{Tracks}}^{\text{sim}}$ correction factors.

| Number of extra tracks | POWHEG+PYTHIA8 f_n^{P} | ALPGEN+HERWIG f_n^{AH} | ALPGEN+PYTHIA6 f_n^{AP} |
|------------------------|---------------------------------|---------------------------------|----------------------------------|
| $n = 0$ | 0.58 | 0.21 | 0.69 |
| $n = 1-4$ | 0.88 | 0.39 | 0.85 |

Table 4: Ratio of exclusivity efficiencies for $Z \rightarrow \mu\mu$ production in data and simulation for different generators after sideband subtraction of nonresonant contributions. The efficiency ratios $f_{n\text{Tracks}}^{\text{sim}}$ are shown for exclusive selection ($n = 0$) as well as for a relaxed selection with one to four additional tracks ($n = 1-4$).

| Mass [GeV] | ALPGEN+HERWIG | ALPGEN+PYTHIA6 | POWHEG+PYTHIA8 |
|-------------|-----------------|-----------------|-----------------|
| 44–60 | 0.81 ± 0.02 | 0.84 ± 0.03 | 0.99 ± 0.09 |
| 60–90 | 1.04 ± 0.02 | 0.98 ± 0.03 | 1.01 ± 0.02 |
| 90–116 | 1.00 ± 0.01 | 1.02 ± 0.02 | 1.00 ± 0.02 |
| 116–200 | 0.89 ± 0.10 | 1.04 ± 0.19 | 0.76 ± 0.10 |

Table 5: Ratio of the exclusivity selection efficiency in Drell-Yan $\mu^+\mu^-$ production as a function of dimuon mass of different generators to SHERPA. A common normalization factor is applied to each column to obtain an average ratio of 1. Only statistical uncertainties are shown. The statistical uncertainty from SHERPA is included and contributes 2.9%, 0.8%, 0.7% and 5.7% in the four mass regions.

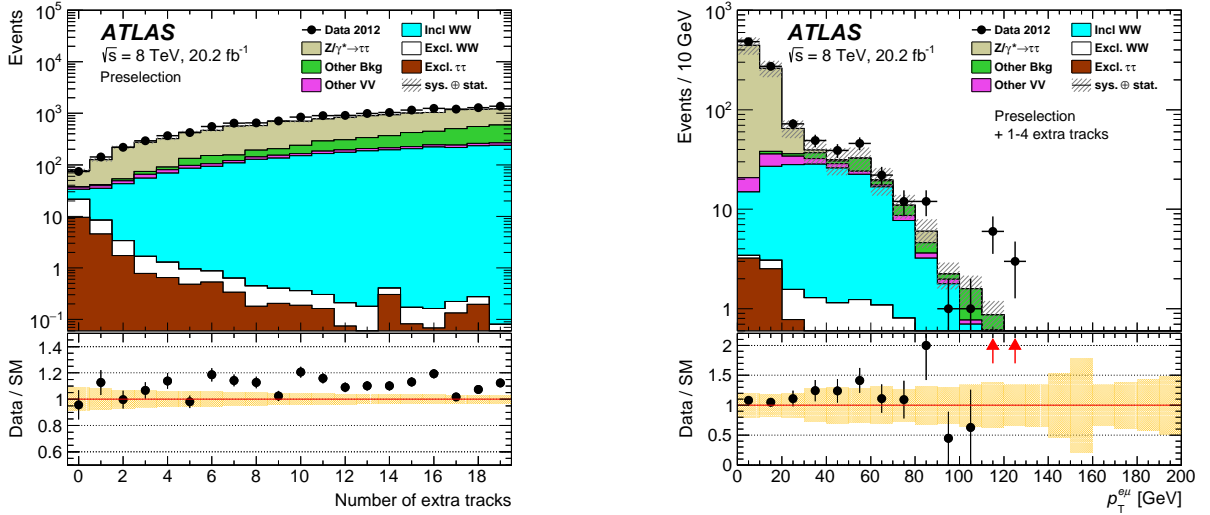


Figure 7: Distribution of track multiplicities after requiring the exclusive W^+W^- preselection (left) with no number of track dependent correction, and the $p_T^{e\mu}$ distribution of candidates that have 1–4 extra tracks (right), with the simulation including all appropriate correction factors such as $f_{nTracks}^{sim}$ (Table 4) for Drell-Yan and inclusive W^+W^- production. The enriched inclusive W^+W^- control region is the 1–4 extra-track region above $p_T^{e\mu} > 30$ GeV. The band around the Data/SM ratio of one illustrates the systemic uncertainties. The upward red arrows indicate ratios outside the plotting range.

To validate the correction factors $f_{nTracks}^{sim}$, an $e^\pm\mu^\mp$ sample was defined. Figure 7 (left) shows the distribution of the number of additional tracks after applying the W^+W^- preselection as defined in Table 3. Applying a relaxed exclusivity selection to select $e^\pm\mu^\mp$ candidates with one to four extra tracks yields a sample that has low enough statistical uncertainties and is dominated by Drell-Yan events for $p_T^{e\mu} < 30$ GeV as illustrated in Fig. 7 (right). Selecting $m_{e\mu} < 90$ GeV further rejects non Drell-Yan contamination as shown in Fig. 8. The correction factor for ALPGEN+PYTHIA6 Drell-Yan, computed in the region defined by $p_T^{e\mu} < 30$ GeV and $m_{e\mu} < 90$ GeV, is found to be 0.90 ± 0.11 , in good agreement with $f_{1-4}^{AP} = 0.85$ found above for $Z \rightarrow \mu^+\mu^-$.

8.3 Inclusive W^+W^- normalization

Inclusive W^+W^- production is a significant background in both the exclusive Higgs boson and exclusive W^+W^- channels. From previous measurements [59, 70], it is known that the NLO prediction for the

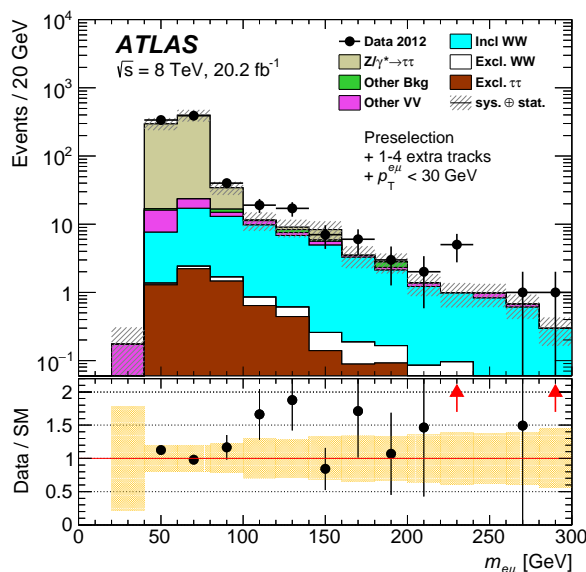


Figure 8: The $m_{e\mu}$ distribution after requiring 1–4 extra tracks within $\Delta z_0^{\text{iso}} = 1.0$ mm and $p_T^{e\mu} < 30$ GeV. The Drell-Yan and inclusive W^+W^- samples are scaled by the factors f_{1-4}^{AP} and f_{1-4}^{P} , respectively. The other samples are normalized as mentioned in the text. In the Data/SM ratio plot, the color band illustrates the systematic uncertainties, the red upward arrows indicate ratios outside the plotting range.

$q\bar{q} \rightarrow W^+W^-$ process as provided by POWHEG+PYTHIA8 underestimates the observed W^+W^- event yield. It is therefore necessary to understand the simulation of this background before requiring the exclusivity selection. A region close in phase space to the exclusive Higgs boson signal region is chosen, referred to here as the Higgs-specific inclusive W^+W^- control region. It has the same definition except: $55 < m_{e\mu} < 110$ GeV, $\Delta\phi_{e\mu} < 2.6$ to reduce Drell-Yan background, no jets to reduce $t\bar{t}$ background, and no requirement on exclusivity. This region is dominated by inclusive W^+W^- production and has a purity of 60%. After subtracting the predicted backgrounds from data, $(20 \pm 5)\%$ more data is observed than is predicted by POWHEG+PYTHIA8. A normalization factor of $1.20 \pm 0.05(\text{stat.})$ is therefore taken as a correction to the cross-section and applied to the inclusive W^+W^- prediction in all regions of phase space studied here, as done in Ref. [59]. The transverse mass m_T distributions in the Higgs-specific inclusive W^+W^- control region after applying the normalization factor to the POWHEG+PYTHIA8 prediction is shown in Fig. 9.

8.4 Sum of inclusive W^+W^- and other background

An estimate of the sum of inclusive W^+W^- background and smaller contributions from Drell-Yan, W +jets, and top-quark production (collectively referred to as other background) is performed using an inclusive W^+W^- -enriched control region defined with the same criteria as the exclusive W^+W^- signal region, except the exclusivity selection requires 1–4 extra tracks within $\Delta z_0^{\text{iso}} = 1$ mm. This control region is shown in Fig. 7 (right) in the region above $p_T^{e\mu} > 30$ GeV. It is dominated by the inclusive W^+W^- process and also has small contributions of exclusive events, non- W^+W^- (other-VV) dibosons, and other background.

Figure 10 shows the leading lepton $p_T^{\ell 1}$ distribution in this control region. The prediction is systematically lower than the data. The processes contributing to this control region can be found in Table 6, and the

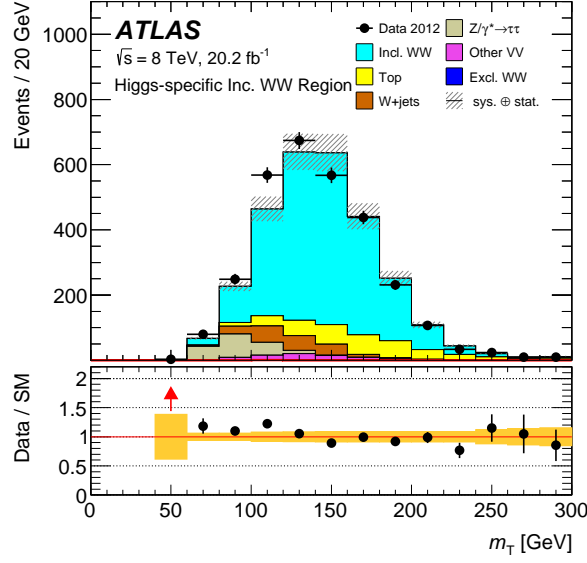


Figure 9: The m_T distributions in the Higgs-specific inclusive W^+W^- control region that is used to determine the scaling for the POWHEG+PYTHIA8 inclusive W^+W^- prediction. In the Data/SM ratio plot, the color band illustrates systematic uncertainties, the red upward arrow indicates a ratio outside the plotting range.

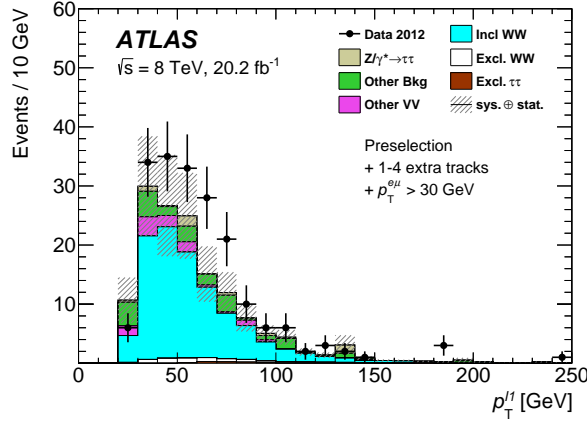


Figure 10: The leading-lepton p_T^{l1} distribution in the inclusive W^+W^- control region. The simulation includes all appropriate correction factors such as f_{1-4}^{sim} for Drell-Yan and f_{1-4}^P for inclusive W^+W^- production.

total SM expectation is compared to the data. The data exceeds the simulation by 2σ . This discrepancy is attributed to a component from jets faking leptons that is unreliably simulated. Events produced with jets such as W +jets, Z +jets, and top-quark production, particularly jets faking leptons, are more easily rejected by the exclusivity selection, while other- VV and Drell-Yan (without accompanying jets) processes are likely to extrapolate from the 1–4 extra-track control region to the zero-track region with a scale factor similar to that for inclusive W^+W^- background. Therefore, this control region is used to constrain the inclusive W^+W^- plus other background involving fake leptons.

For the purpose of estimating the contribution of inclusive W^+W^- events and other background in the zero-track region, the number of these events in the 1–4 extra-track control region is bracketed by the

| Processes | Inclusive W^+W^- |
|--------------------------|--------------------|
| Inclusive W^+W^- | 102 ± 20 |
| Exclusive W^+W^- | 5.5 ± 0.4 |
| Exclusive $\tau^+\tau^-$ | 1.2 ± 0.2 |
| Other diboson | 10.9 ± 2.2 |
| Other background | 27.4 ± 6.2 |
| Total SM | 147 ± 21 |
| Data | 191 |

Table 6: Event yields in the inclusive W^+W^- control region. The uncertainties quoted are statistical and systematic.

number of observed events in the data, after subtracting the exclusive and other- VV contributions, as an upper bound and by the predicted number of inclusive W^+W^- obtained from POWHEG+PYTHIA8 as a lower bound. To obtain the contribution for the exclusive W^+W^- signal region, the two estimates are extrapolated from the 1–4 extra-track control region to the zero-track signal region. In this framework, the lower bound corresponds to the optimistic case where the other background contribution is completely rejected by the zero-track exclusivity requirement, while the upper bound corresponds to the case where all observed candidates in the control region are suppressed by the same factor as the inclusive W^+W^- process. Finally the average of the two estimates (after extrapolation) is taken as the contribution for the signal region.

The extrapolation is achieved by multiplying the estimates by the ratio of the predicted numbers of inclusive W^+W^- events:

$$N_0^{\text{Estimated}} = N_{1-4}^{\text{Estimated}} \times \frac{N_{WW,0}^{\text{Predicted}}}{N_{WW,1-4}^{\text{Predicted}}}, \quad (8)$$

where $N_0^{\text{Estimated}}$ and $N_{1-4}^{\text{Estimated}}$ are the estimates for the lower bound or upper bound mentioned above, and $N_{WW,0}^{\text{Predicted}}$ and $N_{WW,1-4}^{\text{Predicted}}$ are respectively the number of inclusive W^+W^- events predicted by POWHEG+PYTHIA8 for the zero-track and 1–4 extra-track regions. This ratio is found to be 0.048 ± 0.014 , where the uncertainty is dominated by the 20% systematic uncertainties taken to be uncorrelated between the f_0^{P} and f_{1-4}^{P} factors that are included in the predicted numbers of events. As mentioned above, the small exclusive and other- VV contributions are subtracted before the extrapolation. So for inclusive W^+W^- and Drell-Yan processes, the expected number of events in the zero-track region is 20 times less than the prediction for the 1–4 extra-track control region.

As mentioned above, the inclusive W^+W^- and other background contributions to the signal region are taken as the average of the two estimates. Half the difference is included as an additional contribution to the uncertainty in this determination. This results in a final estimate of 6.6 ± 2.5 background candidates for the exclusive W^+W^- signal region.

This background estimate, 6.6 ± 2.5 events in the exclusive W^+W^- signal region, corresponds to scaling the POWHEG+PYTHIA8 W^+W^- prediction by a normalization factor of 0.79. This factor is used to estimate the inclusive W^+W^- and other background contamination in the Higgs boson and aQGC signal regions.

| Source of uncertainty | Uncertainty [%] |
|-------------------------------|-----------------|
| Statistics | 33% |
| Background determination | 18% |
| Exclusivity signal efficiency | 10% |
| All other | < 5% |
| Total | 39% |

Table 7: Sources of uncertainty for the measured exclusive W^+W^- cross-section. All other includes other efficiencies, acceptance, luminosity, and lepton scales and resolution.

9 Systematic uncertainties

The main sources of systematic uncertainty are related to the exclusivity selection and the background determination. The uncertainty in the efficiency of the exclusive signal selection contributes 10% to the exclusive W^+W^- and Higgs boson signal yields, as estimated in Section 7 from the ratios of dimuon event yields without extra tracks and those with exactly one extra track. The prediction of the exclusive W^+W^- process uses the f_γ factor as described in Section 8.1 and thus carries the 7% uncertainty in f_γ . The $\gamma\gamma \rightarrow \tau^+\tau^-$ background has an uncertainty of 14% that is propagated from the f_{EL} factor. As described in Section 7, the f_{EL} uncertainty includes 10% related to the exclusive signal selection and another 10% that results from acoplanarity fits. There is a 38% uncertainty in the inclusive W^+W^- background, as discussed in Section 8.4. This 38% uncertainty contains a component from the $\pm 20\%$ uncertainty in Drell-Yan background described in Section 8.2.

The contributions from these systematic uncertainties to the measured exclusive W^+W^- cross-section can be found in Table 7. The overall background contribution is 18%, predominantly from uncertainty in the extrapolation from the 1–4 track control region. In addition to the systematic uncertainty from the exclusivity selection (10%), other systematic uncertainties (lepton selection efficiencies and acceptance, luminosity and lepton scales and resolution) contribute less than 5%. The statistical uncertainty dominates the uncertainties in the cross-section.

10 Results

This paper presents three main results: the exclusive W^+W^- production cross-section, limits on possible aQGCs, and a limit from a search for exclusive Higgs boson production. Each is summarized in the following. The exclusive W^+W^- signal is the sum of elastic and single- and double-dissociative events through the f_γ factor discussed in Section 8.1.

10.1 Standard Model exclusive W^+W^- production

Before the exclusivity selection, good agreement between data and background prediction is observed. In the $e\mu$ final state, the overall event yield agrees to within 2% and after requiring $p_{\text{T}}^{e\mu} > 30$ GeV it agrees to within 0.5%. The $p_{\text{T}}^{e\mu}$ distribution before the exclusivity requirement is shown in Fig. 11.

The numbers of candidates at various stages of the analysis are listed in Table 8 and the uncertainties quoted include both the statistical and systematic uncertainties. Top-quark and Drell-Yan $Z/\gamma^* \rightarrow \tau^+\tau^-$

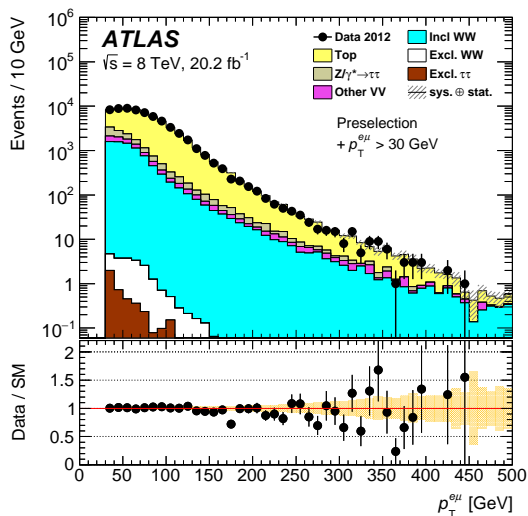


Figure 11: The $p_T^{e\mu}$ distribution before exclusivity, i.e., after requiring $p_T^{e\mu} > 30$ GeV. The main backgrounds at this stage are top-quark production, inclusive W^+W^- and Drell-Yan. In the Data/SM ratio plot, the color band illustrates systematic uncertainties.

processes are the dominant backgrounds before exclusivity, while after requiring exclusivity their contributions are less than 0.5 events. These two backgrounds along with W +jets are grouped together as other background (Table 8). The inclusive W^+W^- estimate (described in Section 8.4) already includes these three processes; thus the other background contribution after requiring exclusivity is not added to the total background. Non- W^+W^- (other- VV) diboson processes are also highly suppressed by the exclusivity selection: they contribute 0.3 ± 0.2 events. Diffractive W^+W^- production was considered as a background and found to be insignificant. The expected signal yield is 9.3 ± 1.2 events, including the dissociative contributions (f_γ factor) discussed in Section 8.1. The total predicted background is 8.3 ± 2.6 , while 23 candidates are observed in the data.

Figure 12 shows the $p_T^{e\mu}$ and $\Delta\phi_{e\mu}$ distributions after applying all selection criteria. The shapes of the signal and the inclusive W^+W^- distributions are similar. The remaining $\tau^+\tau^-$ background has an azimuthal opening angle close to $\Delta\phi_{e\mu} \sim \pi$, i.e., the leptons are back-to-back. No further requirement is applied to $\Delta\phi_{e\mu}$ to reject this background, as the aQGC signal also has an enhancement for $\Delta\phi_{e\mu} \sim \pi$.

| | Expected Signal | Data | Total Bkg | Incl W^+W^- | Excl. $\tau\tau$ | Other- VV | Other Bkg | SM/Data | ϵA (Signal) |
|--------------------------------------------|-----------------|-------|-----------------|-----------------|------------------|---------------|-----------|---------|-----------------------|
| Preselection | 22.6 ± 1.9 | 99424 | 97877 | 11443 | 21.4 | 1385 | 85029 | 0.98 | 0.254 |
| $p_T^{e\mu} > 30$ GeV | 17.6 ± 1.5 | 63329 | 63023 | 8072 | 4.30 | 896.3 | 54051 | 1.00 | 0.198 |
| $\Delta_{\tau_0}^{\text{iso}}$ requirement | 9.3 ± 1.2 | 23 | 8.3 ± 2.6 | 6.6 ± 2.5 | 1.4 ± 0.3 | 0.3 ± 0.2 | – | 0.77 | 0.105 ± 0.012 |
| aQGC signal region | | | | | | | | | |
| $p_T^{e\mu} > 120$ GeV | 0.37 ± 0.04 | 1 | 0.37 ± 0.13 | 0.32 ± 0.12 | 0.05 ± 0.03 | 0 | – | 0.74 | 0.0042 ± 0.0005 |

Table 8: The event yield at different stages of the selection. The expected signal ($\gamma\gamma \rightarrow W^+W^-$) is compared to the data and total background. The SM-to-data ratio (SM/Data) gives the level of agreement between prediction and data. The product of efficiency and acceptance (ϵA) for the signal is computed from the $\gamma\gamma \rightarrow W^+W^- \rightarrow e^\pm\mu^\mp$ MC generator. The statistical and systematic uncertainties are added in quadrature. For the background, the uncertainties are only shown for the yields after exclusivity selection, where they are relevant for the measurement.

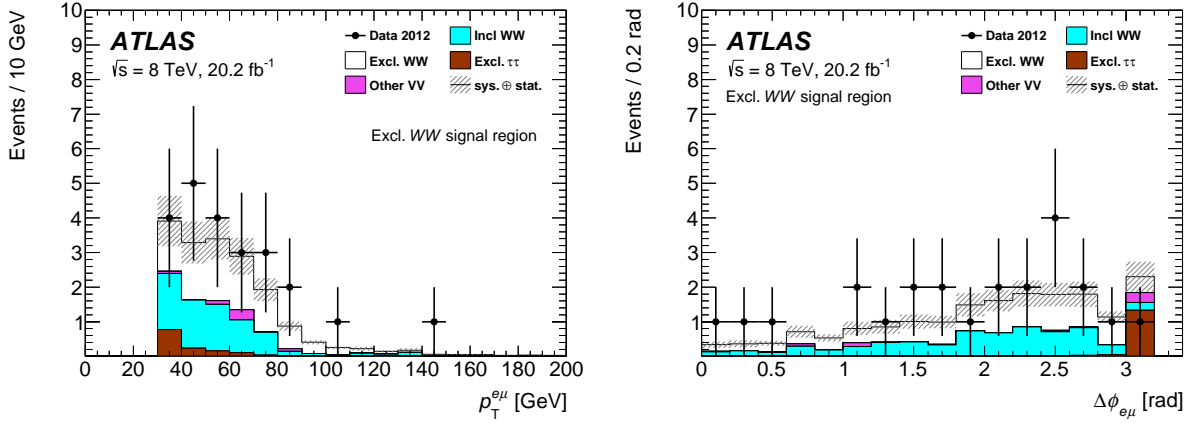


Figure 12: The $p_T^{e\mu}$ (left) and $\Delta\phi_{e\mu}$ (right) distributions in the exclusive W^+W^- signal region. The inclusive W^+W^- estimate includes small contributions from other backgrounds (Drell-Yan, W +jets, and top-quark production).

10.1.1 $\gamma\gamma \rightarrow W^+W^-$ cross-section

The full phase space cross-section predicted by HERWIG++ is $\sigma_{\gamma\gamma \rightarrow W^+W^-}^{\text{HERWIG++}} = 41.6$ fb. This number is well defined but $\sim 20\%$ corrections similar to those for the EPA dilepton prediction are expected, as discussed with Equation (6) above. The branching ratio of the W^+W^- pair decaying to $e^\pm\mu^\mp X$ is $\text{BR}(W^+W^- \rightarrow e^\pm\mu^\mp X) = 3.23\%$ [71] (including the leptonic decays of τ leptons). Therefore, the predicted cross-section corrected for $\text{BR}(W^+W^- \rightarrow e^\pm\mu^\mp X)$ and including the dissociative contributions through the normalization $f_\gamma = 3.30 \pm 0.23$ becomes:

$$\sigma_{\gamma\gamma \rightarrow W^+W^- \rightarrow e^\pm\mu^\mp X}^{\text{Predicted}} = f_\gamma \cdot \sigma_{\gamma\gamma \rightarrow W^+W^-}^{\text{HERWIG++}} \cdot \text{BR}(W^+W^- \rightarrow e^\pm\mu^\mp X) = 4.4 \pm 0.3 \text{ fb}, \quad (9)$$

which corresponds to the prediction of $N_{\text{Predicted}} = 9.3 \pm 1.2$ signal events, quoted in Table 8. The number of candidates observed in the data is $N_{\text{Data}} = 23$, while the predicted background is $N_{\text{Background}} = 8.3 \pm 2.6$ events. So the observation exceeds the prediction by a ratio:

$$R = (N_{\text{Data}} - N_{\text{Background}})/N_{\text{Predicted}} = 1.57 \pm 0.62. \quad (10)$$

The uncertainty in R results from propagation of the uncertainties of each of the numbers that go into the calculation. The uncertainty in the factor f_γ contributes 7%.

The measured cross-section is determined in the exclusive W^+W^- region and extrapolated to the full $W^+W^- \rightarrow e^\pm\mu^\mp + X$ phase space:

$$\sigma_{\gamma\gamma \rightarrow W^+W^- \rightarrow e^\pm\mu^\mp X}^{\text{Measured}} = (N_{\text{Data}} - N_{\text{Background}})/(\mathcal{L} \epsilon A) = 6.9 \pm 2.2 \text{ (stat.)} \pm 1.4 \text{ (sys.) fb}, \quad (11)$$

where $\mathcal{L} = 20.2 \pm 0.4 \text{ fb}^{-1}$. The acceptance (A) is the ratio of the number of simulated events passing the kinematic requirements in Table 3 to the total number of events generated. The efficiencies (ϵ) account for the detector efficiencies due to lepton identification and reconstruction, triggering, and pileup. Both A and ϵ are computed using the HERWIG++ prediction for the elastic $\gamma\gamma \rightarrow W^+W^-$ process. At the end of the event selection, the acceptance is $A = 0.280 \pm 0.001$ and the efficiency, which includes the exclusivity selection efficiency, is $\epsilon = 0.37 \pm 0.04$.

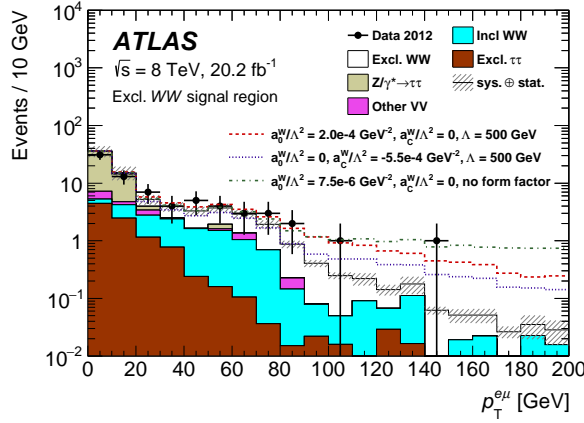


Figure 13: The $p_T^{e\mu}$ distribution for data compared to the SM prediction for events satisfying all the exclusive W^+W^- selection requirements apart from the one on $p_T^{e\mu}$ itself. Also shown are various predictions for aQGC parameters $a_{0,C}^W$.

The efficiency of the exclusivity selection is 0.58 ± 0.06 . The elastic, SD, and DD predicted acceptances can be compared using $\gamma\gamma \rightarrow \mu^+\mu^-$ events with $m_{\mu\mu} > 160$ GeV, and they are found to be the same within 3%. Therefore, the measurement of the cross-section can be performed with the acceptances for elastic $\gamma\gamma \rightarrow W^+W^-$ events. The products of acceptance and efficiencies (ϵA) at different stages of the event selection are given in Table 8.

The sources of uncertainty are given in Table 7. The statistical uncertainty dominates. The contribution from intermediate τ leptons to the accepted signal MC is determined using the HERWIG++ generator to be 9.1%. The background-only hypothesis has a p -value about 0.0012, corresponding to a significance of 3.0σ .

10.1.2 Limits on anomalous Quartic Gauge Couplings

The aQGC limit setting was performed using the region $p_T^{e\mu} > 120$ GeV where the aQGC contributions are expected to be important and Standard Model backgrounds are suppressed. The $p_T^{e\mu}$ distribution is shown in Fig. 13 for data compared to the Standard Model prediction and various aQGC scenarios. The aQGCs enhance the exclusive signal at high $p_T^{e\mu}$, while the background is negligible with $p_T^{e\mu} > 80$ GeV. The 95% CL limits on the couplings a_0^W/Λ^2 and a_C^W/Λ^2 are extracted with a likelihood test using the one observed data event as a constraint.

To extract one-dimensional (1D) limits, one of the aQGCs is set to zero. The 95% CL allowed ranges for the cases with a dipole form factor defined in Equation (2) with $\Lambda_{\text{cutoff}} = 500$ GeV and without a form factor ($\Lambda_{\text{cutoff}} \rightarrow \infty$) are listed in Table 9. The uncertainties in the yields are included in the likelihood test as nuisance parameters. Also, limits on the two aQGC parameters are shown in Fig. 14 for the case with a dipole form factor with $\Lambda_{\text{cutoff}} = 500$ GeV. The region outside the contour is ruled out at 95% confidence-level. The limits are comparable to the CMS combined 7 and 8 TeV results [14].

The 95% CL limits on the dimension-8 $f_{M,0,1,2,3}/\Lambda^4$ couplings are given in Table 10 for the cases with and without a form factor. They are derived from the $a_{0,C}^W/\Lambda^2$ couplings using Equation (3).

| Coupling | Λ_{cutoff} | Observed allowed range [GeV^{-2}] | Expected allowed range [GeV^{-2}] |
|-------------------|---------------------------|-----------------------------------------------|-----------------------------------------------|
| a_0^W/Λ^2 | 500 GeV | $[-0.96 \times 10^{-4}, 0.93 \times 10^{-4}]$ | $[-0.90 \times 10^{-4}, 0.87 \times 10^{-4}]$ |
| a_C^W/Λ^2 | 500 GeV | $[-3.5 \times 10^{-4}, 3.3 \times 10^{-4}]$ | $[-3.3 \times 10^{-4}, 3.1 \times 10^{-4}]$ |
| a_0^W/Λ^2 | ∞ | $[-1.7 \times 10^{-6}, 1.7 \times 10^{-6}]$ | $[-1.5 \times 10^{-6}, 1.6 \times 10^{-6}]$ |
| a_C^W/Λ^2 | ∞ | $[-6.4 \times 10^{-6}, 6.3 \times 10^{-6}]$ | $[-5.9 \times 10^{-6}, 5.8 \times 10^{-6}]$ |

Table 9: The observed allowed ranges for a_0^W/Λ^2 and a_C^W/Λ^2 , for dipole form factor with $\Lambda_{\text{cutoff}} = 500$ GeV and without form factor ($\Lambda_{\text{cutoff}} \rightarrow \infty$). The regions outside the quoted ranges are excluded at 95% confidence-level.

| Coupling | Λ_{cutoff} | Observed allowed range [GeV^{-4}] | Expected allowed range [GeV^{-4}] |
|---------------------|---------------------------|-----------------------------------------------|-----------------------------------------------|
| $f_{M,0}/\Lambda^4$ | 500 GeV | $[-3.7 \times 10^{-9}, 3.6 \times 10^{-9}]$ | $[-3.5 \times 10^{-9}, 3.4 \times 10^{-9}]$ |
| $f_{M,1}/\Lambda^4$ | 500 GeV | $[-13 \times 10^{-9}, 14 \times 10^{-9}]$ | $[-12 \times 10^{-9}, 13 \times 10^{-9}]$ |
| $f_{M,0}/\Lambda^4$ | ∞ | $[-6.6 \times 10^{-11}, 6.6 \times 10^{-11}]$ | $[-5.8 \times 10^{-11}, 6.2 \times 10^{-11}]$ |
| $f_{M,1}/\Lambda^4$ | ∞ | $[-24 \times 10^{-11}, 25 \times 10^{-11}]$ | $[-23 \times 10^{-11}, 23 \times 10^{-11}]$ |

Table 10: The allowed ranges for dimension-8 couplings values derived from the a_0^W and a_C^W parameters, for a dipole form factor with $\Lambda_{\text{cutoff}} = 500$ GeV and without form factor. The regions outside the quoted ranges are excluded at 95% confidence-level. The limits on $f_{M,2,3}/\Lambda^4$ can be determined using the relations: $f_{M,2} = 2 \times f_{M,0}$ and $f_{M,3} = 2 \times f_{M,1}$.

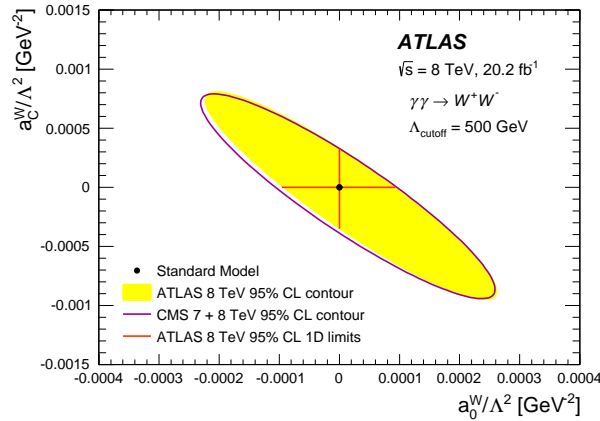


Figure 14: The observed log-likelihood 95% confidence-level contour and 1D limits for the case with a dipole form factor with $\Lambda_{\text{cutoff}} = 500$ GeV. The CMS combined 7 and 8 TeV result [14] is shown for comparison.

10.2 Limits on exclusive Higgs Boson production

As described in Section 3, exclusive production of Higgs bosons is simulated using the FPMC generator. Exclusive W^+W^- contamination in the exclusive Higgs boson signal region is estimated by using HERWIG++ samples that are scaled by $f_\gamma = 3.30$ to account for single-dissociative and double-dissociative processes. The predicted background from exclusive W^+W^- is derived from the observed cross-section in the exclusive W^+W^- signal region (Section 10.1). As discussed in Sections 8.2–8.4, the estimate for inclusive W^+W^- and minor contributions of $Z/\gamma^* \rightarrow \tau^+\tau^-$ and W +jets is obtained from the inclusive W^+W^- samples scaled by a factor of 0.79. The contribution from inclusive Higgs production is expected to be negligible. Exclusive dileptons are not scaled by f_γ because LPAIR simulates SD and DD processes as discussed in Section 7, except for $\gamma\gamma \rightarrow \tau^+\tau^-$ production of which only SD is simulated. The rest of the background sources are scaled by their respective correction factors to account for the mismodeling of the underlying event. Six candidates are observed in the data, while 3.0 ± 0.8 events are predicted from background, and 0.023 ± 0.003 from signal. The quoted uncertainty is the sum in quadrature of systematic uncertainties. Table 11 summarizes expected and observed yields in the signal region and at earlier selection points in the selection criteria summarized in Table 3. The exclusive Higgs boson prediction quoted here is from elastic contribution only. Observed data reasonably agrees with predictions. Figure 15 shows kinematic distributions in the signal region.

| | Excl. H Signal | Data | Total Bkg | Incl. W^+W^- | Excl. W^+W^- | Other Bkg |
|-----------------------------------------------------------------------|-------------------|--------|---------------|----------------|----------------|---------------|
| Preselection | 0.065 ± 0.005 | 129018 | 120090 | 12844 | 43 | 107200 |
| $p_T^{e\mu} > 30$ GeV, $m_{e\mu} < 55$ GeV, $\Delta\phi_{e\mu} < 1.8$ | 0.043 ± 0.004 | 18568 | 17060 | 2026 | 5.7 | 15030 |
| Δz_0^{iso} requirement | 0.023 ± 0.003 | 8 | 4.7 ± 1.3 | 1.4 ± 0.5 | 3.1 ± 1.3 | 0.2 ± 0.1 |
| $m_T < 140$ GeV [Signal Region] | 0.023 ± 0.003 | 6 | 3.0 ± 0.8 | 1.0 ± 0.4 | 1.8 ± 0.8 | 0.2 ± 0.1 |

Table 11: Summary of signal and background yields at different stages of the Higgs boson event selection. Only major background sources are listed explicitly. All the other background sources are summed up in the ‘Other’ category. For the background, the uncertainties are only shown for the yields after exclusivity selection, where they are relevant for the measurement. They include the systematic and statistical components, added in quadrature.

Yields summarized in the preceding paragraph are converted to upper limits on the exclusive Higgs boson total production cross-section using the CL_S technique [72]. The branching ratio $BR(H \rightarrow W^+W^-)$ used to compute these limits is $(21.5 \pm 0.9)\%$ [73]. Table 12 shows a summary of the 95% CL upper limits on the exclusive Higgs boson total production cross-section. The observed upper limit is 1.2 pb, which is 1.1σ higher than the expected upper limit of 0.7 pb. The statistical uncertainty in the predicted background dominates the uncertainty involved in calculating this upper limit, while systematic uncertainties worsen the upper limits by at most 10%. This upper limit value is 400 times the cross-section predicted [24]. However, the limit would not change if the model prediction, which is for elastic production only, increased by an order of magnitude. This limit calculation inherently assumes that the acceptance and efficiency for dissociative events is not significantly different than for elastic events, hence the associated systematic uncertainty is insignificant.

11 Conclusion

A measurement of the exclusive W^+W^- production cross-section and a search for exclusive Higgs boson production via diffraction using $e^\pm\mu^\mp$ final states are presented using a data sample that corre-

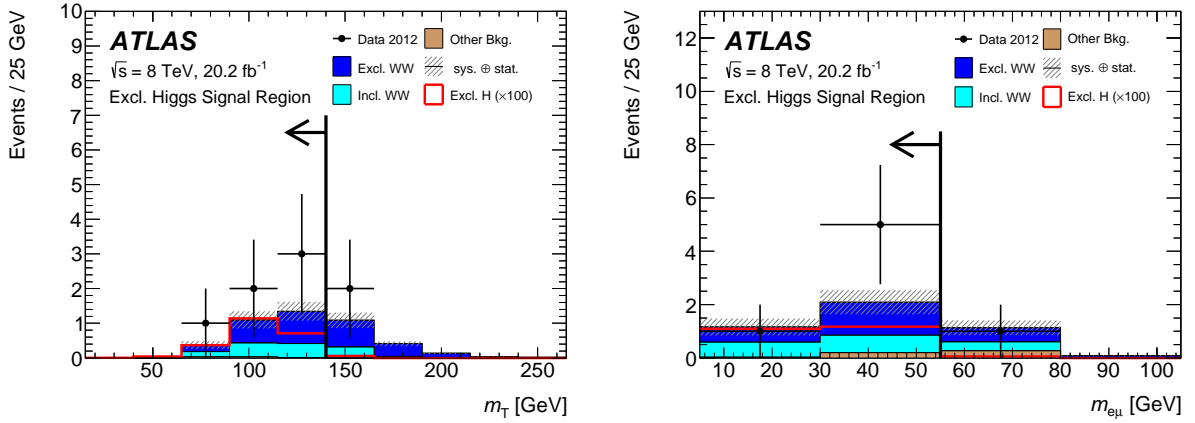


Figure 15: Distributions in the exclusive Higgs boson signal region, without including the selection on the variable plotted. The dominant processes are inclusive and exclusive W^+W^- production. The expected signal is scaled by a factor of 100 for visibility. The arrows denote the selection.

| $+2\sigma$ [pb] | $+1\sigma$ [pb] | Expected [pb] | -1σ [pb] | -2σ [pb] | Observed [pb] |
|-----------------|-----------------|---------------|-----------------|-----------------|---------------|
| 1.6 | 1.0 | 0.7 | 0.5 | 0.4 | 1.2 |

Table 12: Upper limits on σ_H [pb] at 95% CL. The $\pm 1\sigma$ and $\pm 2\sigma$ uncertainties quoted here are on the expected upper limit.

sponds to 20.2 fb^{-1} of LHC pp collisions at $\sqrt{s} = 8 \text{ TeV}$ collected with the ATLAS detector. A track-based technique for selecting exclusive candidates was developed and validated in the $\mu^+\mu^-$ final state, resulting in a ratio of data to the EPA prediction for the exclusive $\gamma\gamma \rightarrow \ell^+\ell^-$ process of $f_{\text{EL}} = 0.76 \pm 0.04(\text{stat.}) \pm 0.10(\text{sys.})$ in agreement with previous ATLAS measurements at $\sqrt{s} = 7 \text{ TeV}$. For exclusive W^+W^- production, the cross-section is determined to be $\sigma(\gamma\gamma \rightarrow W^+W^- \rightarrow e^\pm\mu^\mp X) = 6.9 \pm 2.2(\text{stat.}) \pm 1.4(\text{sys.}) \text{ fb}$ from 23 observed candidates with 8.3 ± 2.6 predicted background events. While evidence of SM exclusive W^+W^- production is at the 3.0σ level, no evidence for an excess was seen in the kinematic region that would be enhanced by anomalous quartic gauge couplings. Rather, independent limits are placed on anomalous quartic gauge couplings that are more stringent than earlier published results from the OPAL, D0, and CMS experiments. Six candidates consistent with exclusive Higgs boson production are observed in the data, with an expected SM background of 3.0 ± 0.8 events. This result corresponds to an upper limit at 95% CL on the total production cross-section of the exclusive Higgs boson of 1.2 pb, whereas the expected limit is 0.7 pb.

Acknowledgments

We thank CERN for the very successful operation of the LHC, as well as the support staff from our institutions without whom ATLAS could not be operated efficiently. We acknowledge the support of ANPCyT, Argentina; YerPhI, Armenia; ARC, Australia; BMWF and FWF, Austria; ANAS, Azerbaijan; SSTC, Belarus; CNPq and FAPESP, Brazil; NSERC, NRC and CFI, Canada; CERN; CONICYT, Chile; CAS, MOST and NSFC, China; COLCIENCIAS, Colombia; MSMT CR, MPO CR and VSC CR,

Czech Republic; DNRF and DNSRC, Denmark; IN2P3-CNRS, CEA-DSM/IRFU, France; GNSF, Georgia; BMBF, HGF, and MPG, Germany; GSRT, Greece; RGC, Hong Kong SAR, China; ISF, I-CORE and Benoziyo Center, Israel; INFN, Italy; MEXT and JSPS, Japan; CNRST, Morocco; FOM and NWO, Netherlands; RCN, Norway; MNiSW and NCN, Poland; FCT, Portugal; MNE/IFA, Romania; MES of Russia and NRC KI, Russian Federation; JINR; MESTD, Serbia; MSSR, Slovakia; ARRS and MIZŠ, Slovenia; DST/NRF, South Africa; MINECO, Spain; SRC and Wallenberg Foundation, Sweden; SERI, SNSF and Cantons of Bern and Geneva, Switzerland; MOST, Taiwan; TAEK, Turkey; STFC, United Kingdom; DOE and NSF, United States of America. In addition, individual groups and members have received support from BCKDF, the Canada Council, CANARIE, CRC, Compute Canada, FQRNT, and the Ontario Innovation Trust, Canada; EPLANET, ERC, FP7, Horizon 2020 and Marie Skłodowska-Curie Actions, European Union; Investissements d’Avenir Labex and Idex, ANR, Région Auvergne and Fondation Partager le Savoir, France; DFG and AvH Foundation, Germany; Herakleitos, Thales and Aristeia programmes co-financed by EU-ESF and the Greek NSRF; BSF, GIF and Minerva, Israel; BRF, Norway; Generalitat de Catalunya, Generalitat Valenciana, Spain; the Royal Society and Leverhulme Trust, United Kingdom. The crucial computing support from all WLCG partners is acknowledged gratefully, in particular from CERN, the ATLAS Tier-1 facilities at TRIUMF (Canada), NDGF (Denmark, Norway, Sweden), CC-IN2P3 (France), KIT/GridKA (Germany), INFN-CNAF (Italy), NL-T1 (Netherlands), PIC (Spain), ASGC (Taiwan), RAL (UK) and BNL (USA), the Tier-2 facilities worldwide and large non-WLCG resource providers. Major contributors of computing resources are listed in Ref. [74].

References

- [1] ATLAS Collaboration, *Observation of a new particle in the search for the Standard Model Higgs boson with the ATLAS detector at the LHC*, *Phys. Lett. B* **716** (2012) 1, arXiv:1207.7214 [hep-ex].
- [2] CMS Collaboration, *Observation of a new boson at a mass of 125 GeV with the CMS experiment at the LHC*, *Phys. Lett. B* **716** (2012) 30, arXiv:1207.7235 [hep-ex].
- [3] G. Belanger and F. Boudjema, $\gamma\gamma \rightarrow WW$ and $\gamma\gamma \rightarrow ZZ$ as tests of novel quartic couplings, *Phys. Lett. B* **288** (1992) 210.
- [4] E. Chapon, C. Royon, and O. Kepka, *Anomalous quartic $WW\gamma\gamma$, $ZZ\gamma\gamma$, and trilinear $WW\gamma$ couplings in two-photon processes at high luminosity at the LHC*, *Phys. Rev. D* **81** (2010) 074003, arXiv:0912.5161 [hep-ph].
- [5] M.-S. Chen et al., *Lepton pair production from two-photon processes*, *Phys. Rev. D* **7** (1973) 3485.
- [6] V. Budnev et al., *The process $pp \rightarrow \gamma\gamma$; $pp \rightarrow e^+e^-$ and the possibility of its calculation by means of quantum electrodynamics only*, *Nucl. Phys. B* **63** (1973) 519.
- [7] CDF Collaboration, A. Abulencia, et al., *Observation of exclusive electron-positron production in hadron-hadron collisions*, *Phys. Rev. Lett.* **98** (2007) 112001, arXiv:hep-ex/0611040 [hep-ex].
- [8] STAR Collaboration, J. Adams, et al., *Production of e^+e^- pairs accompanied by nuclear dissociation in ultra-peripheral heavy ion collisions*, *Phys. Rev. C* **70** (2004) 031902, arXiv:nuc1-ex/0404012 [nuc1-ex].
- [9] CMS Collaboration, *Exclusive $\gamma\gamma \rightarrow \mu^+\mu^-$ production in proton-proton collisions at $\sqrt{s} = 7$ TeV*, *JHEP* **01** (2012) 052, arXiv:1111.5536 [hep-ex].

- [10] CMS Collaboration, *Search for exclusive or semi-exclusive $\gamma\gamma$ production and observation of exclusive and semi-exclusive e^+e^- production in pp collisions at $\sqrt{s} = 7$ TeV*, *JHEP* **11** (2012) 080, arXiv:1209.1666 [hep-ex].
- [11] O. Kepka and C. Royon, *Anomalous $WW\gamma$ coupling in photon-induced processes using forward detectors at the LHC*, *Phys. Rev. D* **78** (2008) 073005, arXiv:0808.0322 [hep-ph].
- [12] OPAL Collaboration, J. Adams, et al., *Constraints on anomalous quartic gauge boson couplings from $\nu\bar{\nu}\gamma\gamma$ and $q\bar{q}\gamma\gamma$ events at CERN LEP2*, *Phys. Rev. D* **70** (2004) 032005, arXiv:hep-ex/0402021 [hep-ex].
- [13] D0 Collaboration, V. M. Abazov, et al., *Search for anomalous quartic $WW\gamma\gamma$ couplings in dielectron and missing energy final states in $p\bar{p}$ collisions at $\sqrt{s} = 1.96$ TeV*, *Phys. Rev. D* **88** (2013) 012005, arXiv:1305.1258 [hep-ex].
- [14] CMS Collaboration, *Evidence for exclusive gamma-gamma to W^+W^- production and constraints on anomalous quartic gauge couplings at $\sqrt{s} = 7$ and 8 TeV*, (2016), arXiv:1604.04464 [hep-ex].
- [15] C. Degrande et al., “Monte Carlo tools for studies of non-standard electroweak gauge boson interactions in multi-boson processes: A Snowmass White Paper,” *Community Summer Study 2013: Snowmass on the Mississippi (CSS2013) Minneapolis, MN, USA, July 29-August 6, 2013*, 2013, arXiv:1309.7890 [hep-ph].
- [16] ATLAS Collaboration, *Study of $(W/Z)H$ production and Higgs boson couplings using $H \rightarrow WW^*$ decays with the ATLAS detector*, *JHEP* **08** (2015) 137, arXiv:1506.06641 [hep-ex].
- [17] S. Heinemeyer et al., *Studying the MSSM Higgs sector by forward proton tagging at the LHC*, *Eur. Phys. J. C* **53** (2008) 231–256, arXiv:0708.3052 [hep-ph].
- [18] B. E. Cox, F. K. Loebinger, and A. D. Pilkington, *Detecting Higgs bosons in the $b\bar{b}$ decay channel using forward proton tagging at the LHC*, *JHEP* **10** (2007) 090, arXiv:0709.3035 [hep-ph].
- [19] M. Tasevsky, *Review of Central Exclusive Production of the Higgs Boson Beyond the Standard Model*, *Int. J. Mod. Phys. A* **29** (2014) 1446012, arXiv:1407.8332 [hep-ph].
- [20] B. E. Cox et al., *Detecting the standard model Higgs boson in the WW decay channel using forward proton tagging at the LHC*, *Eur. Phys. J. C* **45** (2006) 401–407, arXiv:hep-ph/0505240 [hep-ph].
- [21] C. Royon and N. Cartiglia, *The AFP and CT-PPS projects*, *Int. J. Mod. Phys. A* **29** (2014) 1446017.
- [22] L. Adamczyk et al., *Technical Design Report for the ATLAS Forward Proton Detector*, CERN-LHCC-2015-009, 2015, URL: <http://cds.cern.ch/record/2017378/>.
- [23] V. Berardi et al., *Total cross-section, elastic scattering and diffraction dissociation at the Large Hadron Collider at CERN : TOTEM Technical Design Report*, CERN-LHCC-2004-002, 2002, URL: <http://cds.cern.ch/record/704349/>.
- [24] V. Khoze, A. Martin, and M. Ryskin, *Prospects for new physics observations in diffractive processes at the LHC and Tevatron*, *Eur. Phys. J. C* **23** (2002) 311, arXiv:hep-ph/0111078 [hep-ph].
- [25] A. D. Martin and M. Ryskin, *Unintegrated generalized parton distributions*, *Phys. Rev. D* **64** (2001) 094017, arXiv:hep-ph/0107149 [hep-ph].
- [26] J. Cudell et al., *Central exclusive production of dijets at hadronic colliders*, *Eur. Phys. J. C* **61** (2009) 369–390, arXiv:0807.0600 [hep-ph].
- [27] ATLAS Collaboration, *The ATLAS Experiment at the CERN Large Hadron Collider*, *JINST* **3** (2008) S08003.

- [28] ATLAS Collaboration, *Performance of the ATLAS Trigger System in 2010*, *Eur. Phys. J. C* **72** (2012) 1849, arXiv:1110.1530 [hep-ex].
- [29] ATLAS Collaboration, *Luminosity Determination in pp Collisions at $\sqrt{s} = 8$ TeV using the ATLAS Detector at the LHC*, (2016), arXiv:1608.03953 [hep-ex].
- [30] M. Bahr et al., *Herwig++ Physics and Manual*, *Eur. Phys. J. C* **58** (2008) 639, arXiv:0803.0883 [hep-ph].
- [31] M. Boonekamp et al., *FPMC: a generator for forward physics*, (2011), arXiv:1102.2531 [hep-ph].
- [32] V. M. Budnev et al., *The Two photon particle production mechanism. Physical problems. Applications. Equivalent photon approximation*, *Phys. Rept.* **15** (1975) 181.
- [33] J. Vermaseren, *Two-photon processes at very high energies*, *Nucl. Phys. B* **229** (1983) 347.
- [34] T. Sjöstrand, S. Mrenna, and P. Z. Skands, *A Brief Introduction to PYTHIA 8.1*, *Comput. Phys. Commun.* **178** (2008) 852, arXiv:0710.3820 [hep-ph].
- [35] S. Alioli et al., *A general framework for implementing NLO calculations in shower Monte Carlo programs: the POWHEG BOX*, *JHEP* **06** (2010) 043, arXiv:1002.2581 [hep-ph].
- [36] S. Alioli et al., *NLO Higgs boson production via gluon fusion matched with shower in POWHEG*, *JHEP* **04** (2009) 002, arXiv:0812.0578 [hep-ph].
- [37] P. Nason, *A New method for combining NLO QCD with shower Monte Carlo algorithms*, *JHEP* **11** (2004) 040, arXiv:hep-ph/0409146 [hep-ph].
- [38] S. Frixione, P. Nason, and C. Oleari, *Matching NLO QCD computations with Parton Shower simulations: the POWHEG method*, *JHEP* **11** (2007) 070, arXiv:0709.2092 [hep-ph].
- [39] S. Alioli et al., *NLO vector-boson production matched with shower in POWHEG*, *JHEP* **07** (2008) 060, arXiv:0805.4802 [hep-ph].
- [40] ATLAS Collaboration, *Summary of ATLAS Pythia 8 tunes*, ATL-PHYS-PUB-2012-003, 2012, URL: <http://cds.cern.ch/record/1474107>.
- [41] T. Binoth et al., *Gluon-induced W-boson pair production at the LHC*, *JHEP* **12** (2006) 046, arXiv:hep-ph/0611170 [hep-ph].
- [42] G. Corcella et al., *HERWIG 6: An Event generator for hadron emission reactions with interfering gluons (including supersymmetric processes)*, *JHEP* **01** (2001) 010, arXiv:hep-ph/0011363 [hep-ph].
- [43] J. M. Butterworth, J. R. Forshaw, and M. H. Seymour, *Multiparton interactions in photoproduction at HERA*, *Z. Phys. C* **72** (1996) 637, arXiv:hep-ph/9601371 [hep-ph].
- [44] ATLAS Collaboration, *ATLAS tunes of PYTHIA 6 and Pythia 8 for MC11*, ATL-PHYS-PUB-2011-009, 2011, URL: <http://cds.cern.ch/record/1363300>.
- [45] H.-L. Lai et al., *New parton distributions for collider physics*, *Phys. Rev. D* **82** (2010) 074024, arXiv:1007.2241 [hep-ph].
- [46] T. Gleisberg et al., *Event generation with SHERPA 1.1*, *JHEP* **02** (2009) 007, arXiv:0811.4622 [hep-ph].
- [47] M. L. Mangano et al., *ALPGEN, a generator for hard multiparton processes in hadronic collisions*, *JHEP* **07** (2003) 001, arXiv:hep-ph/0206293 [hep-ph].
- [48] T. Sjöstrand, S. Mrenna, and P. Z. Skands, *PYTHIA 6.4 Physics and Manual*, *JHEP* **05** (2006) 026, arXiv:hep-ph/0603175 [hep-ph].

- [49] J. Pumplin et al., *New generation of parton distributions with uncertainties from global QCD analysis*, *JHEP* **07** (2002) 012, arXiv:[hep-ph/0201195](#) [[hep-ph](#)].
- [50] P. Z. Skands, *Tuning Monte Carlo Generators: The Perugia Tunes*, *Phys. Rev. D* **82** (2010) 074018, arXiv:[1005.3457](#) [[hep-ph](#)].
- [51] T. Melia et al., *W^+W^- , WZ and ZZ production in the POWHEG BOX*, *JHEP* **11** (2011) 078, arXiv:[1107.5051](#) [[hep-ph](#)].
- [52] B. P. Kersevan and E. Richter-Was, *The Monte Carlo event generator AcerMC versions 2.0 to 3.8 with interfaces to PYTHIA 6.4, HERWIG 6.5 and ARIADNE 4.1*, *Comput. Phys. Commun.* **184** (2013) 919–985, arXiv:[hep-ph/0405247](#) [[hep-ph](#)].
- [53] S. Frixione et al., *NLO QCD corrections in Herwig++ with MC@NLO*, *JHEP* **01** (2011) 053, arXiv:[1010.0568](#) [[hep-ph](#)].
- [54] ATLAS Collaboration, *The ATLAS Simulation Infrastructure*, *Eur. Phys. J. C* **70** (2010) 823–874, arXiv:[1005.4568](#) [[physics.ins-det](#)].
- [55] S. Agostinelli et al., *Geant4—a simulation toolkit*, *Nucl. Instrum. Meth. A* **506** (2003) 250.
- [56] ATLAS Collaboration, *The simulation principle and performance of the ATLAS fast calorimeter simulation FastCaloSim*, ATL-PHYS-PUB-2010-013, 2010, URL: <http://cds.cern.ch/record/1300517>.
- [57] ATLAS Collaboration, *Electron efficiency measurements with the ATLAS detector using the 2012 LHC proton–proton collision data*, ATLAS-CONF-2014-032, 2014, URL: <http://cdsweb.cern.ch/record/1706245>.
- [58] ATLAS Collaboration, *Measurement of the muon reconstruction performance of the ATLAS detector using the 2011 and 2012 LHC proton-proton collision data*, *Eur. Phys. J. C* **74** (2014) 3130, arXiv:[1407.3935](#) [[hep-ex](#)].
- [59] ATLAS Collaboration, *Observation and measurement of Higgs boson decays to WW^* with the ATLAS detector*, *Phys. Rev. D* **92** (2015) 012006, arXiv:[1412.2641](#) [[hep-ex](#)].
- [60] M. Cacciari and G. P. Salam, *Dispelling the N^3 myth for the k_t jet-finder*, *Phys. Lett. B* **641** (2006) 57, arXiv:[hep-ph/0512210](#) [[hep-ph](#)].
- [61] ATLAS Collaboration, *Performance of Missing Transverse Momentum Reconstruction in Proton-Proton Collisions at 7 TeV with ATLAS*, *Eur. Phys. J. C* **72** (2012) 1844, arXiv:[1108.5602](#) [[hep-ex](#)].
- [62] ATLAS Collaboration, *Dijet production in $\sqrt{s} = 7$ TeV pp collisions with large rapidity gaps at the ATLAS experiment*, *Phys. Lett. B* **754** (2016) 214–234, arXiv:[1511.00502](#) [[hep-ex](#)].
- [63] ATLAS Collaboration, *Rapidity gap cross sections measured with the ATLAS detector in pp collisions at $\sqrt{s} = 7$ TeV*, *Eur. Phys. J. C* **72** (2012) 1926, arXiv:[1201.2808](#) [[hep-ex](#)].
- [64] ATLAS Collaboration, *Performance of the ATLAS Inner Detector Track and Vertex Reconstruction in High Pile-Up LHC Environment*, ATLAS-CONF-2012-042, 2012, URL: <http://cdsweb.cern.ch/record/1435196>.
- [65] ATLAS Collaboration, *Measurement of exclusive $\gamma\gamma \rightarrow \ell^+\ell^-$ production in proton–proton collisions at $\sqrt{s} = 7$ TeV with the ATLAS detector*, *Phys. Lett. B* **749** (2015) 242, arXiv:[1506.07098](#) [[hep-ex](#)].
- [66] M. Dyndal and L. Schoeffel, *The role of finite-size effects on the spectrum of equivalent photons in proton–proton collisions at the LHC*, *Phys. Lett. B* **741** (2015) 66, arXiv:[1410.2983](#) [[hep-ph](#)].

- [67] L. A. Harland-Lang, V. A. Khoze, and M. G. Ryskin, *Exclusive physics at the LHC with SuperChic 2*, *Eur. Phys. J. C* **76** (2016) 9, arXiv:1508.02718 [hep-ph].
- [68] CMS Collaboration, *Study of exclusive two-photon production of W^+W^- in pp collisions at $\sqrt{s} = 7$ TeV and constraints on anomalous quartic gauge couplings*, *JHEP* **07** (2013) 116, arXiv:1305.5596 [hep-ex].
- [69] L. A. Harland-Lang, V. A. Khoze, and M. G. Ryskin, *The photon PDF in events with rapidity gaps*, *Eur. Phys. J. C* **76** (2016) 255, arXiv:1601.03772 [hep-ph].
- [70] ATLAS Collaboration, *Measurement of total and differential W^+W^- production cross sections in proton-proton collisions at $\sqrt{s} = 8$ TeV with the ATLAS detector and limits on anomalous triple-gauge-boson couplings*, (2016), arXiv:1603.01702 [hep-ex].
- [71] K. A. Olive et al., *Review of Particle Physics*, *Chin. Phys. C* **38** (2014) 090001.
- [72] A. L. Read, *Presentation of search results: The $CL(s)$ technique*, *J. Phys. G* **28** (2002) 2693.
- [73] S. Dittmaier et al., *Handbook of LHC Higgs Cross Sections: 2. Differential Distributions*, (2012), arXiv:1201.3084 [hep-ph].
- [74] ATLAS Collaboration, *ATLAS Computing Acknowledgements 2016-2017*, ATL-GEN-PUB-2016-002, 2016, URL: <http://cds.cern.ch/record/2202407>.

The ATLAS Collaboration

M. Aaboud^{135d}, G. Aad⁸⁶, B. Abbott¹¹³, J. Abdallah⁶⁴, O. Abdinov¹², B. Abeloos¹¹⁷, R. Aben¹⁰⁷, O.S. AbouZeid¹³⁷, N.L. Abraham¹⁴⁹, H. Abramowicz¹⁵³, H. Abreu¹⁵², R. Abreu¹¹⁶, Y. Abulaiti^{146a,146b}, B.S. Acharya^{163a,163b,a}, L. Adamczyk^{40a}, D.L. Adams²⁷, J. Adelman¹⁰⁸, S. Adomeit¹⁰⁰, T. Adye¹³¹, A.A. Affolder⁷⁵, T. Agatonovic-Jovin¹⁴, J. Agricola⁵⁶, J.A. Aguilar-Saavedra^{126a,126f}, S.P. Ahlen²⁴, F. Ahmadov^{66,b}, G. Aielli^{133a,133b}, H. Akerstedt^{146a,146b}, T.P.A. Åkesson⁸², A.V. Akimov⁹⁶, G.L. Alberghi^{22a,22b}, J. Albert¹⁶⁸, S. Albrand⁵⁷, M.J. Alconada Verzini⁷², M. Aleksa³², I.N. Aleksandrov⁶⁶, C. Alexa^{28b}, G. Alexander¹⁵³, T. Alexopoulos¹⁰, M. Alhroob¹¹³, B. Ali¹²⁸, M. Aliev^{74a,74b}, G. Alimonti^{92a}, J. Alison³³, S.P. Alkire³⁷, B.M.M. Allbrooke¹⁴⁹, B.W. Allen¹¹⁶, P.P. Allport¹⁹, A. Aloisio^{104a,104b}, A. Alonso³⁸, F. Alonso⁷², C. Alpigiani¹³⁸, M. Alstaty⁸⁶, B. Alvarez Gonzalez³², D. Álvarez Piqueras¹⁶⁶, M.G. Alviggi^{104a,104b}, B.T. Amadio¹⁶, K. Amako⁶⁷, Y. Amaral Coutinho^{26a}, C. Amelung²⁵, D. Amidei⁹⁰, S.P. Amor Dos Santos^{126a,126c}, A. Amorim^{126a,126b}, S. Amoroso³², G. Amundsen²⁵, C. Anastopoulos¹³⁹, L.S. Ancu⁵¹, N. Andari¹⁹, T. Andeen¹¹, C.F. Anders^{59b}, G. Anders³², J.K. Anders⁷⁵, K.J. Anderson³³, A. Andreazza^{92a,92b}, V. Andrei^{59a}, S. Angelidakis⁹, I. Angelozzi¹⁰⁷, P. Anger⁴⁶, A. Angerami³⁷, F. Anghinolfi³², A.V. Anisenkov^{109,c}, N. Anjos¹³, A. Annovi^{124a,124b}, C. Antel^{59a}, M. Antonelli⁴⁹, A. Antonov^{98,*}, F. Anulli^{132a}, M. Aoki⁶⁷, L. Aperio Bella¹⁹, G. Arabidze⁹¹, Y. Arai⁶⁷, J.P. Araque^{126a}, A.T.H. Arce⁴⁷, F.A. Arduh⁷², J-F. Arguin⁹⁵, S. Argyropoulos⁶⁴, M. Arik^{20a}, A.J. Armbruster¹⁴³, L.J. Armitage⁷⁷, O. Arnaez³², H. Arnold⁵⁰, M. Arratia³⁰, O. Arslan²³, A. Artamonov⁹⁷, G. Artoni¹²⁰, S. Artz⁸⁴, S. Asai¹⁵⁵, N. Asbah⁴⁴, A. Ashkenazi¹⁵³, B. Åsman^{146a,146b}, L. Asquith¹⁴⁹, K. Assamagan²⁷, R. Astalos^{144a}, M. Atkinson¹⁶⁵, N.B. Atlay¹⁴¹, K. Augsten¹²⁸, G. Avolio³², B. Axen¹⁶, M.K. Ayoub¹¹⁷, G. Azuelos^{95,d}, M.A. Baak³², A.E. Baas^{59a}, M.J. Baca¹⁹, H. Bachacou¹³⁶, K. Bachas^{74a,74b}, M. Backes¹⁴⁸, M. Backhaus³², P. Bagiacchi^{132a,132b}, P. Bagnaia^{132a,132b}, Y. Bai^{35a}, J.T. Baines¹³¹, O.K. Baker¹⁷⁵, E.M. Baldwin^{109,c}, P. Balek¹⁷¹, T. Balestri¹⁴⁸, F. Balli¹³⁶, W.K. Balunas¹²², E. Banas⁴¹, Sw. Banerjee^{172,e}, A.A.E. Bannoura¹⁷⁴, L. Barak³², E.L. Barberio⁸⁹, D. Barberis^{52a,52b}, M. Barbero⁸⁶, T. Barillari¹⁰¹, M-S Barisits³², T. Barklow¹⁴³, N. Barlow³⁰, S.L. Barnes⁸⁵, B.M. Barnett¹³¹, R.M. Barnett¹⁶, Z. Barnovska⁵, A. Baroncelli^{134a}, G. Barone²⁵, A.J. Barr¹²⁰, L. Barranco Navarro¹⁶⁶, F. Barreiro⁸³, J. Barreiro Guimarães da Costa^{35a}, R. Bartoldus¹⁴³, A.E. Barton⁷³, P. Bartos^{144a}, A. Basalae¹²³, A. Bassalat¹¹⁷, R.L. Bates⁵⁵, S.J. Batista¹⁵⁸, J.R. Batley³⁰, M. Battaglia¹³⁷, M. Bause^{132a,132b}, F. Bauer¹³⁶, H.S. Bawa^{143,f}, J.B. Beacham¹¹¹, M.D. Beattie⁷³, T. Beau⁸¹, P.H. Beauchemin¹⁶¹, P. Bechtel²³, H.P. Beck^{18,g}, K. Becker¹²⁰, M. Becker⁸⁴, M. Beckingham¹⁶⁹, C. Becot¹¹⁰, A.J. Beddall^{20e}, A. Beddall^{20b}, V.A. Bednyakov⁶⁶, M. Bedognetti¹⁰⁷, C.P. Bee¹⁴⁸, L.J. Beemster¹⁰⁷, T.A. Beermann³², M. Begel²⁷, J.K. Behr⁴⁴, C. Belanger-Champagne⁸⁸, A.S. Bell⁷⁹, G. Bella¹⁵³, L. Bellagamba^{22a}, A. Bellerive³¹, M. Bellomo⁸⁷, K. Belotskiy⁹⁸, O. Beltramello³², N.L. Belyaev⁹⁸, O. Benary¹⁵³, D. Benchekroun^{135a}, M. Bender¹⁰⁰, K. Bendtz^{146a,146b}, N. Benekos¹⁰, Y. Benhammou¹⁵³, E. Benhar Nocchioli¹⁷⁵, J. Benitez⁶⁴, D.P. Benjamin⁴⁷, J.R. Bensinger²⁵, S. Bentvelsen¹⁰⁷, L. Beresford¹²⁰, M. Beretta⁴⁹, D. Berge¹⁰⁷, E. Bergeaas Kuutmann¹⁶⁴, N. Berger⁵, J. Beringer¹⁶, S. Berlendis⁵⁷, N.R. Bernard⁸⁷, C. Bernius¹¹⁰, F.U. Bernlochner²³, T. Berry⁷⁸, P. Berta¹²⁹, C. Bertella⁸⁴, G. Bertoli^{146a,146b}, F. Bertolucci^{124a,124b}, I.A. Bertram⁷³, C. Bertsche⁴⁴, D. Bertsche¹¹³, G.J. Besjes³⁸, O. Bessidskaia Bylund^{146a,146b}, M. Bessner⁴⁴, N. Besson¹³⁶, C. Betancourt⁵⁰, A. Bethani⁵⁷, S. Bethke¹⁰¹, A.J. Bevan⁷⁷, R.M. Bianchi¹²⁵, L. Bianchini²⁵, M. Bianco³², O. Biebel¹⁰⁰, D. Biedermann¹⁷, R. Bielski⁸⁵, N.V. Biesuz^{124a,124b}, M. Biglietti^{134a}, J. Bilbao De Mendizabal⁵¹, T.R.V. Billoud⁹⁵, H. Bilokon⁴⁹, M. Bindi⁵⁶, S. Binet¹¹⁷, A. Bingul^{20b}, C. Bini^{132a,132b}, S. Biondi^{22a,22b}, T. Bisanz⁵⁶, D.M. Bjergaard⁴⁷, C.W. Black¹⁵⁰, J.E. Black¹⁴³, K.M. Black²⁴, D. Blackburn¹³⁸, R.E. Blair⁶, J.-B. Blanchard¹³⁶, T. Blazek^{144a}, I. Bloch⁴⁴, C. Blocker²⁵, W. Blum^{84,*}

U. Blumenschein⁵⁶, S. Blunier^{34a}, G.J. Bobbink¹⁰⁷, V.S. Bobrovnikov^{109,c}, S.S. Bocchetta⁸², A. Bocci⁴⁷,
 C. Bock¹⁰⁰, M. Boehler⁵⁰, D. Boerner¹⁷⁴, J.A. Bogaerts³², D. Bogavac¹⁴, A.G. Bogdanchikov¹⁰⁹,
 C. Bohm^{146a}, V. Boisvert⁷⁸, P. Bokan¹⁴, T. Bold^{40a}, A.S. Boldyrev^{163a,163c}, M. Bomben⁸¹, M. Bona⁷⁷,
 M. Boonekamp¹³⁶, A. Borisov¹³⁰, G. Borissov⁷³, J. Bortfeldt³², D. Bortoletto¹²⁰, V. Bortolotto^{61a,61b,61c},
 K. Bos¹⁰⁷, D. Boscherini^{22a}, M. Bosman¹³, J.D. Bossio Sola²⁹, J. Boudreau¹²⁵, J. Bouffard²,
 E.V. Bouhova-Thacker⁷³, D. Boumediene³⁶, C. Bourdarios¹¹⁷, S.K. Boutle⁵⁵, A. Boveia³², J. Boyd³²,
 I.R. Boyko⁶⁶, J. Bracinik¹⁹, A. Brandt⁸, G. Brandt⁵⁶, O. Brandt^{59a}, U. Bratzler¹⁵⁶, B. Brau⁸⁷,
 J.E. Brau¹¹⁶, H.M. Braun^{174,*}, W.D. Breaden Madden⁵⁵, K. Brendlinger¹²², A.J. Brennan⁸⁹,
 L. Brenner¹⁰⁷, R. Brenner¹⁶⁴, S. Bressler¹⁷¹, T.M. Bristow⁴⁸, D. Britton⁵⁵, D. Britzger⁴⁴, F.M. Brochu³⁰,
 I. Brock²³, R. Brock⁹¹, G. Brooijmans³⁷, T. Brooks⁷⁸, W.K. Brooks^{34b}, J. Brosamer¹⁶, E. Brost¹⁰⁸,
 J.H. Broughton¹⁹, P.A. Bruckman de Renstrom⁴¹, D. Bruncko^{144b}, R. Bruneliere⁵⁰, A. Bruni^{22a},
 G. Bruni^{22a}, L.S. Bruni¹⁰⁷, B.H. Brunt³⁰, M. Bruschi^{22a}, N. Bruscino²³, P. Bryant³³, L. Bryngemark⁸²,
 T. Buanes¹⁵, Q. Buat¹⁴², P. Buchholz¹⁴¹, A.G. Buckley⁵⁵, I.A. Budagov⁶⁶, F. Buehrer⁵⁰, M.K. Bugge¹¹⁹,
 O. Bulekov⁹⁸, D. Bullock⁸, H. Burckhart³², S. Burdin⁷⁵, C.D. Burgard⁵⁰, B. Burghgrave¹⁰⁸, K. Burka⁴¹,
 S. Burke¹³¹, I. Burmeister⁴⁵, J.T.P. Burr¹²⁰, E. Busato³⁶, D. Büscher⁵⁰, V. Büscher⁸⁴, P. Bussey⁵⁵,
 J.M. Butler²⁴, C.M. Buttar⁵⁵, J.M. Butterworth⁷⁹, P. Butti¹⁰⁷, W. Buttinger²⁷, A. Buzatu⁵⁵,
 A.R. Buzykaev^{109,c}, S. Cabrera Urbán¹⁶⁶, D. Caforio¹²⁸, V.M. Cairo^{39a,39b}, O. Cakir^{4a}, N. Calace⁵¹,
 P. Calafiura¹⁶, A. Calandri⁸⁶, G. Calderini⁸¹, P. Calfayan¹⁰⁰, G. Callea^{39a,39b}, L.P. Caloba^{26a},
 S. Calvente Lopez⁸³, D. Calvet³⁶, S. Calvet³⁶, T.P. Calvet⁸⁶, R. Camacho Toro³³, S. Camarda³²,
 P. Camarri^{133a,133b}, D. Cameron¹¹⁹, R. Caminal Armadans¹⁶⁵, C. Camincher⁵⁷, S. Campana³²,
 M. Campanelli⁷⁹, A. Camplani^{92a,92b}, A. Campoverde¹⁴¹, V. Canale^{104a,104b}, A. Canepa^{159a},
 M. Cano Bret^{35e}, J. Cantero¹¹⁴, R. Cantrill^{126a}, T. Cao⁴², M.D.M. Capeans Garrido³², I. Caprini^{28b},
 M. Caprini^{28b}, M. Capua^{39a,39b}, R. Caputo⁸⁴, R.M. Carbone³⁷, R. Cardarelli^{133a}, F. Cardillo⁵⁰,
 I. Carli¹²⁹, T. Carli³², G. Carlino^{104a}, L. Carminati^{92a,92b}, S. Caron¹⁰⁶, E. Carquin^{34b},
 G.D. Carrillo-Montoya³², J.R. Carter³⁰, J. Carvalho^{126a,126c}, D. Casadei¹⁹, M.P. Casado^{13,h},
 M. Casolino¹³, D.W. Casper¹⁶², E. Castaneda-Miranda^{145a}, R. Castelijm¹⁰⁷, A. Castelli¹⁰⁷,
 V. Castillo Gimenez¹⁶⁶, N.F. Castro^{126a,i}, A. Catinaccio³², J.R. Catmore¹¹⁹, A. Cattai³², J. Caudron²³,
 V. Cavaliere¹⁶⁵, E. Cavallaro¹³, D. Cavalli^{92a}, M. Cavalli-Sforza¹³, V. Cavasinni^{124a,124b},
 F. Ceradini^{134a,134b}, L. Cerda Alberich¹⁶⁶, B.C. Cerio⁴⁷, A.S. Cerqueira^{26b}, A. Cerri¹⁴⁹,
 L. Cerrito^{133a,133b}, F. Cerutti¹⁶, M. Cerv³², A. Cervelli¹⁸, S.A. Cetin^{20d}, A. Chafaq^{135a},
 D. Chakraborty¹⁰⁸, S.K. Chan⁵⁸, Y.L. Chan^{61a}, P. Chang¹⁶⁵, J.D. Chapman³⁰, D.G. Charlton¹⁹,
 A. Chatterjee⁵¹, C.C. Chau¹⁵⁸, C.A. Chavez Barajas¹⁴⁹, S. Che¹¹¹, S. Cheatham⁷³, A. Chegwidan⁹¹,
 S. Chekanov⁶, S.V. Chekulaev^{159a}, G.A. Chelkov^{66,j}, M.A. Chelstowska⁹⁰, C. Chen⁶⁵, H. Chen²⁷,
 K. Chen¹⁴⁸, S. Chen^{35c}, S. Chen¹⁵⁵, X. Chen^{35f}, Y. Chen⁶⁸, H.C. Cheng⁹⁰, H.J. Cheng^{35a}, Y. Cheng³³,
 A. Cheplakov⁶⁶, E. Cheremushkina¹³⁰, R. Cherkaoui El Moursli^{135e}, V. Chernyatin^{27,*}, E. Cheu⁷,
 L. Chevalier¹³⁶, V. Chiarella⁴⁹, G. Chiarelli^{124a,124b}, G. Chiodini^{74a}, A.S. Chisholm¹⁹, A. Chitan^{28b},
 M.V. Chizhov⁶⁶, K. Choi⁶², A.R. Chomont³⁶, S. Chouridou⁹, B.K.B. Chow¹⁰⁰, V. Christodoulou⁷⁹,
 D. Chromek-Burckhart³², J. Chudoba¹²⁷, A.J. Chuinard⁸⁸, J.J. Chwastowski⁴¹, L. Chytka¹¹⁵,
 G. Ciapetti^{132a,132b}, A.K. Ciftci^{4a}, D. Cinca⁴⁵, V. Cindro⁷⁶, I.A. Cioara²³, C. Ciocca^{22a,22b}, A. Ciocio¹⁶,
 F. Ciotto^{104a,104b}, Z.H. Citron¹⁷¹, M. Citterio^{92a}, M. Ciubancan^{28b}, A. Clark⁵¹, B.L. Clark⁵⁸,
 M.R. Clark³⁷, P.J. Clark⁴⁸, R.N. Clarke¹⁶, C. Clement^{146a,146b}, Y. Coadou⁸⁶, M. Cobal^{163a,163c},
 A. Coccaro⁵¹, J. Cochran⁶⁵, L. Colasurdo¹⁰⁶, B. Cole³⁷, A.P. Colijn¹⁰⁷, J. Collot⁵⁷, T. Colombo³²,
 G. Compostella¹⁰¹, P. Conde Muño^{126a,126b}, E. Coniavitis⁵⁰, S.H. Connell^{145b}, I.A. Connelly⁷⁸,
 V. Consorti⁵⁰, S. Constantinescu^{28b}, G. Conti³², F. Conventi^{104a,k}, M. Cooke¹⁶, B.D. Cooper⁷⁹,
 A.M. Cooper-Sarkar¹²⁰, K.J.R. Cormier¹⁵⁸, T. Cornelissen¹⁷⁴, M. Corradi^{132a,132b}, F. Corriveau^{88,l},
 A. Corso-Radu¹⁶², A. Cortes-Gonzalez³², G. Cortiana¹⁰¹, G. Costa^{92a}, M.J. Costa¹⁶⁶, D. Costanzo¹³⁹,
 G. Cottin³⁰, G. Cowan⁷⁸, B.E. Cox⁸⁵, K. Cranmer¹¹⁰, S.J. Crawley⁵⁵, G. Cree³¹, S. Crépe-Renaudin⁵⁷,

F. Crescioli⁸¹, W.A. Cribbs^{146a,146b}, M. Crispin Ortuzar¹²⁰, M. Cristinziani²³, V. Croft¹⁰⁶,
 G. Crosetti^{39a,39b}, A. Cueto⁸³, T. Cuhadar Donszelmann¹³⁹, J. Cummings¹⁷⁵, M. Curatolo⁴⁹, J. Cúth⁸⁴,
 H. Czirr¹⁴¹, P. Czodrowski³, G. D'amen^{22a,22b}, S. D'Auria⁵⁵, M. D'Onofrio⁷⁵,
 M.J. Da Cunha Sargedas De Sousa^{126a,126b}, C. Da Via⁸⁵, W. Dabrowski^{40a}, T. Dado^{144a}, T. Dai⁹⁰,
 O. Dale¹⁵, F. Dallaire⁹⁵, C. Dallapiccola⁸⁷, M. Dam³⁸, J.R. Dandoy³³, N.P. Dang⁵⁰, A.C. Daniells¹⁹,
 N.S. Dann⁸⁵, M. Danninger¹⁶⁷, M. Dano Hoffmann¹³⁶, V. Dao⁵⁰, G. Darbo^{52a}, S. Darmora⁸,
 J. Dassoulas³, A. Dattagupta⁶², W. Davey²³, C. David¹⁶⁸, T. Davidek¹²⁹, M. Davies¹⁵³, P. Davison⁷⁹,
 E. Dawe⁸⁹, I. Dawson¹³⁹, R.K. Daya-Ishmukhametova⁸⁷, K. De⁸, R. de Asmundis^{104a},
 A. De Benedetti¹¹³, S. De Castro^{22a,22b}, S. De Cecco⁸¹, N. De Groot¹⁰⁶, P. de Jong¹⁰⁷, H. De la Torre⁸³,
 F. De Lorenzi⁶⁵, A. De Maria⁵⁶, D. De Pedis^{132a}, A. De Salvo^{132a}, U. De Sanctis¹⁴⁹, A. De Santo¹⁴⁹,
 J.B. De Vivie De Regie¹¹⁷, W.J. Dearnaley⁷³, R. Debbe²⁷, C. Debenedetti¹³⁷, D.V. Dedovich⁶⁶,
 N. Dehghanian³, I. Deigaard¹⁰⁷, M. Del Gaudio^{39a,39b}, J. Del Peso⁸³, T. Del Prete^{124a,124b},
 D. Delgove¹¹⁷, F. Deliot¹³⁶, C.M. Delitzsch⁵¹, A. Dell'Acqua³², L. Dell'Asta²⁴, M. Dell'Orso^{124a,124b},
 M. Della Pietra^{104a,k}, D. della Volpe⁵¹, M. Delmastro⁵, P.A. Delsart⁵⁷, D.A. DeMarco¹⁵⁸, S. Demers¹⁷⁵,
 M. Demichev⁶⁶, A. Demilly⁸¹, S.P. Denisov¹³⁰, D. Denysiuk¹³⁶, D. Derendarz⁴¹, J.E. Derkaoui^{135d},
 F. Derue⁸¹, P. Dervan⁷⁵, K. Desch²³, C. Deterre⁴⁴, K. Dette⁴⁵, P.O. Deviveiros³², A. Dewhurst¹³¹,
 S. Dhaliwal²⁵, A. Di Ciaccio^{133a,133b}, L. Di Ciaccio⁵, W.K. Di Clemente¹²², C. Di Donato^{132a,132b},
 A. Di Girolamo³², B. Di Girolamo³², B. Di Micco^{134a,134b}, R. Di Nardo³², A. Di Simone⁵⁰,
 R. Di Sipio¹⁵⁸, D. Di Valentino³¹, C. Diaconu⁸⁶, M. Diamond¹⁵⁸, F.A. Dias⁴⁸, M.A. Diaz^{34a},
 E.B. Diehl⁹⁰, J. Dietrich¹⁷, S. Diglio⁸⁶, A. Dimitrievska¹⁴, J. Dingfelder²³, P. Dita^{28b}, S. Dita^{28b},
 F. Dittus³², F. Djama⁸⁶, T. Djobava^{53b}, J.I. Djuvsland^{59a}, M.A.B. do Vale^{26c}, D. Dobos³², M. Dobre^{28b},
 C. Doglioni⁸², J. Dolejsi¹²⁹, Z. Dolezal¹²⁹, M. Donadelli^{26d}, S. Donati^{124a,124b}, P. Dondero^{121a,121b},
 J. Donini³⁶, J. Dopke¹³¹, A. Doria^{104a}, M.T. Dova⁷², A.T. Doyle⁵⁵, E. Drechsler⁵⁶, M. Dris¹⁰, Y. Du^{35d},
 J. Duarte-Campderros¹⁵³, E. Duchovni¹⁷¹, G. Duckeck¹⁰⁰, O.A. Ducu^{95,m}, D. Duda¹⁰⁷, A. Dudarev³²,
 A.Chr. Dudder⁸⁴, E.M. Duffield¹⁶, L. Duflot¹¹⁷, M. Dührssen³², M. Dumancic¹⁷¹, M. Dunford^{59a},
 H. Duran Yildiz^{4a}, M. Düren⁵⁴, A. Durglishvili^{53b}, D. Duschinger⁴⁶, B. Dutta⁴⁴, M. Dyndal⁴⁴,
 C. Eckardt⁴⁴, K.M. Ecker¹⁰¹, R.C. Edgar⁹⁰, N.C. Edwards⁴⁸, T. Eifert³², G. Eigen¹⁵, K. Einsweiler¹⁶,
 T. Ekelof¹⁶⁴, M. El Kacimi^{135c}, V. Ellajosyula⁸⁶, M. Ellert¹⁶⁴, S. Elles⁵, F. Ellinghaus¹⁷⁴, A.A. Elliot¹⁶⁸,
 N. Ellis³², J. Elmsheuser²⁷, M. Elsing³², D. Emelianov¹³¹, Y. Enari¹⁵⁵, O.C. Endner⁸⁴, J.S. Ennis¹⁶⁹,
 J. Erdmann⁴⁵, A. Ereditato¹⁸, G. Ernis¹⁷⁴, J. Ernst², M. Ernst²⁷, S. Errede¹⁶⁵, E. Ertel⁸⁴, M. Escalier¹¹⁷,
 H. Esch⁴⁵, C. Escobar¹²⁵, B. Esposito⁴⁹, A.I. Etienne¹³⁶, E. Etzion¹⁵³, H. Evans⁶², A. Ezhilov¹²³,
 F. Fabbri^{22a,22b}, L. Fabbri^{22a,22b}, G. Facini³³, R.M. Fakhruddinov¹³⁰, S. Falciano^{132a}, R.J. Falla⁷⁹,
 J. Faltova³², Y. Fang^{35a}, M. Fanti^{92a,92b}, A. Farbin⁸, A. Farilla^{134a}, C. Farina¹²⁵, E.M. Farina^{121a,121b},
 T. Faroouque¹³, S. Farrell¹⁶, S.M. Farrington¹⁶⁹, P. Farthouat³², F. Fassi^{135e}, P. Fassnacht³²,
 D. Fassouliotis⁹, M. Fauci Giannelli⁷⁸, A. Favareto^{52a,52b}, W.J. Fawcett¹²⁰, L. Fayard¹¹⁷,
 O.L. Fedin^{123,n}, W. Fedorko¹⁶⁷, S. Feigl¹¹⁹, L. Felgioni⁸⁶, C. Feng^{35d}, E.J. Feng³², H. Feng⁹⁰,
 A.B. Fenyuk¹³⁰, L. Feremenga⁸, P. Fernandez Martinez¹⁶⁶, S. Fernandez Perez¹³, J. Ferrando⁵⁵,
 A. Ferrari¹⁶⁴, P. Ferrari¹⁰⁷, R. Ferrari^{121a}, D.E. Ferreira de Lima^{59b}, A. Ferrer¹⁶⁶, D. Ferrere⁵¹,
 C. Ferretti⁹⁰, A. Ferretto Parodi^{52a,52b}, F. Fiedler⁸⁴, A. Filipčič⁷⁶, M. Filipuzzi⁴⁴, F. Filthaut¹⁰⁶,
 M. Fincke-Keeler¹⁶⁸, K.D. Finelli¹⁵⁰, M.C.N. Fiolhais^{126a,126c}, L. Fiorini¹⁶⁶, A. Firan⁴², A. Fischer²,
 C. Fischer¹³, J. Fischer¹⁷⁴, W.C. Fisher⁹¹, N. Flaschel⁴⁴, I. Fleck¹⁴¹, P. Fleischmann⁹⁰, G.T. Fletcher¹³⁹,
 R.R.M. Fletcher¹²², T. Flick¹⁷⁴, A. Floderus⁸², L.R. Flores Castillo^{61a}, M.J. Flowerdew¹⁰¹,
 G.T. Forcolin⁸⁵, A. Formica¹³⁶, A. Forti⁸⁵, A.G. Foster¹⁹, D. Fournier¹¹⁷, H. Fox⁷³, S. Fracchia¹³,
 P. Francavilla⁸¹, M. Franchini^{22a,22b}, D. Francis³², L. Franconi¹¹⁹, M. Franklin⁵⁸, M. Frate¹⁶²,
 M. Fraternali^{121a,121b}, D. Freeborn⁷⁹, S.M. Fressard-Batraneanu³², F. Friedrich⁴⁶, D. Froidevaux³²,
 J.A. Frost¹²⁰, C. Fukunaga¹⁵⁶, E. Fullana Torregrosa⁸⁴, T. Fusayasu¹⁰², J. Fuster¹⁶⁶, C. Gabaldon⁵⁷,
 O. Gabizon¹⁷⁴, A. Gabrielli^{22a,22b}, A. Gabrielli¹⁶, G.P. Gach^{40a}, S. Gadatsch³², S. Gadomski⁵¹,

G. Gagliardi^{52a,52b}, L.G. Gagnon⁹⁵, P. Gagnon⁶², C. Galea¹⁰⁶, B. Galhardo^{126a,126c}, E.J. Gallas¹²⁰, B.J. Gallop¹³¹, P. Gallus¹²⁸, G. Galster³⁸, K.K. Gan¹¹¹, J. Gao^{35b,86}, Y. Gao⁴⁸, Y.S. Gao^{143,f}, F.M. Garay Walls⁴⁸, C. García¹⁶⁶, J.E. García Navarro¹⁶⁶, M. Garcia-Sciveres¹⁶, R.W. Gardner³³, N. Garelli¹⁴³, V. Garonne¹¹⁹, A. Gascon Bravo⁴⁴, K. Gasnikova⁴⁴, C. Gatti⁴⁹, A. Gaudiello^{52a,52b}, G. Gaudio^{121a}, L. Gauthier⁹⁵, I.L. Gavrilenko⁹⁶, C. Gay¹⁶⁷, G. Gaycken²³, E.N. Gazis¹⁰, Z. Gecse¹⁶⁷, C.N.P. Gee¹³¹, Ch. Geich-Gimbel²³, M. Geisen⁸⁴, M.P. Geisler^{59a}, C. Gemme^{52a}, M.H. Genest⁵⁷, C. Geng^{35b,o}, S. Gentile^{132a,132b}, C. Gentsos¹⁵⁴, S. George⁷⁸, D. Gerbaudo¹³, A. Gershon¹⁵³, S. Ghasemi¹⁴¹, H. Ghazlane^{135b}, M. Ghneimat²³, B. Giacobbe^{22a}, S. Giagu^{132a,132b}, P. Giannetti^{124a,124b}, B. Gibbard²⁷, S.M. Gibson⁷⁸, M. Gignac¹⁶⁷, M. Gilchriese¹⁶, T.P.S. Gillam³⁰, D. Gillberg³¹, G. Gilles¹⁷⁴, D.M. Gingrich^{3,d}, N. Giokaris⁹, M.P. Giordani^{163a,163c}, F.M. Giorgi^{22a}, F.M. Giorgi¹⁷, P.F. Giraud¹³⁶, P. Giromini⁵⁸, D. Giugni^{92a}, F. Giuli¹²⁰, C. Giuliani¹⁰¹, M. Giulini^{59b}, B.K. Gjelsten¹¹⁹, S. Gkaitatzis¹⁵⁴, I. Gkialas¹⁵⁴, E.L. Gkoukousis¹¹⁷, L.K. Gladilin⁹⁹, C. Glasman⁸³, J. Glatzer⁵⁰, P.C.F. Glaysheer⁴⁸, A. Glazov⁴⁴, M. Goblirsch-Kolb²⁵, J. Godlewski⁴¹, S. Goldfarb⁸⁹, T. Golling⁵¹, D. Golubkov¹³⁰, A. Gomes^{126a,126b,126d}, R. Gonçalo^{126a}, J. Goncalves Pinto Firmino Da Costa¹³⁶, G. Gonella⁵⁰, L. Gonella¹⁹, A. Gongadze⁶⁶, S. González de la Hoz¹⁶⁶, G. Gonzalez Parra¹³, S. Gonzalez-Sevilla⁵¹, L. Goossens³², P.A. Gorbounov⁹⁷, H.A. Gordon²⁷, I. Gorelov¹⁰⁵, B. Gorini³², E. Gorini^{74a,74b}, A. Gorišek⁷⁶, E. Gornicki⁴¹, A.T. Goshaw⁴⁷, C. Gössling⁴⁵, M.I. Gostkin⁶⁶, C.R. Goudet¹¹⁷, D. Goujdami^{135c}, A.G. Goussiou¹³⁸, N. Govender^{145b,p}, E. Gozani¹⁵², L. Graber⁵⁶, I. Grabowska-Bold^{40a}, P.O.J. Gradin⁵⁷, P. Grafström^{22a,22b}, J. Gramling⁵¹, E. Gramstad¹¹⁹, S. Grancagnolo¹⁷, V. Gratchev¹²³, P.M. Gravila^{28e}, H.M. Gray³², E. Graziani^{134a}, Z.D. Greenwood^{80,q}, C. Greife²³, K. Gregersen⁷⁹, I.M. Gregor⁴⁴, P. Grenier¹⁴³, K. Grevtsov⁵, J. Griffiths⁸, A.A. Grillo¹³⁷, K. Grimm⁷³, S. Grinstein^{13,r}, Ph. Gris³⁶, J.-F. Grivaz¹¹⁷, S. Groh⁸⁴, J.P. Grohs⁴⁶, E. Gross¹⁷¹, J. Grosse-Knetter⁵⁶, G.C. Grossi⁸⁰, Z.J. Grout⁷⁹, L. Guan⁹⁰, W. Guan¹⁷², J. Guenther⁶³, F. Guescini⁵¹, D. Guest¹⁶², O. Gueta¹⁵³, E. Guido^{52a,52b}, T. Guillemin⁵, S. Guindon², U. Gul⁵⁵, C. Gumpert³², J. Guo^{35e}, Y. Guo^{35b,o}, R. Gupta⁴², S. Gupta¹²⁰, G. Gustavino^{132a,132b}, P. Gutierrez¹¹³, N.G. Gutierrez Ortiz⁷⁹, C. Gutschew⁴⁶, C. Guyot¹³⁶, C. Gwenlan¹²⁰, C.B. Gwilliam⁷⁵, A. Haas¹¹⁰, C. Haber¹⁶, H.K. Hadavand⁸, N. Haddad^{135e}, A. Hadeef⁸⁶, S. Hageböck²³, Z. Hajduk⁴¹, H. Hakobyan^{176,*}, M. Haleem⁴⁴, J. Haley¹¹⁴, G. Halladjian⁹¹, G.D. Hallewell⁸⁶, K. Hamacher¹⁷⁴, P. Hamal¹¹⁵, K. Hamano¹⁶⁸, A. Hamilton^{145a}, G.N. Hamity¹³⁹, P.G. Hamnett⁴⁴, L. Han^{35b}, K. Hanagaki^{67,s}, K. Hanawa¹⁵⁵, M. Hance¹³⁷, B. Haney¹²², S. Hanisch³², P. Hanke^{59a}, R. Hanna¹³⁶, J.B. Hansen³⁸, J.D. Hansen³⁸, M.C. Hansen²³, P.H. Hansen³⁸, K. Hara¹⁶⁰, A.S. Hard¹⁷², T. Harenberg¹⁷⁴, F. Hariri¹¹⁷, S. Harkusha⁹³, R.D. Harrington⁴⁸, P.F. Harrison¹⁶⁹, F. Hartjes¹⁰⁷, N.M. Hartmann¹⁰⁰, M. Hasegawa⁶⁸, Y. Hasegawa¹⁴⁰, A. Hasib¹¹³, S. Hassani¹³⁶, S. Haug¹⁸, R. Hauser⁹¹, L. Hauswald⁴⁶, M. Havranek¹²⁷, C.M. Hawkes¹⁹, R.J. Hawkins³², D. Hayakawa¹⁵⁷, D. Hayden⁹¹, C.P. Hays¹²⁰, J.M. Hays⁷⁷, H.S. Hayward⁷⁵, S.J. Haywood¹³¹, S.J. Head¹⁹, T. Heck⁸⁴, V. Hedberg⁸², L. Heelan⁸, S. Heim¹²², T. Heim¹⁶, B. Heinemann¹⁶, J.J. Heinrich¹⁰⁰, L. Heinrich¹¹⁰, C. Heinz⁵⁴, J. Hejbal¹²⁷, L. Helary³², S. Hellman^{146a,146b}, C. Helsen³², J. Henderson¹²⁰, R.C.W. Henderson⁷³, Y. Heng¹⁷², S. Henkelmann¹⁶⁷, A.M. Henriques Correia³², S. Henrot-Versille¹¹⁷, G.H. Herbert¹⁷, V. Herget¹⁷³, Y. Hernández Jiménez¹⁶⁶, G. Herten⁵⁰, R. Hertenberger¹⁰⁰, L. Hervas³², G.G. Hesketh⁷⁹, N.P. Hesse¹⁰⁷, J.W. Hetherly⁴², R. Hickling⁷⁷, E. Higón-Rodríguez¹⁶⁶, E. Hill¹⁶⁸, J.C. Hill³⁰, K.H. Hiller⁴⁴, S.J. Hillier¹⁹, I. Hinchliffe¹⁶, E. Hines¹²², R.R. Hinman¹⁶, M. Hirose⁵⁰, D. Hirschbuehl¹⁷⁴, J. Hobbs¹⁴⁸, N. Hod^{159a}, M.C. Hodgkinson¹³⁹, P. Hodgson¹³⁹, A. Hoecker³², M.R. Hoferkamp¹⁰⁵, F. Hoenig¹⁰⁰, D. Hohn²³, T.R. Holmes¹⁶, M. Homann⁴⁵, T.M. Hong¹²⁵, B.H. Hooberman¹⁶⁵, W.H. Hopkins¹¹⁶, Y. Horii¹⁰³, A.J. Horton¹⁴², J.-Y. Hostachy⁵⁷, S. Hou¹⁵¹, A. Hoummada^{135a}, J. Howarth⁴⁴, M. Hrabovsky¹¹⁵, I. Hristova¹⁷, J. Hrivnac¹¹⁷, T. Hryn'ova⁵, A. Hrynevich⁹⁴, C. Hsu^{145c}, P.J. Hsu^{151,t}, S.-C. Hsu¹³⁸, D. Hu³⁷, Q. Hu^{35b}, S. Hu^{35e}, Y. Huang⁴⁴, Z. Hubacek¹²⁸, F. Hubaut⁸⁶, F. Huegging²³, T.B. Huffman¹²⁰, E.W. Hughes³⁷, G. Hughes⁷³,

M. Huhtinen³², P. Huo¹⁴⁸, N. Huseynov^{66,b}, J. Huston⁹¹, J. Huth⁵⁸, G. Iacobucci⁵¹, G. Iakovidis²⁷,
I. Ibragimov¹⁴¹, L. Iconomidou-Fayard¹¹⁷, E. Ideal¹⁷⁵, Z. Idrissi^{135e}, P. Iengo³², O. Igonkina^{107,u},
T. Iizawa¹⁷⁰, Y. Ikegami⁶⁷, M. Ikeno⁶⁷, Y. Ilchenko^{11,v}, D. Iliadis¹⁵⁴, N. Ilic¹⁴³, T. Ince¹⁰¹,
G. Introzzi^{121a,121b}, P. Ioannou^{9,*}, M. Iodice^{134a}, K. Iordanidou³⁷, V. Ippolito⁵⁸, N. Ishijima¹¹⁸,
M. Ishino¹⁵⁵, M. Ishitsuka¹⁵⁷, R. Ishmukhametov¹¹¹, C. Issever¹²⁰, S. Istin^{20a}, F. Ito¹⁶⁰,
J.M. Iturbe Ponce⁸⁵, R. Iuppa³⁰⁸, W. Iwanski⁴¹, H. Iwasaki⁶⁷, J.M. Izen⁴³, V. Izzo^{104a}, S. Jabbar³,
B. Jackson¹²², P. Jackson¹, V. Jain², K.B. Jakobi⁸⁴, K. Jakobs⁵⁰, S. Jakobsen³², T. Jakoubek¹²⁷,
D.O. Jamin¹¹⁴, D.K. Jana⁸⁰, E. Jansen⁷⁹, R. Jansky⁶³, J. Janssen²³, M. Janus⁵⁶, G. Jarlskog⁸²,
N. Javadov^{66,b}, T. Javůrek⁵⁰, F. Jeanneau¹³⁶, L. Jeanty¹⁶, J. Jejelava^{53a,w}, G.-Y. Jeng¹⁵⁰, D. Jennens⁸⁹,
P. Jenni^{50,x}, C. Jeske¹⁶⁹, S. Jézéquel⁵, H. Ji¹⁷², J. Jia¹⁴⁸, H. Jiang⁶⁵, Y. Jiang^{35b}, S. Jiggins⁷⁹,
J. Jimenez Pena¹⁶⁶, S. Jin^{35a}, A. Jinaru^{28b}, O. Jinnouchi¹⁵⁷, P. Johansson¹³⁹, K.A. Johns⁷,
W.J. Johnson¹³⁸, K. Jon-And^{146a,146b}, G. Jones¹⁶⁹, R.W.L. Jones⁷³, S. Jones⁷, T.J. Jones⁷⁵,
J. Jongmanns^{59a}, P.M. Jorge^{126a,126b}, J. Jovicevic^{159a}, X. Ju¹⁷², A. Juste Rozas^{13,r}, M.K. Köhler¹⁷¹,
A. Kaczmarska⁴¹, M. Kado¹¹⁷, H. Kagan¹¹¹, M. Kagan¹⁴³, S.J. Kahn⁸⁶, T. Kaji¹⁷⁰, E. Kajomovitz⁴⁷,
C.W. Kalderon¹²⁰, A. Kaluza⁸⁴, S. Kama⁴², A. Kamenshchikov¹³⁰, N. Kanaya¹⁵⁵, S. Kaneti³⁰,
L. Kanjir⁷⁶, V.A. Kantserov⁹⁸, J. Kanzaki⁶⁷, B. Kaplan¹¹⁰, L.S. Kaplan¹⁷², A. Kapliy³³, D. Kar^{145c},
K. Karakostas¹⁰, A. Karamaoun³, N. Karastathis¹⁰, M.J. Kareem⁵⁶, E. Karentzos¹⁰, M. Karnevskiy⁸⁴,
S.N. Karpov⁶⁶, Z.M. Karpova⁶⁶, K. Karthik¹¹⁰, V. Kartvelishvili⁷³, A.N. Karyukhin¹³⁰, K. Kasahara¹⁶⁰,
L. Kashif¹⁷², R.D. Kass¹¹¹, A. Kastanas¹⁵, Y. Kataoka¹⁵⁵, C. Kato¹⁵⁵, A. Katre⁵¹, J. Katzy⁴⁴,
K. Kawagoe⁷¹, T. Kawamoto¹⁵⁵, G. Kawamura⁵⁶, V.F. Kazanin^{109,c}, R. Keeler¹⁶⁸, R. Kehoe⁴²,
J.S. Keller⁴⁴, J.J. Kempster⁷⁸, K. Kentaro¹⁰³, H. Keoshkerian¹⁵⁸, O. Kepka¹²⁷, B.P. Kerševan⁷⁶,
S. Kersten¹⁷⁴, R.A. Keyes⁸⁸, M. Khader¹⁶⁵, F. Khalil-zada¹², A. Khanov¹¹⁴, A.G. Kharlamov^{109,c},
T.J. Khoo⁵¹, V. Khovanskiy⁹⁷, E. Khramov⁶⁶, J. Khubua^{53b,y}, S. Kido⁶⁸, C.R. Kilby⁷⁸, H.Y. Kim⁸,
S.H. Kim¹⁶⁰, Y.K. Kim³³, N. Kimura¹⁵⁴, O.M. Kind¹⁷, B.T. King⁷⁵, M. King¹⁶⁶, S.B. King¹⁶⁷,
J. Kirk¹³¹, A.E. Kiryunin¹⁰¹, T. Kishimoto¹⁵⁵, D. Kisielewska^{40a}, F. Kiss⁵⁰, K. Kiuchi¹⁶⁰,
O. Kivernyk¹³⁶, E. Kladiva^{144b}, M.H. Klein³⁷, M. Klein⁷⁵, U. Klein⁷⁵, K. Kleinknecht⁸⁴, P. Klimek¹⁰⁸,
A. Klimentov²⁷, R. Klingenberg⁴⁵, J.A. Klinger¹³⁹, T. Klioutchnikova³², E.-E. Kluge^{59a}, P. Kluit¹⁰⁷,
S. Kluth¹⁰¹, J. Knapik⁴¹, E. Kneringer⁶³, E.B.F.G. Knoop⁸⁶, A. Knue⁵⁵, A. Kobayashi¹⁵⁵,
D. Kobayashi¹⁵⁷, T. Kobayashi¹⁵⁵, M. Kobel⁴⁶, M. Kocian¹⁴³, P. Kodys¹²⁹, N.M. Koehler¹⁰¹, T. Koffas³¹,
E. Koffeman¹⁰⁷, T. Koi¹⁴³, H. Kolanoski¹⁷, M. Kolb^{59b}, I. Koletsou⁵, A.A. Komar^{96,*}, Y. Komori¹⁵⁵,
T. Kondo⁶⁷, N. Kondrashova⁴⁴, K. Köneke⁵⁰, A.C. König¹⁰⁶, T. Kono^{67,z}, R. Konoplich^{110,aa},
N. Konstantinidis⁷⁹, R. Kopeliansky⁶², S. Koperny^{40a}, L. Köpke⁸⁴, A.K. Kopp⁵⁰, K. Korcyl⁴¹,
K. Kordas¹⁵⁴, A. Korn⁷⁹, A.A. Korol^{109,c}, I. Korolkov¹³, E.V. Korolkova¹³⁹, O. Kortner¹⁰¹, S. Kortner¹⁰¹,
T. Kosek¹²⁹, V.V. Kostyukhin²³, A. Kotwal⁴⁷, A. Kourkumeli-Charalampidi^{121a,121b}, C. Kourkumelis⁹,
V. Kouskoura²⁷, A.B. Kowalewska⁴¹, R. Kowalewski¹⁶⁸, T.Z. Kowalski^{40a}, C. Kozakai¹⁵⁵,
W. Kozanecki¹³⁶, A.S. Kozhin¹³⁰, V.A. Kramarenko⁹⁹, G. Kramerberger⁷⁶, D. Krasnopevtsev⁹⁸,
M.W. Krasny⁸¹, A. Krasznahorkay³², A. Kravchenko²⁷, M. Kretz^{59c}, J. Kretzschmar⁷⁵, K. Kreutzfeldt⁵⁴,
P. Krieger¹⁵⁸, K. Krizka³³, K. Kroeninger⁴⁵, H. Kroha¹⁰¹, J. Kroll¹²², J. Kroseberg²³, J. Krstic¹⁴,
U. Kruchonak⁶⁶, H. Krüger²³, N. Krumnack⁶⁵, A. Kruse¹⁷², M.C. Kruse⁴⁷, M. Kruskal²⁴, T. Kubota⁸⁹,
H. Kucuk⁷⁹, S. Kuday^{4b}, J.T. Kuechler¹⁷⁴, S. Kuehn⁵⁰, A. Kugel^{59c}, F. Kuger¹⁷³, A. Kuhl¹³⁷, T. Kuhl⁴⁴,
V. Kukhtin⁶⁶, R. Kukla¹³⁶, Y. Kulchitsky⁹³, S. Kuleshov^{34b}, M. Kuna^{132a,132b}, T. Kunigo⁶⁹, A. Kupco¹²⁷,
H. Kurashige⁶⁸, Y.A. Kurochkin⁹³, V. Kus¹²⁷, E.S. Kuwertz¹⁶⁸, M. Kuze¹⁵⁷, J. Kvita¹¹⁵, T. Kwan¹⁶⁸,
D. Kyriazopoulos¹³⁹, A. La Rosa¹⁰¹, J.L. La Rosa Navarro^{26d}, L. La Rotonda^{39a,39b}, C. Lacasta¹⁶⁶,
F. Lacava^{132a,132b}, J. Lacey³¹, H. Lacker¹⁷, D. Lacour⁸¹, V.R. Lacuesta¹⁶⁶, E. Ladygin⁶⁶, R. Lafaye⁵,
B. Laforge⁸¹, T. Lagouri¹⁷⁵, S. Lai⁵⁶, S. Lammers⁶², W. Lampl⁷, E. Lançon¹³⁶, U. Landgraf⁵⁰,
M.P.J. Landon⁷⁷, M.C. Lanfermann⁵¹, V.S. Lang^{59a}, J.C. Lange¹³, A.J. Lankford¹⁶², F. Lanni²⁷,
K. Lantzscht²³, A. Lanza^{121a}, S. Laplace⁸¹, C. Lapoire³², J.F. Laporte¹³⁶, T. Lari^{92a},

F. Lasagni Manghi^{22a,22b}, M. Lassnig³², P. Laurelli⁴⁹, W. Lavrijsen¹⁶, A.T. Law¹³⁷, P. Laycock⁷⁵, T. Lazovich⁵⁸, M. Lazzaroni^{92a,92b}, B. Le⁸⁹, O. Le Dortz⁸¹, E. Le Guirriec⁸⁶, E.P. Le Quilleuc¹³⁶, M. LeBlanc¹⁶⁸, T. LeCompte⁶, F. Ledroit-Guillon⁵⁷, C.A. Lee²⁷, S.C. Lee¹⁵¹, L. Lee¹, B. Lefebvre⁸⁸, G. Lefebvre⁸¹, M. Lefebvre¹⁶⁸, F. Legger¹⁰⁰, C. Leggett¹⁶, A. Lehan⁷⁵, G. Lehmann Miotto³², X. Lei⁷, W.A. Leight³¹, A. Leisos^{154,ab}, A.G. Leister¹⁷⁵, M.A.L. Leite^{26d}, R. Leitner¹²⁹, D. Lellouch¹⁷¹, B. Lemmer⁵⁶, K.J.C. Leney⁷⁹, T. Lenz²³, B. Lenzi³², R. Leone⁷, S. Leone^{124a,124b}, C. Leonidopoulos⁴⁸, S. Leontsinis¹⁰, G. Lerner¹⁴⁹, C. Leroy⁹⁵, A.A.J. Lesage¹³⁶, C.G. Lester³⁰, M. Levchenko¹²³, J. Levêque⁵, D. Levin⁹⁰, L.J. Levinson¹⁷¹, M. Levy¹⁹, D. Lewis⁷⁷, A.M. Leyko²³, M. Leyton⁴³, B. Li^{35b,o}, C. Li^{35b}, H. Li¹⁴⁸, H.L. Li³³, L. Li⁴⁷, L. Li^{35e}, Q. Li^{35a}, S. Li⁴⁷, X. Li⁸⁵, Y. Li¹⁴¹, Z. Liang^{35a}, B. Liberti^{133a}, A. Liblong¹⁵⁸, P. Lichard³², K. Lie¹⁶⁵, J. Liebal²³, W. Liebig¹⁵, A. Limosani¹⁵⁰, S.C. Lin^{151,ac}, T.H. Lin⁸⁴, B.E. Lindquist¹⁴⁸, A.E. Lioni⁵¹, E. Lipeles¹²², A. Lipniacka¹⁵, M. Lisovyi^{59b}, T.M. Liss¹⁶⁵, A. Lister¹⁶⁷, A.M. Litke¹³⁷, B. Liu^{151,ad}, D. Liu¹⁵¹, H. Liu⁹⁰, H. Liu²⁷, J. Liu⁸⁶, J.B. Liu^{35b}, K. Liu⁸⁶, L. Liu¹⁶⁵, M. Liu⁴⁷, M. Liu^{35b}, Y.L. Liu^{35b}, Y. Liu^{35b}, M. Livan^{121a,121b}, A. Lleres⁵⁷, J. Llorente Merino^{35a}, S.L. Lloyd⁷⁷, F. Lo Sterzo¹⁵¹, E. Lobodzinska⁴⁴, P. Loch⁷, W.S. Lockman¹³⁷, F.K. Loebinger⁸⁵, A.E. Loevschall-Jensen³⁸, K.M. Loew²⁵, A. Loginov^{175,*}, T. Lohse¹⁷, K. Lohwasser⁴⁴, M. Lokajicek¹²⁷, B.A. Long²⁴, J.D. Long¹⁶⁵, R.E. Long⁷³, L. Longo^{74a,74b}, K.A. Looper¹¹¹, L. Lopes^{126a}, D. Lopez Mateos⁵⁸, B. Lopez Paredes¹³⁹, I. Lopez Paz¹³, A. Lopez Solis⁸¹, J. Lorenz¹⁰⁰, N. Lorenzo Martinez⁶², M. Losada²¹, P.J. Lösel¹⁰⁰, X. Lou^{35a}, A. Lounis¹¹⁷, J. Love⁶, P.A. Love⁷³, H. Lu^{61a}, N. Lu⁹⁰, H.J. Lubatti¹³⁸, C. Luci^{132a,132b}, A. Lucotte⁵⁷, C. Luedtke⁵⁰, F. Luehring⁶², W. Lukas⁶³, L. Luminari^{132a}, O. Lundberg^{146a,146b}, B. Lund-Jensen¹⁴⁷, P.M. Luzi⁸¹, D. Lynn²⁷, R. Lysak¹²⁷, E. Lytken⁸², V. Lyubushkin⁶⁶, H. Ma²⁷, L.L. Ma^{35d}, Y. Ma^{35d}, G. Maccarrone⁴⁹, A. Macchiolo¹⁰¹, C.M. Macdonald¹³⁹, B. Maček⁷⁶, J. Machado Miguens^{122,126b}, D. Madaffari⁸⁶, R. Madar³⁶, H.J. Maddocks¹⁶⁴, W.F. Mader⁴⁶, A. Madsen⁴⁴, J. Maeda⁶⁸, S. Maeland¹⁵, T. Maeno²⁷, A. Maeviskiy⁹⁹, E. Magradze⁵⁶, J. Mahlstedt¹⁰⁷, C. Maiani¹¹⁷, C. Maidantchik^{26a}, A.A. Maier¹⁰¹, T. Maier¹⁰⁰, A. Maio^{126a,126b,126d}, S. Majewski¹¹⁶, Y. Makida⁶⁷, N. Makovec¹¹⁷, B. Malaescu⁸¹, Pa. Malecki⁴¹, V.P. Maleev¹²³, F. Malek⁵⁷, U. Mallik⁶⁴, D. Malon⁶, C. Malone¹⁴³, S. Maltezos¹⁰, S. Malyukov³², J. Mamuzic¹⁶⁶, G. Mancini⁴⁹, B. Mandelli³², L. Mandelli^{92a}, I. Mandić⁷⁶, J. Maneira^{126a,126b}, L. Manhaes de Andrade Filho^{26b}, J. Manjarres Ramos^{159b}, A. Mann¹⁰⁰, A. Manousos³², B. Mansoulie¹³⁶, J.D. Mansour^{35a}, R. Mantifel⁸⁸, M. Mantoani⁵⁶, S. Manzoni^{92a,92b}, L. Mapelli³², G. Marceca²⁹, L. March⁵¹, G. Marchiori⁸¹, M. Marcisovsky¹²⁷, M. Marjanovic¹⁴, D.E. Marley⁹⁰, F. Marroquim^{26a}, S.P. Marsden⁸⁵, Z. Marshall¹⁶, S. Marti-Garcia¹⁶⁶, B. Martin⁹¹, T.A. Martin¹⁶⁹, V.J. Martin⁴⁸, B. Martin dit Latour¹⁵, M. Martinez^{13,r}, V.I. Martinez Outschoorn¹⁶⁵, S. Martin-Haugh¹³¹, V.S. Martoiu^{28b}, A.C. Martyniuk⁷⁹, M. Marx¹³⁸, A. Marzin³², L. Masetti⁸⁴, T. Mashimo¹⁵⁵, R. Mashinistov⁹⁶, J. Masik⁸⁵, A.L. Maslennikov^{109,c}, I. Massa^{22a,22b}, L. Massa^{22a,22b}, P. Mastrandrea⁵, A. Mastroberardino^{39a,39b}, T. Masubuchi¹⁵⁵, P. Mättig¹⁷⁴, J. Mattmann⁸⁴, J. Maurer^{28b}, S.J. Maxfield⁷⁵, D.A. Maximov^{109,c}, R. Mazini¹⁵¹, S.M. Mazza^{92a,92b}, N.C. Mc Fadden¹⁰⁵, G. Mc Goldrick¹⁵⁸, S.P. Mc Kee⁹⁰, A. McCarn⁹⁰, R.L. McCarthy¹⁴⁸, T.G. McCarthy¹⁰¹, L.I. McClymont⁷⁹, E.F. McDonald⁸⁹, J.A. Mcfayden⁷⁹, G. Mchedlidze⁵⁶, S.J. McMahon¹³¹, R.A. McPherson^{168,l}, M. Medinnis⁴⁴, S. Meehan¹³⁸, S. Mehlhase¹⁰⁰, A. Mehta⁷⁵, K. Meier^{59a}, C. Meineck¹⁰⁰, B. Meirose⁴³, D. Melini¹⁶⁶, B.R. Mellado Garcia^{145c}, M. Melo^{144a}, F. Meloni¹⁸, A. Mengarelli^{22a,22b}, S. Menke¹⁰¹, E. Meoni¹⁶¹, S. Mergelmeyer¹⁷, P. Mermod⁵¹, L. Merola^{104a,104b}, C. Meroni^{92a}, F.S. Merritt³³, A. Messina^{132a,132b}, J. Metcalfe⁶, A.S. Mete¹⁶², C. Meyer⁸⁴, C. Meyer¹²², J-P. Meyer¹³⁶, J. Meyer¹⁰⁷, H. Meyer Zu Theenhausen^{59a}, F. Miano¹⁴⁹, R.P. Middleton¹³¹, S. Miglioranzi^{52a,52b}, L. Mijovic⁴⁸, G. Mikenberg¹⁷¹, M. Mikesikova¹²⁷, M. Mikuž⁷⁶, M. Milesi⁸⁹, A. Milic⁶³, D.W. Miller³³, C. Mills⁴⁸, A. Milov¹⁷¹, D.A. Milstead^{146a,146b}, A.A. Minaenko¹³⁰, Y. Minami¹⁵⁵, I.A. Minashvili⁶⁶, A.I. Mincer¹¹⁰, B. Mindur^{40a}, M. Mineev⁶⁶, Y. Ming¹⁷², L.M. Mir¹³, K.P. Mistry¹²², T. Mitani¹⁷⁰, J. Mitrevski¹⁰⁰, V.A. Mitsou¹⁶⁶, A. Miucci⁵¹, P.S. Miyagawa¹³⁹,

J.U. Mjörnmark⁸², T. Moa^{146a,146b}, K. Mochizuki⁹⁵, S. Mohapatra³⁷, S. Molander^{146a,146b}, R. Moles-Valls²³, R. Monden⁶⁹, M.C. Mondragon⁹¹, K. Mönig⁴⁴, J. Monk³⁸, E. Monnier⁸⁶, A. Montalbano¹⁴⁸, J. Montejo Berlingen³², F. Monticelli⁷², S. Monzani^{92a,92b}, R.W. Moore³, N. Morange¹¹⁷, D. Moreno²¹, M. Moreno Llácer⁵⁶, P. Morettini^{52a}, D. Mori¹⁴², T. Mori¹⁵⁵, M. Morii⁵⁸, M. Morinaga¹⁵⁵, V. Morisbak¹¹⁹, S. Moritz⁸⁴, A.K. Morley¹⁵⁰, G. Mornacchi³², J.D. Morris⁷⁷, S.S. Mortensen³⁸, L. Morvaj¹⁴⁸, M. Mosidze^{53b}, J. Moss¹⁴³, K. Motohashi¹⁵⁷, R. Mount¹⁴³, E. Mountricha²⁷, S.V. Mouraviev^{96,*}, E.J.W. Moyses⁸⁷, S. Muanza⁸⁶, R.D. Mudd¹⁹, F. Mueller¹⁰¹, J. Mueller¹²⁵, R.S.P. Mueller¹⁰⁰, T. Mueller³⁰, D. Muenstermann⁷³, P. Mullen⁵⁵, G.A. Mullier¹⁸, F.J. Munoz Sanchez⁸⁵, J.A. Murillo Quijada¹⁹, W.J. Murray^{169,131}, H. Musheghyan⁵⁶, M. Muškinja⁷⁶, A.G. Myagkov^{130,ae}, M. Myska¹²⁸, B.P. Nachman¹⁴³, O. Nackenhorst⁵¹, K. Nagai¹²⁰, R. Nagai^{67,z}, K. Nagano⁶⁷, Y. Nagasaka⁶⁰, K. Nagata¹⁶⁰, M. Nagel⁵⁰, E. Nagy⁸⁶, A.M. Nairz³², Y. Nakahama¹⁰³, K. Nakamura⁶⁷, T. Nakamura¹⁵⁵, I. Nakano¹¹², H. Namasivayam⁴³, R.F. Naranjo Garcia⁴⁴, R. Narayan¹¹, D.I. Narrias Villar^{59a}, I. Naryshkin¹²³, T. Naumann⁴⁴, G. Navarro²¹, R. Nayyar⁷, H.A. Neal⁹⁰, P.Yu. Nechaeva⁹⁶, T.J. Neep⁸⁵, A. Negri^{121a,121b}, M. Negrini^{22a}, S. Nektarijevic¹⁰⁶, C. Nellist¹¹⁷, A. Nelson¹⁶², S. Nemecek¹²⁷, P. Nemethy¹¹⁰, A.A. Nepomuceno^{26a}, M. Nessi^{32,af}, M.S. Neubauer¹⁶⁵, M. Neumann¹⁷⁴, R.M. Neves¹¹⁰, P. Nevski²⁷, P.R. Newman¹⁹, D.H. Nguyen⁶, T. Nguyen Manh⁹⁵, R.B. Nickerson¹²⁰, R. Nicolaidou¹³⁶, J. Nielsen¹³⁷, A. Nikiforov¹⁷, V. Nikolaenko^{130,ae}, I. Nikolic-Audit⁸¹, K. Nikolopoulos¹⁹, J.K. Nilsen¹¹⁹, P. Nilsson²⁷, Y. Ninomiya¹⁵⁵, A. Nisati^{132a}, R. Nisius¹⁰¹, T. Nobe¹⁵⁵, L. Nodulman⁶, M. Nomachi¹¹⁸, I. Nomidis³¹, T. Nooney⁷⁷, S. Norberg¹¹³, M. Nordberg³², N. Norjoharuddeen¹²⁰, O. Novgorodova⁴⁶, S. Nowak¹⁰¹, M. Nozaki⁶⁷, L. Nozka¹¹⁵, K. Ntekas¹⁰, E. Nurse⁷⁹, F. Nuti⁸⁹, F. O'grady⁷, D.C. O'Neil¹⁴², A.A. O'Rourke⁴⁴, V. O'Shea⁵⁵, F.G. Oakham^{31,d}, H. Oberlack¹⁰¹, T. Obermann²³, J. Ocariz⁸¹, A. Ochi⁶⁸, I. Ochoa³⁷, J.P. Ochoa-Ricoux^{34a}, S. Oda⁷¹, S. Odaka⁶⁷, H. Ogren⁶², A. Oh⁸⁵, S.H. Oh⁴⁷, C.C. Ohm¹⁶, H. Ohman¹⁶⁴, H. Oide³², H. Okawa¹⁶⁰, Y. Okumura¹⁵⁵, T. Okuyama⁶⁷, A. Olariu^{28b}, L.F. Oleiro Seabra^{126a}, S.A. Olivares Pino⁴⁸, D. Oliveira Damazio²⁷, A. Olszewski⁴¹, J. Olszowska⁴¹, A. Onofre^{126a,126e}, K. Onogi¹⁰³, P.U.E. Onyisi^{11,v}, M.J. Oreglia³³, Y. Oren¹⁵³, D. Orestano^{134a,134b}, N. Orlando^{61b}, R.S. Orr¹⁵⁸, B. Osculati^{52a,52b}, R. Ospanov⁸⁵, G. Otero y Garzon²⁹, H. Otono⁷¹, M. Ouchrif^{135d}, F. Ould-Saada¹¹⁹, A. Ouraou¹³⁶, K.P. Oussoren¹⁰⁷, Q. Ouyang^{35a}, M. Owen⁵⁵, R.E. Owen¹⁹, V.E. Ozcan^{20a}, N. Ozturk⁸, K. Pachal¹⁴², A. Pacheco Pages¹³, L. Pacheco Rodriguez¹³⁶, C. Padilla Aranda¹³, M. Pagáčová⁵⁰, S. Pagan Griso¹⁶, F. Paige²⁷, P. Pais⁸⁷, K. Pajchel¹¹⁹, G. Palacino^{159b}, S. Palazzo^{39a,39b}, S. Palestini³², M. Palka^{40b}, D. Pallin³⁶, E.St. Panagiotopoulou¹⁰, C.E. Pandini⁸¹, J.G. Panduro Vazquez⁷⁸, P. Pani^{146a,146b}, S. Panitkin²⁷, D. Pantea^{28b}, L. Paolozzi⁵¹, Th.D. Papadopoulou¹⁰, K. Papageorgiou¹⁵⁴, A. Paramonov⁶, D. Paredes Hernandez¹⁷⁵, A.J. Parker⁷³, M.A. Parker³⁰, K.A. Parker¹³⁹, F. Parodi^{52a,52b}, J.A. Parsons³⁷, U. Parzefall⁵⁰, V.R. Pascuzzi¹⁵⁸, E. Pasqualucci^{132a}, S. Passaggio^{52a}, Fr. Pastore⁷⁸, G. Pásztor^{31,ag}, S. Pataria¹⁷⁴, J.R. Pater⁸⁵, T. Pauly³², J. Pearce¹⁶⁸, B. Pearson¹¹³, L.E. Pedersen³⁸, M. Pedersen¹¹⁹, S. Pedraza Lopez¹⁶⁶, R. Pedro^{126a,126b}, S.V. Peleganchuk^{109,c}, O. Penc¹²⁷, C. Peng^{35a}, H. Peng^{35b}, J. Penwell⁶², B.S. Peralva^{26b}, M.M. Perego¹³⁶, D.V. Perepelitsa²⁷, E. Perez Codina^{159a}, L. Perini^{92a,92b}, H. Pernegger³², S. Perrella^{104a,104b}, R. Peschke⁴⁴, V.D. Peshekhonov⁶⁶, K. Peters⁴⁴, R.F.Y. Peters⁸⁵, B.A. Petersen³², T.C. Petersen³⁸, E. Petit⁵⁷, A. Petridis¹, C. Petridou¹⁵⁴, P. Petroff¹¹⁷, E. Petrolo^{132a}, M. Petrov¹²⁰, F. Petrucci^{134a,134b}, N.E. Pettersson⁸⁷, A. Peyaud¹³⁶, R. Pezoa^{34b}, P.W. Phillips¹³¹, G. Piacquadio¹⁴³, E. Pianori¹⁶⁹, A. Picazio⁸⁷, E. Piccaro⁷⁷, M. Piccinini^{22a,22b}, M.A. Pickering¹²⁰, R. Piegai²⁹, J.E. Pilcher³³, A.D. Pilkington⁸⁵, A.W.J. Pin⁸⁵, M. Pinamonti^{163a,163c,ah}, J.L. Pinfold³, A. Pingel³⁸, S. Pires⁸¹, H. Pirumov⁴⁴, M. Pitt¹⁷¹, L. Plazak^{144a}, M.-A. Pleier²⁷, V. Pleskot⁸⁴, E. Plotnikova⁶⁶, P. Plucinski⁹¹, D. Pluth⁶⁵, R. Poettgen^{146a,146b}, L. Poggioli¹¹⁷, D. Pohl²³, G. Polesello^{121a}, A. Poley⁴⁴, A. Policicchio^{39a,39b}, R. Polifka¹⁵⁸, A. Polini^{22a}, C.S. Pollard⁵⁵, V. Polychronakos²⁷, K. Pommès³², L. Pontecorvo^{132a}, B.G. Pope⁹¹, G.A. Popeneciu^{28c}, D.S. Popovic¹⁴, A. Poppleton³², S. Pospisil¹²⁸,

K. Potamianos¹⁶, I.N. Potrap⁶⁶, C.J. Potter³⁰, C.T. Potter¹¹⁶, G. Poulard³², J. Poveda³²,
 V. Pozdnyakov⁶⁶, M.E. Pozo Astigarraga³², P. Pralavorio⁸⁶, A. Pranko¹⁶, S. Prell⁶⁵, D. Price⁸⁵,
 L.E. Price⁶, M. Primavera^{74a}, S. Prince⁸⁸, K. Prokofiev^{61c}, F. Prokoshin^{34b}, S. Protopopescu²⁷,
 J. Proudfoot⁶, M. Przybycien^{40a}, D. Puddu^{134a,134b}, M. Purohit^{27,ai}, P. Puzo¹¹⁷, J. Qian⁹⁰, G. Qin⁵⁵,
 Y. Qin⁸⁵, A. Quadt⁵⁶, W.B. Quayle^{163a,163b}, M. Queitsch-Maitland⁸⁵, D. Quilty⁵⁵, S. Raddum¹¹⁹,
 V. Radeka²⁷, V. Radescu¹²⁰, S.K. Radhakrishnan¹⁴⁸, P. Radloff¹¹⁶, P. Rados⁸⁹, F. Ragusa^{92a,92b},
 G. Rahal¹⁷⁷, J.A. Raine⁸⁵, S. Rajagopalan²⁷, M. Rammensee³², C. Rangel-Smith¹⁶⁴, M.G. Ratti^{92a,92b},
 F. Rauscher¹⁰⁰, S. Rave⁸⁴, T. Ravenscroft⁵⁵, I. Ravinovich¹⁷¹, M. Raymond³², A.L. Read¹¹⁹,
 N.P. Readioff⁷⁵, M. Reale^{74a,74b}, D.M. Rebuzzi^{121a,121b}, A. Redelbach¹⁷³, G. Redlinger²⁷, R. Reece¹³⁷,
 K. Reeves⁴³, L. Rehnisch¹⁷, J. Reichert¹²², H. Reisin²⁹, C. Rembser³², H. Ren^{35a}, M. Rescigno^{132a},
 S. Resconi^{92a}, O.L. Rezanova^{109,c}, P. Reznicek¹²⁹, R. Rezvani⁹⁵, R. Richter¹⁰¹, S. Richter⁷⁹,
 E. Richter-Was^{40b}, O. Ricken²³, M. Ridel⁸¹, P. Rieck¹⁷, C.J. Riegel¹⁷⁴, J. Rieger⁵⁶, O. Rifki¹¹³,
 M. Rijssenbeek¹⁴⁸, A. Rimoldi^{121a,121b}, M. Rimoldi¹⁸, L. Rinaldi^{22a}, B. Ristic⁵¹, E. Ritsch³², I. Riu¹³,
 F. Rizatdinova¹¹⁴, E. Rizvi⁷⁷, C. Rizzi¹³, S.H. Robertson^{88,l}, A. Robichaud-Veronneau⁸⁸, D. Robinson³⁰,
 J.E.M. Robinson⁴⁴, A. Robson⁵⁵, C. Roda^{124a,124b}, Y. Rodina⁸⁶, A. Rodriguez Perez¹³,
 D. Rodriguez Rodriguez¹⁶⁶, S. Roe³², C.S. Rogan⁵⁸, O. Røhne¹¹⁹, A. Romaniouk⁹⁸, M. Romano^{22a,22b},
 S.M. Romano Saez³⁶, E. Romero Adam¹⁶⁶, N. Rompotis¹³⁸, M. Ronzani⁵⁰, L. Roos⁸¹, E. Ros¹⁶⁶,
 S. Rosati^{132a}, K. Rosbach⁵⁰, P. Rose¹³⁷, O. Rosenthal¹⁴¹, N.-A. Rosien⁵⁶, V. Rossetti^{146a,146b},
 E. Rossi^{104a,104b}, L.P. Rossi^{52a}, J.H.N. Rosten³⁰, R. Rosten¹³⁸, M. Rotaru^{28b}, I. Roth¹⁷¹, J. Rothberg¹³⁸,
 D. Rousseau¹¹⁷, C.R. Royon¹³⁶, A. Rozanov⁸⁶, Y. Rozen¹⁵², X. Ruan^{145c}, F. Rubbo¹⁴³,
 M.S. Rudolph¹⁵⁸, F. Rühr⁵⁰, A. Ruiz-Martinez³¹, Z. Rurikova⁵⁰, N.A. Rusakovich⁶⁶, A. Ruschke¹⁰⁰,
 H.L. Russell¹³⁸, J.P. Rutherford⁷, N. Ruthmann³², Y.F. Ryabov¹²³, M. Rybar¹⁶⁵, G. Rybkin¹¹⁷, S. Ryu⁶,
 A. Ryzhov¹³⁰, G.F. Rzehorz⁵⁶, A.F. Saavedra¹⁵⁰, G. Sabato¹⁰⁷, S. Sacerdoti²⁹, H.F.-W. Sadrozinski¹³⁷,
 R. Sadykov⁶⁶, F. Safai Tehrani^{132a}, P. Saha¹⁰⁸, M. Sahinsoy^{59a}, M. Saimpert¹³⁶, T. Saito¹⁵⁵,
 H. Sakamoto¹⁵⁵, Y. Sakurai¹⁷⁰, G. Salamanna^{134a,134b}, A. Salamon^{133a,133b}, J.E. Salazar Loyola^{34b},
 D. Salek¹⁰⁷, P.H. Sales De Bruin¹³⁸, D. Salihagic¹⁰¹, A. Salnikov¹⁴³, J. Salt¹⁶⁶, D. Salvatore^{39a,39b},
 F. Salvatore¹⁴⁹, A. Salvucci^{61a}, A. Salzburger³², D. Sammel⁵⁰, D. Sampsonidis¹⁵⁴, A. Sanchez^{104a,104b},
 J. Sánchez¹⁶⁶, V. Sanchez Martinez¹⁶⁶, H. Sandaker¹¹⁹, R.L. Sandbach⁷⁷, H.G. Sander⁸⁴,
 M. Sandhoff¹⁷⁴, C. Sandoval²¹, R. Sandstroem¹⁰¹, D.P.C. Sankey¹³¹, M. Sannino^{52a,52b}, A. Sansoni⁴⁹,
 C. Santoni³⁶, R. Santonico^{133a,133b}, H. Santos^{126a}, I. Santoyo Castillo¹⁴⁹, K. Sapp¹²⁵, A. Saponov⁶⁶,
 J.G. Saraiva^{126a,126d}, B. Sarrazin²³, O. Sasaki⁶⁷, Y. Sasaki¹⁵⁵, K. Sato¹⁶⁰, G. Sauvage^{5,*}, E. Sauvan⁵,
 G. Savage⁷⁸, P. Savard^{158,d}, N. Savic¹⁰¹, C. Sawyer¹³¹, L. Sawyer^{80,q}, J. Saxon³³, C. Sbarra^{22a},
 A. Sbrizzi^{22a,22b}, T. Scanlon⁷⁹, D.A. Scannicchio¹⁶², M. Scarcella¹⁵⁰, V. Scarfone^{39a,39b},
 J. Schaarschmidt¹⁷¹, P. Schacht¹⁰¹, B.M. Schachtner¹⁰⁰, D. Schaefer³², L. Schaefer¹²², R. Schaefer⁴⁴,
 J. Schaeffer⁸⁴, S. Schaepe²³, S. Schaetzel^{59b}, U. Schäfer⁸⁴, A.C. Schaffer¹¹⁷, D. Schaile¹⁰⁰,
 R.D. Schamberger¹⁴⁸, V. Scharf^{59a}, V.A. Schegelsky¹²³, D. Scheirich¹²⁹, M. Schernau¹⁶²,
 C. Schiavi^{52a,52b}, S. Schier¹³⁷, C. Schillo⁵⁰, M. Schioppa^{39a,39b}, S. Schlenker³²,
 K.R. Schmidt-Sommerfeld¹⁰¹, K. Schmieden³², C. Schmitt⁸⁴, S. Schmitt⁴⁴, S. Schmitz⁸⁴,
 B. Schneider^{159a}, U. Schnoor⁵⁰, L. Schoeffel¹³⁶, A. Schoening^{59b}, B.D. Schoenrock⁹¹, E. Schopf²³,
 M. Schott⁸⁴, J. Schovancova⁸, S. Schramm⁵¹, M. Schreyer¹⁷³, N. Schuh⁸⁴, A. Schulte⁸⁴,
 M.J. Schultens²³, H.-C. Schultz-Coulon^{59a}, H. Schulz¹⁷, M. Schumacher⁵⁰, B.A. Schumm¹³⁷,
 Ph. Schune¹³⁶, A. Schwartzman¹⁴³, T.A. Schwarz⁹⁰, H. Schweiger⁸⁵, Ph. Schwemling¹³⁶,
 R. Schwienhorst⁹¹, J. Schwindling¹³⁶, T. Schwindt²³, G. Sciolla²⁵, F. Scuri^{124a,124b}, F. Scutti⁸⁹,
 J. Searcy⁹⁰, P. Seema²³, S.C. Seidel¹⁰⁵, A. Seiden¹³⁷, F. Seifert¹²⁸, J.M. Seixas^{26a}, G. Sekhniaidze^{104a},
 K. Sekhon⁹⁰, S.J. Sekula⁴², D.M. Seliverstov^{123,*}, N. Semprini-Cesari^{22a,22b}, C. Serfon¹¹⁹, L. Serin¹¹⁷,
 L. Serkin^{163a,163b}, M. Sessa^{134a,134b}, R. Seuster¹⁶⁸, H. Severini¹¹³, T. Sfiligoj⁷⁶, F. Sforza³², A. Sfyrla⁵¹,
 E. Shabalina⁵⁶, N.W. Shaikh^{146a,146b}, L.Y. Shan^{35a}, R. Shang¹⁶⁵, J.T. Shank²⁴, M. Shapiro¹⁶,

P.B. Shatalov⁹⁷, K. Shaw^{163a,163b}, S.M. Shaw⁸⁵, A. Shcherbakova^{146a,146b}, C.Y. Shehu¹⁴⁹, P. Sherwood⁷⁹,
 L. Shi^{151,aj}, S. Shimizu⁶⁸, C.O. Shimmin¹⁶², M. Shimojima¹⁰², M. Shiyakova^{66,ak}, A. Shmeleva⁹⁶,
 D. Shoaleh Saadi⁹⁵, M.J. Shochet³³, S. Shojaii^{92a,92b}, S. Shrestha¹¹¹, E. Shulga⁹⁸, M.A. Shupe⁷,
 P. Sicho¹²⁷, A.M. Sickles¹⁶⁵, P.E. Sidebo¹⁴⁷, O. Sidiropoulou¹⁷³, D. Sidorov¹¹⁴, A. Sidoti^{22a,22b},
 F. Siegert⁴⁶, Dj. Sijacki¹⁴, J. Silva^{126a,126d}, S.B. Silverstein^{146a}, V. Simak¹²⁸, Lj. Simic¹⁴, S. Simion¹¹⁷,
 E. Simioni⁸⁴, B. Simmons⁷⁹, D. Simon³⁶, M. Simon⁸⁴, P. Sinervo¹⁵⁸, N.B. Sinev¹¹⁶, M. Sioli^{22a,22b},
 G. Siragusa¹⁷³, S.Yu. Sivoklokov⁹⁹, J. Sjölin^{146a,146b}, M.B. Skinner⁷³, H.P. Skottowe⁵⁸, P. Skubic¹¹³,
 M. Slater¹⁹, T. Slavicek¹²⁸, M. Slawinska¹⁰⁷, K. Sliwa¹⁶¹, R. Slovak¹²⁹, V. Smakhtin¹⁷¹, B.H. Smart⁵,
 L. Smestad¹⁵, J. Smiesko^{144a}, S.Yu. Smirnov⁹⁸, Y. Smirnov⁹⁸, L.N. Smirnova^{99,al}, O. Smirnova⁸²,
 M.N.K. Smith³⁷, R.W. Smith³⁷, M. Smizanska⁷³, K. Smolek¹²⁸, A.A. Snesarev⁹⁶, S. Snyder²⁷,
 R. Sobie^{168,l}, F. Socher⁴⁶, A. Soffer¹⁵³, D.A. Soh¹⁵¹, G. Sokhrannyi⁷⁶, C.A. Solans Sanchez³²,
 M. Solar¹²⁸, E.Yu. Soldatov⁹⁸, U. Soldevila¹⁶⁶, A.A. Solodkov¹³⁰, A. Soloshenko⁶⁶,
 O.V. Solovyanov¹³⁰, V. Solovyev¹²³, P. Sommer⁵⁰, H. Son¹⁶¹, H.Y. Song^{35b,am}, A. Sood¹⁶,
 A. Sopczak¹²⁸, V. Sopko¹²⁸, V. Sorin¹³, D. Sosa^{59b}, C.L. Sotiropoulou^{124a,124b}, R. Soualah^{163a,163c},
 A.M. Soukharev^{109,c}, D. South⁴⁴, B.C. Sowden⁷⁸, S. Spagnolo^{74a,74b}, M. Spalla^{124a,124b},
 M. Spangenberg¹⁶⁹, F. Spanò⁷⁸, D. Sperlich¹⁷, F. Spettel¹⁰¹, R. Spighi^{22a}, G. Spigo³², L.A. Spiller⁸⁹,
 M. Spousta¹²⁹, R.D. St. Denis^{55,*}, A. Stabile^{92a}, R. Stamen^{59a}, S. Stamm¹⁷, E. Stanecka⁴¹, R.W. Stanek⁶,
 C. Stanescu^{134a}, M. Stanescu-Bellu⁴⁴, M.M. Stanitzki⁴⁴, S. Stapnes¹¹⁹, E.A. Starchenko¹³⁰,
 G.H. Stark³³, J. Stark⁵⁷, P. Staroba¹²⁷, P. Starovoitov^{59a}, S. Stärz³², R. Staszewski⁴¹, P. Steinberg²⁷,
 B. Stelzer¹⁴², H.J. Stelzer³², O. Stelzer-Chilton^{159a}, H. Stenzel⁵⁴, G.A. Stewart⁵⁵, J.A. Stillings²³,
 M.C. Stockton⁸⁸, M. Stoebe⁸⁸, G. Stoica^{28b}, P. Stolte⁵⁶, S. Stonjek¹⁰¹, A.R. Stradling⁸, A. Straessner⁴⁶,
 M.E. Stramaglia¹⁸, J. Strandberg¹⁴⁷, S. Strandberg^{146a,146b}, A. Strandlie¹¹⁹, M. Strauss¹¹³,
 P. Strizenc^{144b}, R. Ströhmer¹⁷³, D.M. Strom¹¹⁶, R. Stroynowski⁴², A. Strubig¹⁰⁶, S.A. Stucci²⁷,
 B. Stugu¹⁵, N.A. Styles⁴⁴, D. Su¹⁴³, J. Su¹²⁵, S. Suchek^{59a}, Y. Sugaya¹¹⁸, M. Suk¹²⁸, V.V. Sulin⁹⁶,
 S. Sultansoy^{4c}, T. Sumida⁶⁹, S. Sun⁵⁸, X. Sun^{35a}, J.E. Sundermann⁵⁰, K. Suruliz¹⁴⁹, G. Susinno^{39a,39b},
 M.R. Sutton¹⁴⁹, S. Suzuki⁶⁷, M. Svatos¹²⁷, M. Swiatlowski³³, I. Sykora^{144a}, T. Sykora¹²⁹, D. Ta⁵⁰,
 C. Taccini^{134a,134b}, K. Tackmann⁴⁴, J. Taenzer¹⁵⁸, A. Taffard¹⁶², R. Tafirout^{159a}, N. Taiblum¹⁵³,
 H. Takai²⁷, R. Takashima⁷⁰, T. Takeshita¹⁴⁰, Y. Takubo⁶⁷, M. Talby⁸⁶, A.A. Talyshv^{109,c}, K.G. Tan⁸⁹,
 J. Tanaka¹⁵⁵, M. Tanaka¹⁵⁷, R. Tanaka¹¹⁷, S. Tanaka⁶⁷, B.B. Tannenwald¹¹¹, S. Tapia Araya^{34b},
 S. Tapprogge⁸⁴, S. Tarem¹⁵², G.F. Tartarelli^{92a}, P. Tas¹²⁹, M. Tasevsky¹²⁷, T. Tashiro⁶⁹, E. Tassi^{39a,39b},
 A. Tavares Delgado^{126a,126b}, Y. Tayalati^{135e}, A.C. Taylor¹⁰⁵, G.N. Taylor⁸⁹, P.T.E. Taylor⁸⁹,
 W. Taylor^{159b}, F.A. Teischinger³², P. Teixeira-Dias⁷⁸, K.K. Temming⁵⁰, D. Temple¹⁴², H. Ten Kate³²,
 P.K. Teng¹⁵¹, J.J. Teoh¹¹⁸, F. Tepel¹⁷⁴, S. Terada⁶⁷, K. Terashi¹⁵⁵, J. Terron⁸³, S. Terzo¹⁰¹, M. Testa⁴⁹,
 R.J. Teuscher^{158,l}, T. Thevenaux-Pelzer⁸⁶, J.P. Thomas¹⁹, J. Thomas-Wilsker⁷⁸, E.N. Thompson³⁷,
 P.D. Thompson¹⁹, A.S. Thompson⁵⁵, L.A. Thomsen¹⁷⁵, E. Thomson¹²², M. Thomson³⁰, M.J. Tibbetts¹⁶,
 R.E. Ticse Torres⁸⁶, V.O. Tikhomirov^{96,am}, Yu.A. Tikhonov^{109,c}, S. Timoshenko⁹⁸, P. Tipton¹⁷⁵,
 S. Tisserant⁸⁶, K. Todome¹⁵⁷, T. Todorov^{5,*}, S. Todorova-Nova¹²⁹, J. Tojo⁷¹, S. Tokár^{144a},
 K. Tokushuku⁶⁷, E. Tolley⁵⁸, L. Tomlinson⁸⁵, M. Tomoto¹⁰³, L. Tompkins^{143,ao}, K. Toms¹⁰⁵, B. Tong⁵⁸,
 E. Torrence¹¹⁶, H. Torres¹⁴², E. Torró Pastor¹³⁸, J. Toth^{86,ap}, F. Touchard⁸⁶, D.R. Tovey¹³⁹,
 T. Trefzger¹⁷³, A. Tricoli²⁷, I.M. Trigger^{159a}, S. Trincaz-Duvoid⁸¹, M.F. Tripiana¹³, W. Trischuk¹⁵⁸,
 B. Trocmé⁵⁷, A. Trofymov⁴⁴, C. Troncon^{92a}, M. Trotter-McDonald¹⁶, M. Trovatelli¹⁶⁸,
 L. Truong^{163a,163c}, M. Trzebinski⁴¹, A. Trzupek⁴¹, J.C-L. Tseng¹²⁰, P.V. Tsiarehka⁹³, G. Tsipolitis¹⁰,
 N. Tsirintanis⁹, S. Tsiskaridze¹³, V. Tsiskaridze⁵⁰, E.G. Tskhadadze^{53a}, K.M. Tsui^{61a}, I.I. Tsukerman⁹⁷,
 V. Tsulaia¹⁶, S. Tsuno⁶⁷, D. Tsybychev¹⁴⁸, Y. Tu^{61b}, A. Tudorache^{28b}, V. Tudorache^{28b}, A.N. Tuna⁵⁸,
 S.A. Tuppiti^{22a,22b}, S. Turchikhin⁶⁶, D. Turecek¹²⁸, D. Turgeman¹⁷¹, R. Turra^{92a,92b}, A.J. Turvey⁴²,
 P.M. Tuts³⁷, M. Tyndel¹³¹, G. Ucchielli^{22a,22b}, I. Ueda¹⁵⁵, M. Ughetto^{146a,146b}, F. Ukegawa¹⁶⁰, G. Unal³²,
 A. Undrus²⁷, G. Unel¹⁶², F.C. Ungaro⁸⁹, Y. Unno⁶⁷, C. Unverdorben¹⁰⁰, J. Urban^{144b}, P. Urquijo⁸⁹,

P. Urrejola⁸⁴, G. Usai⁸, A. Usanova⁶³, L. Vacavant⁸⁶, V. Vacek¹²⁸, B. Vachon⁸⁸, C. Valderanis¹⁰⁰, E. Valdes Santurio^{146a,146b}, N. Valencio¹⁰⁷, S. Valentinetti^{22a,22b}, A. Valero¹⁶⁶, L. Valery¹³, S. Valkar¹²⁹, J.A. Valls Ferrer¹⁶⁶, W. Van Den Wollenberg¹⁰⁷, P.C. Van Der Deijl¹⁰⁷, H. van der Graaf¹⁰⁷, N. van Eldik¹⁵², P. van Gemmeren⁶, J. Van Nieuwkoop¹⁴², I. van Vulpen¹⁰⁷, M.C. van Woerden³², M. Vanadia^{132a,132b}, W. Vandelli³², R. Vanguri¹²², A. Vaniachine¹³⁰, P. Vankov¹⁰⁷, G. Vardanyan¹⁷⁶, R. Vari^{132a}, E.W. Varnes⁷, T. Varol⁴², D. Varouchas⁸¹, A. Vartapetian⁸, K.E. Varvell¹⁵⁰, J.G. Vasquez¹⁷⁵, F. Vazeille³⁶, T. Vazquez Schroeder⁸⁸, J. Veatch⁵⁶, V. Veeraraghavan⁷, L.M. Veloce¹⁵⁸, F. Veloso^{126a,126c}, S. Veneziano^{132a}, A. Ventura^{74a,74b}, M. Venturi¹⁶⁸, N. Venturi¹⁵⁸, A. Venturini²⁵, V. Vercesi^{121a}, M. Verducci^{132a,132b}, W. Verkerke¹⁰⁷, J.C. Vermeulen¹⁰⁷, A. Vest^{46,47}, M.C. Vetterli^{142,d}, O. Viazlo⁸², I. Vichou^{165,*}, T. Vickey¹³⁹, O.E. Vickey Boeriu¹³⁹, G.H.A. Viehhauser¹²⁰, S. Viel¹⁶, L. Vigani¹²⁰, M. Villa^{22a,22b}, M. Villaplana Perez^{92a,92b}, E. Vilucchi⁴⁹, M.G. Vincter³¹, V.B. Vinogradov⁶⁶, C. Vittori^{22a,22b}, I. Vivarelli¹⁴⁹, S. Vlachos¹⁰, M. Vlasak¹²⁸, M. Vogel¹⁷⁴, P. Vokac¹²⁸, G. Volpi^{124a,124b}, M. Volpi⁸⁹, H. von der Schmitt¹⁰¹, E. von Toerne²³, V. Vorobel¹²⁹, K. Vorobev⁹⁸, M. Vos¹⁶⁶, R. Voss³², J.H. Vossebeld⁷⁵, N. Vranjes¹⁴, M. Vranjes Milosavljevic¹⁴, V. Vrba¹²⁷, M. Vreeswijk¹⁰⁷, R. Vuillermet³², I. Vukotic³³, Z. Vykydal¹²⁸, P. Wagner²³, W. Wagner¹⁷⁴, H. Wahlberg⁷², S. Wahrenmund⁴⁶, J. Wakabayashi¹⁰³, J. Walder⁷³, R. Walker¹⁰⁰, W. Walkowiak¹⁴¹, V. Wallangen^{146a,146b}, C. Wang^{35c}, C. Wang^{35d,86}, F. Wang¹⁷², H. Wang¹⁶, H. Wang⁴², J. Wang⁴⁴, J. Wang¹⁵⁰, K. Wang⁸⁸, R. Wang⁶, S.M. Wang¹⁵¹, T. Wang²³, T. Wang³⁷, W. Wang^{35b}, X. Wang¹⁷⁵, C. Wanotayaroj¹¹⁶, A. Warburton⁸⁸, C.P. Ward³⁰, D.R. Wardrope⁷⁹, A. Washbrook⁴⁸, P.M. Watkins¹⁹, A.T. Watson¹⁹, M.F. Watson¹⁹, G. Watts¹³⁸, S. Watts⁸⁵, B.M. Waugh⁷⁹, S. Webb⁸⁴, M.S. Weber¹⁸, S.W. Weber¹⁷³, J.S. Webster⁶, A.R. Weidberg¹²⁰, B. Weinert⁶², J. Weingarten⁵⁶, C. Weiser⁵⁰, H. Weits¹⁰⁷, P.S. Wells³², T. Wenaus²⁷, T. Wengler³², S. Wenig³², N. Wermes²³, M. Werner⁵⁰, M.D. Werner⁶⁵, P. Werner³², M. Wessels^{59a}, J. Wetter¹⁶¹, K. Whalen¹¹⁶, N.L. Whallon¹³⁸, A.M. Wharton⁷³, A. White⁸, M.J. White¹, R. White^{34b}, D. Whiteson¹⁶², F.J. Wickens¹³¹, W. Wiedenmann¹⁷², M. Wielers¹³¹, P. Wienemann²³, C. Wiglesworth³⁸, L.A.M. Wiik-Fuchs²³, A. Wildauer¹⁰¹, F. Wilk⁸⁵, H.G. Wilkens³², H.H. Williams¹²², S. Williams¹⁰⁷, C. Willis⁹¹, S. Willocq⁸⁷, J.A. Wilson¹⁹, I. Wingerter-Seez⁵, F. Winklmeier¹¹⁶, O.J. Winston¹⁴⁹, B.T. Winter²³, M. Wittgen¹⁴³, J. Wittkowski¹⁰⁰, T.M.H. Wolf¹⁰⁷, M.W. Wolter⁴¹, H. Wolters^{126a,126c}, S.D. Worm¹³¹, B.K. Wosiek⁴¹, J. Wotschack³², M.J. Woudstra⁸⁵, K.W. Wozniak⁴¹, M. Wu⁵⁷, M. Wu³³, S.L. Wu¹⁷², X. Wu⁵¹, Y. Wu⁹⁰, T.R. Wyatt⁸⁵, B.M. Wynne⁴⁸, S. Xella³⁸, D. Xu^{35a}, L. Xu²⁷, B. Yabsley¹⁵⁰, S. Yacoob^{145a}, D. Yamaguchi¹⁵⁷, Y. Yamaguchi¹¹⁸, A. Yamamoto⁶⁷, S. Yamamoto¹⁵⁵, T. Yamanaka¹⁵⁵, K. Yamauchi¹⁰³, Y. Yamazaki⁶⁸, Z. Yan²⁴, H. Yang^{35e}, H. Yang¹⁷², Y. Yang¹⁵¹, Z. Yang¹⁵, W-M. Yao¹⁶, Y.C. Yap⁸¹, Y. Yasu⁶⁷, E. Yatsenko⁵, K.H. Yau Wong²³, J. Ye⁴², S. Ye²⁷, I. Yeletskikh⁶⁶, A.L. Yen⁵⁸, E. Yildirim⁸⁴, K. Yorita¹⁷⁰, R. Yoshida⁶, K. Yoshihara¹²², C. Young¹⁴³, C.J.S. Young³², S. Youssef²⁴, D.R. Yu¹⁶, J. Yu⁸, J.M. Yu⁹⁰, J. Yu⁶⁵, L. Yuan⁶⁸, S.P.Y. Yuen²³, I. Yusuff^{30,ar}, B. Zabinski⁴¹, R. Zaidan^{35d}, A.M. Zaitsev^{130,ae}, N. Zakharchuk⁴⁴, J. Zalieckas¹⁵, A. Zaman¹⁴⁸, S. Zambito⁵⁸, L. Zanello^{132a,132b}, D. Zanzi⁸⁹, C. Zeitnitz¹⁷⁴, M. Zeman¹²⁸, A. Zemla^{40a}, J.C. Zeng¹⁶⁵, Q. Zeng¹⁴³, K. Zengel²⁵, O. Zenin¹³⁰, T. Ženiš^{144a}, D. Zerwas¹¹⁷, D. Zhang⁹⁰, F. Zhang¹⁷², G. Zhang^{35b,am}, H. Zhang^{35c}, J. Zhang⁶, L. Zhang⁵⁰, R. Zhang²³, R. Zhang^{35b,as}, X. Zhang^{35d}, Z. Zhang¹¹⁷, X. Zhao⁴², Y. Zhao^{35d}, Z. Zhao^{35b}, A. Zhemchugov⁶⁶, J. Zhong¹²⁰, B. Zhou⁹⁰, C. Zhou⁴⁷, L. Zhou³⁷, L. Zhou⁴², M. Zhou¹⁴⁸, N. Zhou^{35f}, C.G. Zhu^{35d}, H. Zhu^{35a}, J. Zhu⁹⁰, Y. Zhu^{35b}, X. Zhuang^{35a}, K. Zhukov⁹⁶, A. Zibell¹⁷³, D. Zieminska⁶², N.I. Zimine⁶⁶, C. Zimmermann⁸⁴, S. Zimmermann⁵⁰, Z. Zinonos⁵⁶, M. Zinser⁸⁴, M. Ziolkowski¹⁴¹, L. Živković¹⁴, G. Zobernig¹⁷², A. Zoccoli^{22a,22b}, M. zur Nedden¹⁷, L. Zwalinski³².

¹ Department of Physics, University of Adelaide, Adelaide, Australia

² Physics Department, SUNY Albany, Albany NY, United States of America

³ Department of Physics, University of Alberta, Edmonton AB, Canada

- ⁴ ^(a) Department of Physics, Ankara University, Ankara; ^(b) Istanbul Aydin University, Istanbul; ^(c) Division of Physics, TOBB University of Economics and Technology, Ankara, Turkey
- ⁵ LAPP, CNRS/IN2P3 and Université Savoie Mont Blanc, Annecy-le-Vieux, France
- ⁶ High Energy Physics Division, Argonne National Laboratory, Argonne IL, United States of America
- ⁷ Department of Physics, University of Arizona, Tucson AZ, United States of America
- ⁸ Department of Physics, The University of Texas at Arlington, Arlington TX, United States of America
- ⁹ Physics Department, University of Athens, Athens, Greece
- ¹⁰ Physics Department, National Technical University of Athens, Zografou, Greece
- ¹¹ Department of Physics, The University of Texas at Austin, Austin TX, United States of America
- ¹² Institute of Physics, Azerbaijan Academy of Sciences, Baku, Azerbaijan
- ¹³ Institut de Física d'Altes Energies (IFAE), The Barcelona Institute of Science and Technology, Barcelona, Spain, Spain
- ¹⁴ Institute of Physics, University of Belgrade, Belgrade, Serbia
- ¹⁵ Department for Physics and Technology, University of Bergen, Bergen, Norway
- ¹⁶ Physics Division, Lawrence Berkeley National Laboratory and University of California, Berkeley CA, United States of America
- ¹⁷ Department of Physics, Humboldt University, Berlin, Germany
- ¹⁸ Albert Einstein Center for Fundamental Physics and Laboratory for High Energy Physics, University of Bern, Bern, Switzerland
- ¹⁹ School of Physics and Astronomy, University of Birmingham, Birmingham, United Kingdom
- ²⁰ ^(a) Department of Physics, Bogazici University, Istanbul; ^(b) Department of Physics Engineering, Gaziantep University, Gaziantep; ^(d) Istanbul Bilgi University, Faculty of Engineering and Natural Sciences, Istanbul, Turkey; ^(e) Bahcesehir University, Faculty of Engineering and Natural Sciences, Istanbul, Turkey, Turkey
- ²¹ Centro de Investigaciones, Universidad Antonio Narino, Bogota, Colombia
- ²² ^(a) INFN Sezione di Bologna; ^(b) Dipartimento di Fisica e Astronomia, Università di Bologna, Bologna, Italy
- ²³ Physikalisches Institut, University of Bonn, Bonn, Germany
- ²⁴ Department of Physics, Boston University, Boston MA, United States of America
- ²⁵ Department of Physics, Brandeis University, Waltham MA, United States of America
- ²⁶ ^(a) Universidade Federal do Rio De Janeiro COPPE/EE/IF, Rio de Janeiro; ^(b) Electrical Circuits Department, Federal University of Juiz de Fora (UFJF), Juiz de Fora; ^(c) Federal University of Sao Joao del Rei (UFSJ), Sao Joao del Rei; ^(d) Instituto de Fisica, Universidade de Sao Paulo, Sao Paulo, Brazil
- ²⁷ Physics Department, Brookhaven National Laboratory, Upton NY, United States of America
- ²⁸ ^(a) Transilvania University of Brasov, Brasov, Romania; ^(b) National Institute of Physics and Nuclear Engineering, Bucharest; ^(c) National Institute for Research and Development of Isotopic and Molecular Technologies, Physics Department, Cluj Napoca; ^(d) University Politehnica Bucharest, Bucharest; ^(e) West University in Timisoara, Timisoara, Romania
- ²⁹ Departamento de Física, Universidad de Buenos Aires, Buenos Aires, Argentina
- ³⁰ Cavendish Laboratory, University of Cambridge, Cambridge, United Kingdom
- ³¹ Department of Physics, Carleton University, Ottawa ON, Canada
- ³² CERN, Geneva, Switzerland
- ³³ Enrico Fermi Institute, University of Chicago, Chicago IL, United States of America
- ³⁴ ^(a) Departamento de Física, Pontificia Universidad Católica de Chile, Santiago; ^(b) Departamento de Física, Universidad Técnica Federico Santa María, Valparaíso, Chile
- ³⁵ ^(a) Institute of High Energy Physics, Chinese Academy of Sciences, Beijing; ^(b) Department of Modern Physics, University of Science and Technology of China, Anhui; ^(c) Department of Physics,

Nanjing University, Jiangsu; ^(d) School of Physics, Shandong University, Shandong; ^(e) Department of Physics and Astronomy, Shanghai Key Laboratory for Particle Physics and Cosmology, Shanghai Jiao Tong University, Shanghai; (also affiliated with PKU-CHEP); ^(f) Physics Department, Tsinghua University, Beijing 100084, China

³⁶ Laboratoire de Physique Corpusculaire, Clermont Université and Université Blaise Pascal and CNRS/IN2P3, Clermont-Ferrand, France

³⁷ Nevis Laboratory, Columbia University, Irvington NY, United States of America

³⁸ Niels Bohr Institute, University of Copenhagen, Kobenhavn, Denmark

³⁹ ^(a) INFN Gruppo Collegato di Cosenza, Laboratori Nazionali di Frascati; ^(b) Dipartimento di Fisica, Università della Calabria, Rende, Italy

⁴⁰ ^(a) AGH University of Science and Technology, Faculty of Physics and Applied Computer Science, Krakow; ^(b) Marian Smoluchowski Institute of Physics, Jagiellonian University, Krakow, Poland

⁴¹ Institute of Nuclear Physics Polish Academy of Sciences, Krakow, Poland

⁴² Physics Department, Southern Methodist University, Dallas TX, United States of America

⁴³ Physics Department, University of Texas at Dallas, Richardson TX, United States of America

⁴⁴ DESY, Hamburg and Zeuthen, Germany

⁴⁵ Institut für Experimentelle Physik IV, Technische Universität Dortmund, Dortmund, Germany

⁴⁶ Institut für Kern- und Teilchenphysik, Technische Universität Dresden, Dresden, Germany

⁴⁷ Department of Physics, Duke University, Durham NC, United States of America

⁴⁸ SUPA - School of Physics and Astronomy, University of Edinburgh, Edinburgh, United Kingdom

⁴⁹ INFN Laboratori Nazionali di Frascati, Frascati, Italy

⁵⁰ Fakultät für Mathematik und Physik, Albert-Ludwigs-Universität, Freiburg, Germany

⁵¹ Section de Physique, Université de Genève, Geneva, Switzerland

⁵² ^(a) INFN Sezione di Genova; ^(b) Dipartimento di Fisica, Università di Genova, Genova, Italy

⁵³ ^(a) E. Andronikashvili Institute of Physics, Iv. Javakhishvili Tbilisi State University, Tbilisi; ^(b) High Energy Physics Institute, Tbilisi State University, Tbilisi, Georgia

⁵⁴ II Physikalisches Institut, Justus-Liebig-Universität Giessen, Giessen, Germany

⁵⁵ SUPA - School of Physics and Astronomy, University of Glasgow, Glasgow, United Kingdom

⁵⁶ II Physikalisches Institut, Georg-August-Universität, Göttingen, Germany

⁵⁷ Laboratoire de Physique Subatomique et de Cosmologie, Université Grenoble-Alpes, CNRS/IN2P3, Grenoble, France

⁵⁸ Laboratory for Particle Physics and Cosmology, Harvard University, Cambridge MA, United States of America

⁵⁹ ^(a) Kirchhoff-Institut für Physik, Ruprecht-Karls-Universität Heidelberg, Heidelberg; ^(b) Physikalisches Institut, Ruprecht-Karls-Universität Heidelberg, Heidelberg; ^(c) ZITI Institut für technische Informatik, Ruprecht-Karls-Universität Heidelberg, Mannheim, Germany

⁶⁰ Faculty of Applied Information Science, Hiroshima Institute of Technology, Hiroshima, Japan

⁶¹ ^(a) Department of Physics, The Chinese University of Hong Kong, Shatin, N.T., Hong Kong; ^(b) Department of Physics, The University of Hong Kong, Hong Kong; ^(c) Department of Physics, The Hong Kong University of Science and Technology, Clear Water Bay, Kowloon, Hong Kong, China

⁶² Department of Physics, Indiana University, Bloomington IN, United States of America

⁶³ Institut für Astro- und Teilchenphysik, Leopold-Franzens-Universität, Innsbruck, Austria

⁶⁴ University of Iowa, Iowa City IA, United States of America

⁶⁵ Department of Physics and Astronomy, Iowa State University, Ames IA, United States of America

⁶⁶ Joint Institute for Nuclear Research, JINR Dubna, Dubna, Russia

⁶⁷ KEK, High Energy Accelerator Research Organization, Tsukuba, Japan

⁶⁸ Graduate School of Science, Kobe University, Kobe, Japan

- ⁶⁹ Faculty of Science, Kyoto University, Kyoto, Japan
- ⁷⁰ Kyoto University of Education, Kyoto, Japan
- ⁷¹ Department of Physics, Kyushu University, Fukuoka, Japan
- ⁷² Instituto de Física La Plata, Universidad Nacional de La Plata and CONICET, La Plata, Argentina
- ⁷³ Physics Department, Lancaster University, Lancaster, United Kingdom
- ⁷⁴ ^(a) INFN Sezione di Lecce; ^(b) Dipartimento di Matematica e Fisica, Università del Salento, Lecce, Italy
- ⁷⁵ Oliver Lodge Laboratory, University of Liverpool, Liverpool, United Kingdom
- ⁷⁶ Department of Physics, Jožef Stefan Institute and University of Ljubljana, Ljubljana, Slovenia
- ⁷⁷ School of Physics and Astronomy, Queen Mary University of London, London, United Kingdom
- ⁷⁸ Department of Physics, Royal Holloway University of London, Surrey, United Kingdom
- ⁷⁹ Department of Physics and Astronomy, University College London, London, United Kingdom
- ⁸⁰ Louisiana Tech University, Ruston LA, United States of America
- ⁸¹ Laboratoire de Physique Nucléaire et de Hautes Energies, UPMC and Université Paris-Diderot and CNRS/IN2P3, Paris, France
- ⁸² Fysiska institutionen, Lunds universitet, Lund, Sweden
- ⁸³ Departamento de Física Teórica C-15, Universidad Autónoma de Madrid, Madrid, Spain
- ⁸⁴ Institut für Physik, Universität Mainz, Mainz, Germany
- ⁸⁵ School of Physics and Astronomy, University of Manchester, Manchester, United Kingdom
- ⁸⁶ CPPM, Aix-Marseille Université and CNRS/IN2P3, Marseille, France
- ⁸⁷ Department of Physics, University of Massachusetts, Amherst MA, United States of America
- ⁸⁸ Department of Physics, McGill University, Montreal QC, Canada
- ⁸⁹ School of Physics, University of Melbourne, Victoria, Australia
- ⁹⁰ Department of Physics, The University of Michigan, Ann Arbor MI, United States of America
- ⁹¹ Department of Physics and Astronomy, Michigan State University, East Lansing MI, United States of America
- ⁹² ^(a) INFN Sezione di Milano; ^(b) Dipartimento di Fisica, Università di Milano, Milano, Italy
- ⁹³ B.I. Stepanov Institute of Physics, National Academy of Sciences of Belarus, Minsk, Republic of Belarus
- ⁹⁴ National Scientific and Educational Centre for Particle and High Energy Physics, Minsk, Republic of Belarus
- ⁹⁵ Group of Particle Physics, University of Montreal, Montreal QC, Canada
- ⁹⁶ P.N. Lebedev Physical Institute of the Russian Academy of Sciences, Moscow, Russia
- ⁹⁷ Institute for Theoretical and Experimental Physics (ITEP), Moscow, Russia
- ⁹⁸ National Research Nuclear University MEPhI, Moscow, Russia
- ⁹⁹ D.V. Skobeltsyn Institute of Nuclear Physics, M.V. Lomonosov Moscow State University, Moscow, Russia
- ¹⁰⁰ Fakultät für Physik, Ludwig-Maximilians-Universität München, München, Germany
- ¹⁰¹ Max-Planck-Institut für Physik (Werner-Heisenberg-Institut), München, Germany
- ¹⁰² Nagasaki Institute of Applied Science, Nagasaki, Japan
- ¹⁰³ Graduate School of Science and Kobayashi-Maskawa Institute, Nagoya University, Nagoya, Japan
- ¹⁰⁴ ^(a) INFN Sezione di Napoli; ^(b) Dipartimento di Fisica, Università di Napoli, Napoli, Italy
- ¹⁰⁵ Department of Physics and Astronomy, University of New Mexico, Albuquerque NM, United States of America
- ¹⁰⁶ Institute for Mathematics, Astrophysics and Particle Physics, Radboud University Nijmegen/Nikhef, Nijmegen, Netherlands
- ¹⁰⁷ Nikhef National Institute for Subatomic Physics and University of Amsterdam, Amsterdam,

Netherlands

¹⁰⁸ Department of Physics, Northern Illinois University, DeKalb IL, United States of America

¹⁰⁹ Budker Institute of Nuclear Physics, SB RAS, Novosibirsk, Russia

¹¹⁰ Department of Physics, New York University, New York NY, United States of America

¹¹¹ Ohio State University, Columbus OH, United States of America

¹¹² Faculty of Science, Okayama University, Okayama, Japan

¹¹³ Homer L. Dodge Department of Physics and Astronomy, University of Oklahoma, Norman OK, United States of America

¹¹⁴ Department of Physics, Oklahoma State University, Stillwater OK, United States of America

¹¹⁵ Palacký University, RCPTM, Olomouc, Czech Republic

¹¹⁶ Center for High Energy Physics, University of Oregon, Eugene OR, United States of America

¹¹⁷ LAL, Univ. Paris-Sud, CNRS/IN2P3, Université Paris-Saclay, Orsay, France

¹¹⁸ Graduate School of Science, Osaka University, Osaka, Japan

¹¹⁹ Department of Physics, University of Oslo, Oslo, Norway

¹²⁰ Department of Physics, Oxford University, Oxford, United Kingdom

¹²¹ ^(a) INFN Sezione di Pavia; ^(b) Dipartimento di Fisica, Università di Pavia, Pavia, Italy

¹²² Department of Physics, University of Pennsylvania, Philadelphia PA, United States of America

¹²³ National Research Centre "Kurchatov Institute" B.P.Konstantinov Petersburg Nuclear Physics Institute, St. Petersburg, Russia

¹²⁴ ^(a) INFN Sezione di Pisa; ^(b) Dipartimento di Fisica E. Fermi, Università di Pisa, Pisa, Italy

¹²⁵ Department of Physics and Astronomy, University of Pittsburgh, Pittsburgh PA, United States of America

¹²⁶ ^(a) Laboratório de Instrumentação e Física Experimental de Partículas - LIP, Lisboa; ^(b) Faculdade de Ciências, Universidade de Lisboa, Lisboa; ^(c) Department of Physics, University of Coimbra, Coimbra; ^(d) Centro de Física Nuclear da Universidade de Lisboa, Lisboa; ^(e) Departamento de Física, Universidade do Minho, Braga; ^(f) Departamento de Física Teórica y del Cosmos and CAFPE, Universidad de Granada, Granada (Spain); ^(g) Dep Física and CEFITEC of Faculdade de Ciências e Tecnologia, Universidade Nova de Lisboa, Caparica, Portugal

¹²⁷ Institute of Physics, Academy of Sciences of the Czech Republic, Praha, Czech Republic

¹²⁸ Czech Technical University in Prague, Praha, Czech Republic

¹²⁹ Faculty of Mathematics and Physics, Charles University in Prague, Praha, Czech Republic

¹³⁰ State Research Center Institute for High Energy Physics (Protvino), NRC KI, Russia

¹³¹ Particle Physics Department, Rutherford Appleton Laboratory, Didcot, United Kingdom

¹³² ^(a) INFN Sezione di Roma; ^(b) Dipartimento di Fisica, Sapienza Università di Roma, Roma, Italy

¹³³ ^(a) INFN Sezione di Roma Tor Vergata; ^(b) Dipartimento di Fisica, Università di Roma Tor Vergata, Roma, Italy

¹³⁴ ^(a) INFN Sezione di Roma Tre; ^(b) Dipartimento di Matematica e Fisica, Università Roma Tre, Roma, Italy

¹³⁵ ^(a) Faculté des Sciences Ain Chock, Réseau Universitaire de Physique des Hautes Energies - Université Hassan II, Casablanca; ^(b) Centre National de l'Énergie des Sciences Techniques Nucleaires, Rabat; ^(c) Faculté des Sciences Semlalia, Université Cadi Ayyad, LPHEA-Marrakech; ^(d) Faculté des Sciences, Université Mohamed Premier and LTPM, Oujda; ^(e) Faculté des sciences, Université Mohammed V, Rabat, Morocco

¹³⁶ DSM/IRFU (Institut de Recherches sur les Lois Fondamentales de l'Univers), CEA Saclay (Commissariat à l'Énergie Atomique et aux Énergies Alternatives), Gif-sur-Yvette, France

¹³⁷ Santa Cruz Institute for Particle Physics, University of California Santa Cruz, Santa Cruz CA, United States of America

- 138 Department of Physics, University of Washington, Seattle WA, United States of America
- 139 Department of Physics and Astronomy, University of Sheffield, Sheffield, United Kingdom
- 140 Department of Physics, Shinshu University, Nagano, Japan
- 141 Fachbereich Physik, Universität Siegen, Siegen, Germany
- 142 Department of Physics, Simon Fraser University, Burnaby BC, Canada
- 143 SLAC National Accelerator Laboratory, Stanford CA, United States of America
- 144 ^(a) Faculty of Mathematics, Physics & Informatics, Comenius University, Bratislava; ^(b) Department of Subnuclear Physics, Institute of Experimental Physics of the Slovak Academy of Sciences, Kosice, Slovak Republic
- 145 ^(a) Department of Physics, University of Cape Town, Cape Town; ^(b) Department of Physics, University of Johannesburg, Johannesburg; ^(c) School of Physics, University of the Witwatersrand, Johannesburg, South Africa
- 146 ^(a) Department of Physics, Stockholm University; ^(b) The Oskar Klein Centre, Stockholm, Sweden
- 147 Physics Department, Royal Institute of Technology, Stockholm, Sweden
- 148 Departments of Physics & Astronomy and Chemistry, Stony Brook University, Stony Brook NY, United States of America
- 149 Department of Physics and Astronomy, University of Sussex, Brighton, United Kingdom
- 150 School of Physics, University of Sydney, Sydney, Australia
- 151 Institute of Physics, Academia Sinica, Taipei, Taiwan
- 152 Department of Physics, Technion: Israel Institute of Technology, Haifa, Israel
- 153 Raymond and Beverly Sackler School of Physics and Astronomy, Tel Aviv University, Tel Aviv, Israel
- 154 Department of Physics, Aristotle University of Thessaloniki, Thessaloniki, Greece
- 155 International Center for Elementary Particle Physics and Department of Physics, The University of Tokyo, Tokyo, Japan
- 156 Graduate School of Science and Technology, Tokyo Metropolitan University, Tokyo, Japan
- 157 Department of Physics, Tokyo Institute of Technology, Tokyo, Japan
- 158 Department of Physics, University of Toronto, Toronto ON, Canada
- 159 ^(a) TRIUMF, Vancouver BC; ^(b) Department of Physics and Astronomy, York University, Toronto ON, Canada
- 160 Faculty of Pure and Applied Sciences, and Center for Integrated Research in Fundamental Science and Engineering, University of Tsukuba, Tsukuba, Japan
- 161 Department of Physics and Astronomy, Tufts University, Medford MA, United States of America
- 162 Department of Physics and Astronomy, University of California Irvine, Irvine CA, United States of America
- 163 ^(a) INFN Gruppo Collegato di Udine, Sezione di Trieste, Udine; ^(b) ICTP, Trieste; ^(c) Dipartimento di Chimica, Fisica e Ambiente, Università di Udine, Udine, Italy
- 164 Department of Physics and Astronomy, University of Uppsala, Uppsala, Sweden
- 165 Department of Physics, University of Illinois, Urbana IL, United States of America
- 166 Instituto de Física Corpuscular (IFIC) and Departamento de Física Atómica, Molecular y Nuclear and Departamento de Ingeniería Electrónica and Instituto de Microelectrónica de Barcelona (IMB-CNM), University of Valencia and CSIC, Valencia, Spain
- 167 Department of Physics, University of British Columbia, Vancouver BC, Canada
- 168 Department of Physics and Astronomy, University of Victoria, Victoria BC, Canada
- 169 Department of Physics, University of Warwick, Coventry, United Kingdom
- 170 Waseda University, Tokyo, Japan
- 171 Department of Particle Physics, The Weizmann Institute of Science, Rehovot, Israel

- ¹⁷² Department of Physics, University of Wisconsin, Madison WI, United States of America
- ¹⁷³ Fakultät für Physik und Astronomie, Julius-Maximilians-Universität, Würzburg, Germany
- ¹⁷⁴ Fakultät für Mathematik und Naturwissenschaften, Fachgruppe Physik, Bergische Universität Wuppertal, Wuppertal, Germany
- ¹⁷⁵ Department of Physics, Yale University, New Haven CT, United States of America
- ¹⁷⁶ Yerevan Physics Institute, Yerevan, Armenia
- ¹⁷⁷ Centre de Calcul de l'Institut National de Physique Nucléaire et de Physique des Particules (IN2P3), Villeurbanne, France
- ^a Also at Department of Physics, King's College London, London, United Kingdom
- ^b Also at Institute of Physics, Azerbaijan Academy of Sciences, Baku, Azerbaijan
- ^c Also at Novosibirsk State University, Novosibirsk, Russia
- ^d Also at TRIUMF, Vancouver BC, Canada
- ^e Also at Department of Physics & Astronomy, University of Louisville, Louisville, KY, United States of America
- ^f Also at Department of Physics, California State University, Fresno CA, United States of America
- ^g Also at Department of Physics, University of Fribourg, Fribourg, Switzerland
- ^h Also at Departament de Física de la Universitat Autònoma de Barcelona, Barcelona, Spain
- ⁱ Also at Departamento de Física e Astronomia, Faculdade de Ciências, Universidade do Porto, Portugal
- ^j Also at Tomsk State University, Tomsk, Russia
- ^k Also at Università di Napoli Parthenope, Napoli, Italy
- ^l Also at Institute of Particle Physics (IPP), Canada
- ^m Also at National Institute of Physics and Nuclear Engineering, Bucharest, Romania
- ⁿ Also at Department of Physics, St. Petersburg State Polytechnical University, St. Petersburg, Russia
- ^o Also at Department of Physics, The University of Michigan, Ann Arbor MI, United States of America
- ^p Also at Centre for High Performance Computing, CSIR Campus, Rosebank, Cape Town, South Africa
- ^q Also at Louisiana Tech University, Ruston LA, United States of America
- ^r Also at Institutio Catalana de Recerca i Estudis Avancats, ICREA, Barcelona, Spain
- ^s Also at Graduate School of Science, Osaka University, Osaka, Japan
- ^t Also at Department of Physics, National Tsing Hua University, Taiwan
- ^u Also at Institute for Mathematics, Astrophysics and Particle Physics, Radboud University Nijmegen/Nikhef, Nijmegen, Netherlands
- ^v Also at Department of Physics, The University of Texas at Austin, Austin TX, United States of America
- ^w Also at Institute of Theoretical Physics, Ilia State University, Tbilisi, Georgia
- ^x Also at CERN, Geneva, Switzerland
- ^y Also at Georgian Technical University (GTU), Tbilisi, Georgia
- ^z Also at Ochadai Academic Production, Ochanomizu University, Tokyo, Japan
- ^{aa} Also at Manhattan College, New York NY, United States of America
- ^{ab} Also at Hellenic Open University, Patras, Greece
- ^{ac} Also at Academia Sinica Grid Computing, Institute of Physics, Academia Sinica, Taipei, Taiwan
- ^{ad} Also at School of Physics, Shandong University, Shandong, China
- ^{ae} Also at Moscow Institute of Physics and Technology State University, Dolgoprudny, Russia
- ^{af} Also at Section de Physique, Université de Genève, Geneva, Switzerland
- ^{ag} Also at Eotvos Lorand University, Budapest, Hungary
- ^{ah} Also at International School for Advanced Studies (SISSA), Trieste, Italy
- ^{ai} Also at Department of Physics and Astronomy, University of South Carolina, Columbia SC, United States of America
- ^{aj} Also at School of Physics and Engineering, Sun Yat-sen University, Guangzhou, China

ak Also at Institute for Nuclear Research and Nuclear Energy (INRNE) of the Bulgarian Academy of Sciences, Sofia, Bulgaria

al Also at Faculty of Physics, M.V.Lomonosov Moscow State University, Moscow, Russia

am Also at Institute of Physics, Academia Sinica, Taipei, Taiwan

an Also at National Research Nuclear University MEPhI, Moscow, Russia

ao Also at Department of Physics, Stanford University, Stanford CA, United States of America

ap Also at Institute for Particle and Nuclear Physics, Wigner Research Centre for Physics, Budapest, Hungary

aq Also at Flensburg University of Applied Sciences, Flensburg, Germany

ar Also at University of Malaya, Department of Physics, Kuala Lumpur, Malaysia

as Also at CPPM, Aix-Marseille Université and CNRS/IN2P3, Marseille, France

* Deceased